Copper Based Nanomaterials for Oxidation Catalysis

by

Theunis Jacobus Muller

A dissertation submitted to meet the requirements for the degree of

Magister Scientiae

in the

Department of Chemistry

Faculty of Science

at the

University of the Free State

Supervisor: Prof. Gideon Steyl

Co-Supervisor: Prof. Andreas Roodt

November 2009

Acknowledgements

I wish to express my gratitude to the following:

Firstly I would like the thank my God and Heavenly Father for the countless blessings that You have bestowed on me and for allowing me to understand great and unsearchable things which I did not know. The honour and the glory of all belong to You for I am nothing without You.

Thank you to Prof Andreas Roodt for all his guidance, patience, endurance, leadership and perseverance throughout the course of this work. Your enthusiasm for chemistry makes learning an adventure. It is a privilege to be known as your student.

To Prof Gideon Steyl, thank you for your help and encouragement. Your encouragement to learn as much as I can and for always being available to give advice is greatly appreciated.

To my fellow students and the personnel of the Inorganic group at UFS who contributed in any way, for their support and enjoyable times we shared.

To my friends Leo Kirsten, Nicoline Cloete, Marietjie Schutte, Bradley Miller, Ilana Engelbrecht and Cyril Young for all the help, continuous encouragement, support and selflessly sharing your knowledge with me. If it were not for friends none of this would have been possible.

To my parents, Theunis and Ria Muller, and my brothers, Gert and Joubert Muller, without your love, support, faith, sacrifices, understanding and continuous encouragement this would not be possible.

The financial assistance from the University of the Free State, MNS cluster, Sasol, Thrip and the National Research Foundation (NRF) towards this research is hereby gratefully acknowledged. Opinions expressed and conclusions arrived at, are those of the author and not necessarily those of the NRF

Table of Contents

Abbreviations and Symbols VII

Abstract IX

Opsomming XI

1 Introduction and Aim 1

1.1 Introduction 1

1.2 Aim of the Study 5

2 Theoretical Aspects of Catalysis 6

2.1 Introduction 6

2.2 Copper in Organometallic Chemistry 6

2.2.1 Copper Metal 6

2.2.2 Oxidation States of Copper 8

2.3 Oxidation-Reduction Reaction of Transition Metal Ions 10

2.3.1 Introduction 10

2.3.2 Outer-Sphere Reactions 11

2.3.3 Inner-Sphere Reactions 11

2.4 Oxidation 12

2.4.1 Introduction 12

2.4.2 Mechanisms of Oxidation 16

2.4.2.1 Wacker Oxidation 16

2.4.2.2 Oxidation of Acetylenes 16

2.4.2.3 Oxidation of Aldehydes 20

2.4.2.4 Oxidation of Alcohols 21

2.4.2.5 Oxidation of Amines 24

2.4.2.6 Oxidation of Organometallic Compounds 26

2.4.2.7 Oxidation of Carboxylic Acids 28

2.4.3 Factors Influencing Oxidation 35

2.4.3.1 Ligand Parameters 37

2.5 Metal-Catalyzed Oxidation 42

2.5.1 Introduction 42

2.5.2 Mechanistic Principles of Metal-Catalyzed Oxidation 45

2.5.3 Homogeneous and Heterogeneous Catalysis 49

2.6 Oxidation of 3,5-di-*tert*-butylcatechol 50

2.6.1 Introduction 50

2.6.2 Factors Influencing the Oxidation 51

2.6.3 Mechanistic Investigation 52

2.7 Conclusion 52

3 Synthesis and Characterisation of Copper Complexes 54

3.1 Introduction 54

3.2 Spectroscopic Techniques 54

3.2.1 Infrared Spectroscopy 54

3.2.2 Ultraviolet-Visible Spectroscopy 56

3.2.3 Nuclear Magnetic Resonance Spectrocopy 58

3.3 Theoretical Aspects of X-Ray Crystallography 60

3.3.1 Introduction 60

3.3.2 X-Ray Diffraction 60

3.3.3 Bragg`s Law 63

3.3.4 Structure Factor 64

3.3.5 The'Phase Problem' 66

3.3.5.1 Direct Methods 66

3.3.5.2 The Patterson Function 66

3.3.6 Least-Squares Refinement 67

3.4 Synthesis and Spectroscopic Characterisation of Compounds 67

3.4.1 Chemicals and Instrumentation 67

3.4.2 Synthesis of Compounds 68

3.4.2.1 Synthesis of Bis(tropolonato) Copper(II) 68

3.4.2.2 Synthesis of Bis(tri-bromotropolonato) Copper(II) 68

3.4.2.3 Synthesis of Bis(2-methyl-3-hydroxy-4-pyrone) Copper(II) 69

3.4.2.4 Synthesis of Bis(2-ethyl-3-hydroxy-4-pyrone) Copper(II) 70

3.5 Crystal Structure Determination of Bis(tri-bromotropolonato) Bis(dimethylsulphoxide) Copper(II) Complex and 3,5-di-*tert*-butylcatechol 70

3.5.1 Experimental 70

3.5.2 Crystal Structure of Bis(tri-bromotropolonato) Bis (dimethylsulphoxide) Copper(II) 73

3.5.3 Crystal Structure of 3,5-di-*tert*-butylcatechol 78

3.6 Conclusion 84

4 Kinetic Study of the Oxidation of 3,5-di-*tert*-butylcatechol by Different Copper Complexes 85

4.1 Introduction 85

4.2 Theoretical Principles of Chemical Kinetic 86

4.2.1 Reaction Rates and Rate Laws 86

4.2.2 Reaction Order 87

4.2.3 Reaction Rates in Practice 88

4.2.4 Reaction Half-Life 92

4.2.5 Reaction Thermodynamics 92

4.2.6 Transition State Theory 93

4.3 Oxidation of 3,5-di-*tert*-butylcatechol by [Cu(Memal)$_2$], [Cu(Etmal)$_2$], [Cu(Trop)$_2$] and [Cu(TropBr$_3$)$_2$] 95

4.3.1 Introductition 95

4.3.2 Experimental 95

4.3.3 Mechanistic Investigation 96

4.3.3.1 Arguments and Results from Literature and Preliminary Experiments used 96

4.3.3.2 Possible Reaction Mechanisms for the Catalytic Cycle 101

4.3.4 Results and Discussion 105

4.3.4.1 Kinetic Studie 106

4.4 Conclusion 112

5 Study Evaluation 114

5.1 Introduction 114

5.2 Scientific Relevance of the Study 114

5.3 Future Research 115

Appendix 116

ABBREVIATIONS AND SYMBOLS

Abbreviation	Meaning
Å	Angstrom
NMR	Nuclear magnetic resonance spectroscopy
ppm	(Unit of chemical shift) parts per million
IR	Infrared spectroscopy
ν	Stretching frequency on IR
MO	Molecular orbital
π	Pi
σ	Sigma
α	Alpha
β	Beta
γ	Gamma
σ*	Sigma anti-bonding
λ	Wavelength
θ	Sigma
°	Degree
°C	Degree Celsius
$X^{\neq}$	Activated state
TON	Turn over number
TOF	Turn over frequency
cm	Centimeter
g	Gram
mg	Milligram
M	($mol.dm^{-3}$)
$\Delta H^{\neq}$	Enthalpy of activation
$\Delta S^{\neq}$	Entropy of activation
ΔG	Gibbs free energy
h	Planck's constant
k_B	Boltzman's constant
k_{obs}	Observed pseudo first-order rate constant
Me	Methyl
T or temp	Temperature
UV	Ultraviolet region in light spectrum

ABBREVIATIONS AND SYMBOLS

Vis	Visible region in light spectrum
MeOH	Methanol
Z	Number of molecules in a unit cell
cat or catechol	3,5-di-*tert*-butylcatechol
quin or quinone	3,5-di-*tert*-butyl-1,2-benzoquinone
δ	Chemical shift
Δ	Interval
J	Coupling constant
ΔE	Energy difference
Abs	Absorbance
NH_3	Ammonia
py	Pyridine
Memal	2-methyl-3-hydroxy-4-pyrone
Etmal	2-ethyl-3-hydroxy-4-pyrone
Trop	Tropolonato
$TropBr_3$	tri-bromotropolonato
DMSO	Dimethyl sulfoxide

Abstract

The aim of this study was the synthesis simple O,O-bidentate ligand copper complexes of the type $[Cu(Memal)_2]$, $[Cu(Etmal)_2]$, $[Cu(Trop)_2]$ and $[Cu(TropBr_3)_2]$, where Memal = 2-methyl-3-hydroxy-4-pyrone, Etmal = 2-ethyl-3-hydroxy-4-pyrone, Trop = Tropolonato and $TropBr_3$ = tri-bromotropolonato and to do an evaluation of the oxidation catalysis of 3,5-di-*tert*-butylcatechol to the 3,5-di-*tert*-butyl-1,2-benzoquinone and study the kinetics associated therewith. The ligands were selected to provide a systematic range of electronic and steric variation at the Cu(II) metal centre.

Characterisation of the complexes was done by infrared spectroscopy (IR) and elemental analysis, as well as an X-ray crystallographic structure determination of selected compounds i.e., $[Cu(TropBr_3)_2(DMSO)_2]$ and 3,5-di-*tert*-butylcatechol. $[Cu(TropBr_3)_2(DMSO)_2]$ crystallised in the monoclinic space group C2/c with Z = 4 in the unit cell dimensions a = 18.002(7) Å, b = 20.351(7) Å, c = 7.578(3) Å, β = 108.331(2) ° and the data were collected at -173 °C. Least-squares refinement led to a value of the conventional R_1 index of 0.0320 and R_w = 0.0571 for 2873 reflections having I > 2σ(I). The copper ion is coordinated by four oxygen atoms from two tri-bromotropolonato ligands. In addition there are two oxygen atoms from the two dimethylsulphoxide molecules coordinated to the copper centre in the axial positions, ensuring an overall octahedral geometry. The Cu-O(DMSO) bond lengths in the axial positions are significantly longer than the Cu-O bonds in the equatorial positions due to Jahn-Teller distortions. The 3,5-di-*tert*-butylcatechol crystallised in the triclinic space group $P\bar{1}$ with Z = 4 in the unit cell dimensions a = 9.101(5) Å, b = 11.394(5) Å, c = 13.203(5) Å, α = 83.653(5) °, β = 79.601(5) °, γ = 85.091(5) °; and the data were collected at -173 °C. Least-squares refinement led to a value of the conventional R_1 index of 0.0124 and R_w = 0.3548 for 5675 reflections having I > 2σ(I). The *tert*-butyl group on the 5 position of the phenyl ring crystallises in a 45:55 % statistically disordered position.

A kinetic investigation was conducted to study the catalytic oxidation of 3,5-di-*tert*-butylcatechol to 3,5-di-*tert*-butyl-1,2-benzoquinone by the copper complexes listed above. The reaction was studied by two techniques namely, UV-Vis and GC in order to characterise the final product. All four complexes have the ability to oxidize 3,5-di-*tert*-butylcatechol, but there is a significant difference in the rate of oxidation between the complexes. $[Cu(Memal)_2]$ and $[CuEtmal)_2]$ have comparable rates and it is much faster than the rate of $[Cu(Trop)_2]$ and

[Cu(TropBr$_3$)$_2$]. Different solvents also have an effect on the rate of the reaction: in acetonitrile the reaction only proceed to 14% completeness, but in methanol a 52% conversion is achieved in 24 hr under the same conditions. The rate of the reaction exhibits a limiting relationship with respect to molecular oxygen concentration.

The catalytic mechanism that best describes the kinetics consists of five reversible steps. The first steps involves the coordination of 3,5-di-*tert*-butylcatechol to the copper followed by a second 3,5-di-*tert*-butylcatechol coordinating to the copper in the subsequent step. The third step involves the interaction with oxygen and the loss of one 3,5-di-*tert*-butylcatechol. A limiting value for the rate constant of the copper complex with molecular oxygen, k_2 = 3.4(3) s^{-1} for [Cu(Memal)$_2$] was determined. The fourth step is the rate determining formation of 3,5-di-*tert*-butyl-1,2 benzoquinone, defined by rate constants k_3 and k_{-3}, for [Cu(Memal)] is determined to be 3.7(6) x 10^{-5} M^{-1} s^{-1} and 2(5) x10^{-6} s^{-1}. The fifth step completes the catalytic cycle and regenerates the starting complex *i.e.* the coordination of the Memal to the copper. The rates of the reaction seem to be both sterically and electronically dependent. TON and TOF values of 70.4 and 2.93 h^{-1} were observed for [Cu(Memal)$_2$].

Key terms:

Copper

Oxidation

Electonic parameters

Steric parameters

Crystal structure

Kinetics

3,5-di-*tert*-butylcatechol

3,5-di-*tert*-butyl-1,2 benzoquinone

Catalysis

Limiting kinetics

Opsomming

Die doel van hierdie studie was die sintese van eenvoudige O,O-bidentate ligand koper komplekse van die tipe $[Cu(Memal)_2]$, $[Cu(Etmal)_2]$, $[Cu(Trop)_2]$ en $[Cu(TropBr_3)_2]$ waar Memal = 2-metiel-3-hydroksie-4-piroon, Etmal = 2-etiel-3-hydroksie-4-piroon, Trop = Tropolonato en $TropBr_3$ = *tri*-bromrtroplonato en om `n evalueering van die katalitiese oksidasie van 3,5-di-*tert*-butielkatekol na die 3,5-di-*tert*-butiel-1,2-bensokinoon en die kinetika daarmee geassosieer te doen. Die ligande is gekies om `n sistematiese reeks elektroniese en steriese verandering op die Cu(II) metaal senter.

Karakterisering van die komplekse is gedoen deur middel van infrarooi spektroskopie (IR) en elementele analise, asook X-straal kristallografiese struktuurbepaling van gekose verbindings bv. $[Cu(TropBr_3)_2(DMSO)_2]$ en 3,5-di-*tert*-butielkatekol. $[Cu(TropBr_3)_2(DMSO)_2]$ het gekristalliseer in die monokliniese ruimtegroep C2/*c* met Z = 4 in die eenheidsel met dimensies a = 18.002(7) Å, b = 20.351(7) Å, c = 7.578(3) Å, β = 108.331(2) °, en die data was by -173 °C gekollekteer. Kleinste kwadraat verfyning het gelei na `n konvensionele R_1 indeks waarde van 0.0320 en R_w = 0.0571 vir 2873 refleksies met $I > 2\sigma(I)$. Die koper ioon is gekoördineer deur vier suurstof atome van twee tri-bromotropoloon ligande. Bykomend hiertoe is daar twee suurstof atome van die twee dimetielsulfoksied molekule aan die koper senter gekoördineer in aksiale posisies; dus is die algehele geometrie oktahedries. Die Cu-O(DMSO) bindingsafstande in die aksiale posisies is langer as die Cu-O bindingsafstande in die ekwatoriale posisies as gevolg van die Jahn-Teller effek. Die 3,5-di-*tert*-butielkatekol kristalliseer in die trikliniese ruimtegroep $P\bar{1}$ met Z = 4 in `n eenheidsel met dimensies a = 9.101(5) Å, b = 11.394(5) Å, c = 13.203(5) Å, α = 83.653(5) °, β = 79.601(5) °, γ = 85.091(5) ° en die data was by -173 °C gekollekteer. Kleinste kwadraat verfyning het gelei na `n konvensionele R_1 indeks waarde van 0.0124 en R_w = 0.3548 vir 5675 refleksies met $I > 2\sigma(I)$. Die *tert*-butiel groep op die 5-posisie van die feniel ring het uit gekristaliseer in `n 45:55 % statistiese vervormde posisie.

`n Kinetiese ondersoek is uitgevoer om die katalitiese oksidasie van 3,5-di-*tert*-butielkatekol na 3,5-di-*tert*-butiel-1,2-bensokinoon deur die bogenoemde koper komplekse te bestudeer. Die reaksie is met behulp van twee metodes bestudeer, naamlik UV-Vis spektroskopie en gaskromatografie (GC) ten einde die finale produk te karakteriseer. Al vier komplekse het die

vermoë om 3,5-di-*tert*-butielkatekol te oksideer, maar daar is `n noemenswaardige verskil in die tempo van oksidasie tussen die verskillende komplekse. $[Cu(Memal)_2]$ en $[CuEtmal)_2]$ het vergelykbare tempos wat aansienlik vinniger is as die tempos van $[Cu(Trop)_2]$ en $[Cu(TropBr_3)_2]$. Verskillende oplosmiddels beïnvloed ook die tempo van die reaksie: in asetonitriel bereik die reaksie slegs 14% volledigheid maar in metanol bereik die reaksie 52% omskakeling binne 24 uur onder dieselfde reaksietoestande. Die tempo van die reaksie stel `n beperkende verhouding ten toon, ten opsigte van molekulêre suurstof konsentrasie.

Die katalitiese meganisme wat die kinetika die beste beskryf bestaan uit vyf omkeerbare stappe. Die eerste stap behels die koördinasie van 3,5-di-*tert*-butielkatekol aan die koper en `n tweede 3,5-di-*tert*-butielkatekol wat aan die koper koördineer in die daaropvolgende stap. Die derde stap behels die interaksie van suurstof en die verlies van een 3,5-di-*tert*-butielkatekol. `n Beperkende waarde vir die tempo konstante van die koper kompleks met molekulêre suurstof, k_2 = 3.4(3) s^{-1} vir $[Cu(Memal)_2]$ is bepaal. Die vierde stap is die tempobepalende vorming van 3,5-di-*tert*-butiel-1,2-bensokinoon gedefinieer deur tempo konstantes k_3 en k_{-3}, en is onderskeidelik bepaal as 3.7(6) x 10^{-5} $M^{-1}.s^{-1}$ en 2(5) x 10^{-6} s^{-1} vir [Cu(Memal)]. Die vyfde stap voltooi die katalitiese kringloop en vorm die begin kompleks, met ander woorde die koördinasie van die Memal aan die koper. Die tempos van die reakse blyk beide steries en elektronies afhanklik te wees. TON en TOF waardes van 70.4 en 2.93 h^{-1} was waargeneem vir $[Cu(Memal)_2]$.

Sleutelterme:

Koper

Oksidasie

Elektroniese parameters

Steriese parameters

Kristalstruktuur

Kinetika

3,5-di-*tert*-butielkatekol

3,5-di-*tert*-butiel-1,2 bensokinoon

Katalise

Beperkende kinetika

1. Introduction and Aim

1.1 Introduction:

The name copper and the symbol Cu are derived from *aes cyprium* since it was from Cyprus that the Romans first obtained their copper metal. The discovery of copper dates back to prehistoric times: it is said to be mined for more than 5000 years. It is one of man`s most important metals. Copper is reddish colored, takes on a bright metallic luster, and is malleable, ductile, and a good conductor of heat and electricity (second only to silver in electrical conductivity) and the electrical industry is thus one of the largest users. Copper occasionally occurs native, and is found in many minerals such as cuprite, malcite, azurite chacopurite and bornite. Large copper ore deposits are found in the U.S., Chile, Zambia, DRC, Peru and Canada, mainly as the sulfide, oxide or carbonate, its major ores being copper pyrite (chalcopyrite), $CuFeS_2$, which is estimated to account for about 50% of all Cu deposits; copper glance (chalcocite), Cu_2S; cuprite, Cu_2O and malachite, $Cu_2CO_3(OH)_2$. From these, copper is obtained by smelting, leaching and by electrolysis. The native copper found near Lake Superior is extremely pure but the vast majority of current supplies of copper are obtained from low-grade ores containing only about 1% Cu. Its alloys, brass and bronze, long used are still very important; all American coins are now copper alloy, while money and gun metals also contain copper. The most important compounds are the oxides and the sulfate, blue vitriol. The latter has a wide use as an agriculture poison and as an algaecide in water purification. Copper compounds such as Fehling`s solution are widely used in analytical chemistry in tests for sugar.

The relative abundances of copper, silver and gold in the earth's crust (Cu 68 ppm, Ag 0.08 ppm, Au 0.004 ppm) are comparable to those of the preceding triad - Ni, Pd and Pt.

Table 1.1 Some properties of the elements copper, silver and gold.

Property	Cu	Ag	Au
Atomic number	29	47	79
Number of naturally occurring isotopes	2	2	1
Atomic weight	63.546(3)	107.8682(2)	196.96655(2)
Electronic configuration	$[Ar]3d^{10}4s^1$	$[Kr]4d^{10}5s^1$	$[Xe]4f^{14}5d^{10}6s^1$
Electonegativety	1.9	1.9	2.4
Metal radius (12-coordinate)/pm	128	144	144
Effective ionic radius (6-coordinate)/6			
V	-	-	57
III	54	75	85
II	73	94	-
I	77	115	137
Ionization energy/kJ mol^{-1}			
1st	745.3	730.8	889.9
2nd	1957.3	2072.6	1973.3
3rd	3577.6	3359.4	(2895)
MP/°C	1083	961	1064
BP/°C	2570	2155	2808
ΔH_{fus}/kJ mol^{-1}	13.0	11.1	12.8
ΔH_{vap}/kJ mol^{-1}	307(±6)	258(±6)	343(±11)
$\Delta H_{(monoatomic\ gas)}$/kJ mol^{-1}	337(±6)	284(±4)	379(±8)
Density (20 °C)/g cm^{-3}	8.95	10.49	19.32
Electrical resistivity (20 °C)/μohm cm	1.673	1.59	2.35

Due to the traditional designation of Cu, Ag and Au as a subdivision of the group containing the alkali metals (justified by their respective $d^{10}s^1$ and p^6s electron configuration) some similarities in properties might be expected. Such similarities as do occur, however, are confined almost entirely to the stoichiometry (as distinct from the chemical properties) of the compounds of the +1 oxidation states. The reasons are not hard to find: a filled d shell is far less effective than a filled p shell in shielding an outer s electron from the attraction of the nucleus. As a result the first ionization energies of the coinage metals are much higher, and their ionic radii smaller than those of the corresponding alkali metals (Table 1.1). Cu, Ag and Au consequently have higher melting points, are harder, denser, less reactive, less soluble in liquid ammonia and their compounds more covalent. Again, whereas the alkali metals stand at the top of the electrochemical series (with *E″* between -3.045 and -2.714 V), the coinage metals are near the bottom: Cu^+/Cu +0.521, Ag^+/Ag +0.799, Au^+/Au +1.691 V. On the other hand, a filled d shell is more easily disrupted than a filled p shell. The second and third ionization energies of the coinage metals are therefore *lower* than those of the alkali metals so that they are able to adopt oxidation states higher than +l. Cu, Ag and Au also more readily form coordination complexes. In short, Cu, Ag and Au are transition metals whereas the alkali metals are not.

CHAPTER 1

Copper, silver and gold are notable in forming an extensive series of alloys with many other metals and many of these have played an important part in the development of technology through the ages. In many cases the alloys can be thought of as nonstoichiometric intermetallic compounds of definite structural types and, despite the apparently bizarre formulae that emerge from the succession of phases, they can readily be classified by a set of rules first outlined by W. Hume-Rothery in 1926. The determining feature is the ratio of the number of electrons to the number of atoms ("electron concentration"), and because of this the phases are sometimes referred to as "electron compounds".

The reactivity of Cu, Ag and Au decreases down the group. All three metals are stable in pure dry air at room temperature but copper forms Cu_2^0 at red heat. Copper is also attacked by sulfur and halogens, and when exposed to air containing sulphur, copper forms a green coating of a basic sulfate.

Typical compounds of the elements, reveal a further reduction in the range of oxidation states consequent on the stabilization of d orbitals at the end of the transition series. Apart from a single Cu^{IV} fluoro-complex and possibly one or two Cu^{IV} oxo-species, neither Cu nor Ag is known to exceed the oxidation state +3 and even Au does so only in a few Au^{V} fluoro-compounds: these may owe their existence at least in part to the stabilizing effect of the t^6_{2g} configuration. It is also significant that, in a number of instances, the +1 oxidation state no longer requires the presence of presumed π-acceptor ligands even though the M^1 metals are to be regarded mainly as class b in character. Stable, zero-valent compounds are not found, but a number of cluster compounds with the metal in a fractional (< 1) oxidation state are known. The only aqua ions of this group are those of Cu^1 (unstable), Cu^2, Ag^1 and Ag^2 (unstable). The best-known oxidation states, particularly in aqueous solution, are +2 for Cu, +1 for Ag, and +3 for Au. This accords with their ionization energies though, of course, few of the compounds are completely ionic. Silver has the lowest first ionization energy, while the sum of first and second is lowest for Cu and the sum of first, second, and third is lowest for Au. This is an erratic sequence and illustrates the most notable feature of the triad from a chemical point of view, namely that the elements are not well related either, as three elements showing a monotonic gradation in properties or as a triad comprising a single lighter element together with a pair of closely similar heavier elements. "Horizontal" similarities with their neighbors in the periodic table are in fact more noticeable than "vertical" ones. The reasons

are by no means certain but no doubt involve several factors, of which size is probably a major one. Thus the Cu^{II} ion is smaller than Cu^{I} and, having twice the charge, interacts much more strongly with solvent water (heats of hydration are -2100 and -580 kJ mol^{-1} respectively). The difference is evidently sufficient to outweigh the second ionization energy of copper and to render Cu^{II} more stable in aqueous solution (and in ionic solids) than Cu^{1}, in spite of the stable d^{10} configuration of the latter.

Coordination numbers in this triad are again rarely higher than 6, but the univalent metals provide examples of the coordination number 2, which tends to be uncommon in transition metals proper (i.e. excluding Zn, Cd and Hg). Organometallic chemistry is not particularly extensive, even though gold alkyls were amongst the first organo-transition metal compounds to be prepared. Those of Au^{III} are the most stable in this group, while Cu^{1} and Ag^{1} (but not Au^{1}) form complexes, of lower stability, with unsaturated hydrocarbons.

Copper is best known for its ability to oxidize various organic substrates ranging from the Wacker process[1] to the oxidation of acetylenes[2], aldehydes[3], alcohols[4], amines[5], carboxylic acids[6] and it is also used in the making of Grignard reagents.[7]

1.2 Aim of the Study

It is clear from Section 1.1 that copper finds wide application in many biological processes. The fact that it is used as an oxidation catalyst provides interesting possibilities for systematic investigation. New ligand systems available might provide new applications in this regard.
With this in mind, the following stepwise aims were set for this study.

1. The synthesis of different copper complexes with different O,O- ligand systems and to characterize these systems as fully as possible.

[1] J. Smidt, W. Hafner, R. Jira, J. Sedlmeier, R. Sieber, R. Rüttinger and H. Kojer, *Angew. Chem.*, **71**, 176, (1959).
[2] W.G. Nigh, *Oxidation by Cupric Ion* 11 Academic Press New York, (1973).
[3] B. Moteiro, S. Gago, S.S. Balua, A.A. Valente, I.S. Goncalves and M. Pillinger, *J. Mol. Catal. A: Chem.*, **312**, 23, (2009).
[4] M.J. Schultz and M.S. Sigman, *Tetrahedron*, **62**, 8227, (2006).
[5] K. Muniz, A. Iglasias and Y. Fang, *Chem Commun.*, 2551, (2009).
[6] O. Das, S. Paria and T.K. Paine, *Tetrahedron Lett.*, **49**, 5924, (2008).
[7] A. Kraak, A.K. Wiersma, P. Jordens and H. Wynberg, *Tetrahedron,* **24**, 3381 (1968).

2. The crystallographic characterization of selected Cu-O,O ligands systems to study coordination mode, bond lengths and distortions of the complexes.
3. The kinetic investigation of the oxidation of 3,5-di-*tert*-butylchatechol by molecular oxygen and $[Cu(Memal)_2]$, $[Cu(Etmal)_2]$, $[Cu(Trop)_2]$ and $[Cu(tri\text{-}Brtrop)_2]$ complexes.
4. The analysis of results with respect to oxidation reactivity and coordination ability and comparison to other catalytic systems available in literature.

2. Theoretical Aspects of Catalysis

2.1 Introduction

The use of copper(II) as an oxidizing agent for organic compounds dates back to a medieval practice involving what is generally known as Egyptian ointment. This concoction was prepared by heating a mixture of honey (fructose and glucose), vinegar (acetic acid) and verdigris (cupric acetate). Alchemists dispensed this mixture for both medicinal and cosmetic purposes. It was, however, not until 1815 that the reddish brown precipitate produced in this reaction, was shown to be cuprous oxide.[1]

The first indication of the potential value of this reaction occurred in 1841, when it was observed that D-glucose precipitated cuprous oxide from an alkaline solution of cupric sulphate, whereas sucrose was unreactive toward this reagent.[2] Further work with carbohydrates led Barreswil to suggest that an alkaline solution of cupric tartrate might be used as a qualitative test for reducing sugars.[3] A few years later, Fehling worked out a useful analytical procedure based on Barreswil`s suggestion.[4]

Since these early beginnings, copper(II) has been found to be a useful oxidizing agent for a wide range of organic substrates. It offers the advantages of having a high selectivity as a result of its mild oxidizing power and its compatibility with a variety of solvent systems.

2.2 Copper in Organometallic Chemistry

2.2.1 Copper Metal

Copper (pronounced /kɒpɚ/) is a chemical element with the symbol **Cu** (Latin: *cuprum*) and atomic number 29. It is a ductile metal with excellent electrical conductivity. In its pure state, copper is rather supple and has a pinkish lustre, which is, with the exception of gold, unusual

---

[1] Vogel, *Schweigger`s J*. **13**, 162, (1815).
[2] Trommer, *Ann. Chem. Pharm*. **39**, 360, (1841); *Chem. Zentra*. **12**, 762, (1841).
[3] C. Barreswil, *J. Pharm*. **6**, 301, (1844).
[4] H. Fehling, *Ann. Chem. Pharm*. **72**, 106, (1849).

for metals, which are usually silvery white. Its uses are wide, ranging from heat conductors, electrical conductors, as building material to that of a component of various metal alloys.

Copper is an essential trace nutrient to all plants and animals. In animals, including humans, it is found primarily in the bloodstream, as a co-factor in various enzymes and in copper-based pigments. However, in sufficient amounts, copper can be poisonous and even fatal to organisms.

This easily accessible, uncompounded metal has been used by mankind for thousands of years, as it was the first mineral to be extracted from the earth and has played a significant part in the history of man, as, along with tin, it gave rise to the Bronze Age. Evidence of the extensive use of copper has been preserved from several early civilisations. In the Roman Era, copper was principally mined on the island of Cyprus, from which the metal's name originated as Cyprium, "metal of Cyprus", of which it was later shortened to Cuprum.

A number of countries, such as Chile and the United States, still have sizable reserves of the metal, which is extracted through large, open pit mines. However, like tin, there may be insufficient reserves to sustain current rates of consumption. A high demand relative to the available supply caused a price spike early in the 21st century.

Copper is an excellent conductor of electricity, and as such one of its main industrial uses is for the production of cable, wire and electrical products for both the electrical and building industries. The construction industry accounts for the second largest consumer of copper in areas such as pipes for plumbing, heating and ventilation as well as building wire and sheet metal facing. It also has many other uses, as copper has a significant presence in the industry of decorative metal art, and its uses as an anti-germ surface can also add to the anti-bacterial and anti-microbial features of buildings such as hospitals.

Like gold and silver, copper has one s-orbital electron on top of a filled electron shell, and as a result all three of these metals are found in the same family on the periodic table. This similarity in electron structure results in many shared characteristics amongst these three metals. All three have very high thermal and electrical conductivity, and all are malleable metals. Of all pure metals at room temperature, copper has the second highest electrical and thermal conductivity, with only silver having a higher conductivity.

2.2.2 Oxidation States of Copper

Copper is known to exist in the 0, 1+, 2+, and 3+ oxidation states. Of these, copper(III) is the least encountered because of its very large oxidation potential. The few known compounds containing copper(III) appear to exist as paramagnetic octahedral salts. The steel-blue $KCuO_2$, however, is diamagnetic, which suggests that it is a square-planer complex. Copper(III) has been suggested as an intermediate in certain reactions involving catalytic amounts of cupric ion and oxidizing agents such as hydrogen peroxide, hexachloroiridate(IV), peroxydisulfate, and hypochlorite (see Scheme 2.1):

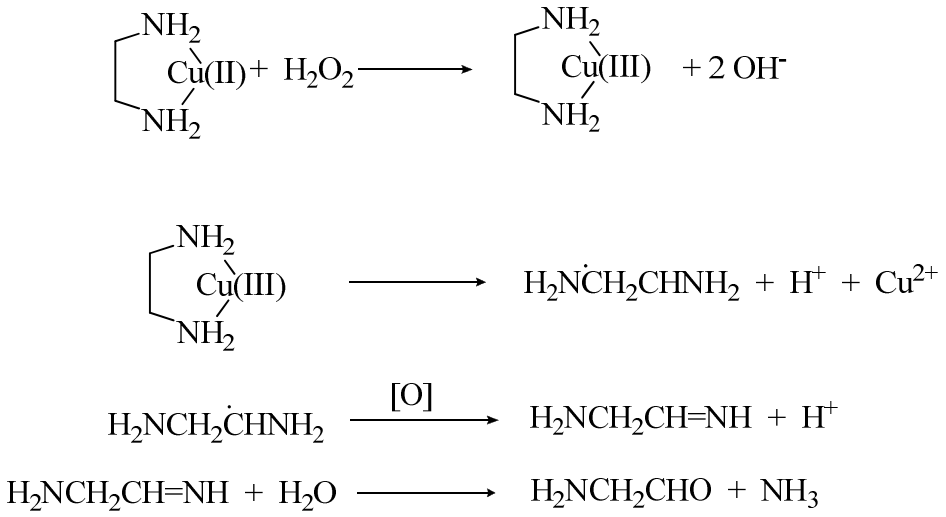

Scheme 2.1 Copper(III) as an intermediate in certain reactions involving catalytic amounts of cupric ion and oxidizing agents.

It has also been suggested that the oxidation potential of copper(III) is decreased by complex formation to a point which is low enough to allow its formation with much milder oxidizing agents (Scheme2.2).

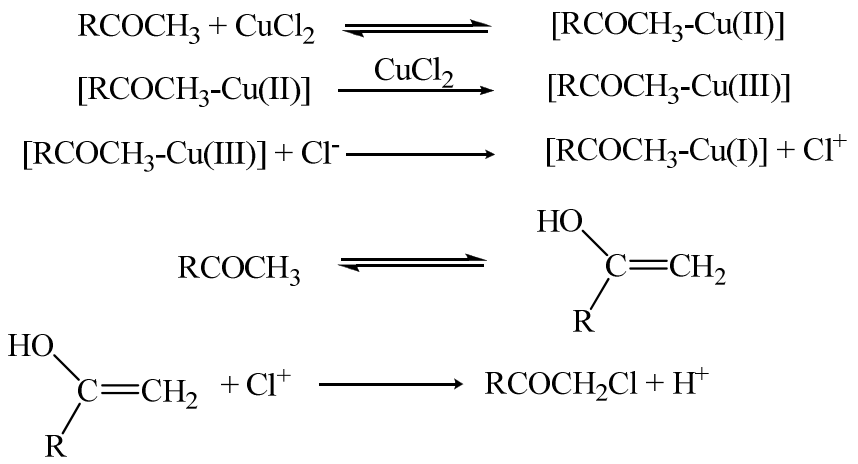

Scheme 2.2 An example of complex formation of copper(III) leading to a reduction in oxidation potential.

There is, however, no direct evidence of the intermediary of copper(III) in the absence of strong oxidizing agents. On the contrary, cupric ion oxidation appears to involve only the cupric-cuprous couple.

In contrast to copper(III), copper(II) is a relatively mild oxidizing agent. Copper(II) is the most common valance state of the metal and generally exhibits a coordination number of four or six. In the majority of cases, it possesses either a square-planer or an octahedral bond orientation. As a result of its d^9-electronic configuration, octahedral copper(II) complexes usually exhibit a Jahn-Teller distortion. Therefore two of the trans metal-ligand distances are greater than the other four, resulting in an elongated octahedral structure. Less commonly, cupric ion may form distorted tetrahedral, square-pyramidal or trigonal-bipyramidal complexes. All mononuclear copper(II) complexes are paramagnetic. However, in those cases where two copper(II) ions are held close together, there is a considerable amount of quenching of the spin moment. In the dimeric copper(II) salt of diazoaminobenzene ($C_6H_5NH{-}N{=}N{-}C_6H_5$) the spins of the two cupric ions are so strongly coupled that the salt is diamagnetic.[5]

As a result of its d^{10}-electronic structure, copper(I) is always diamagnetic. Cuprous ion is normally either two- or four-coordinated. While monodentate ligands exhibits a preference for a linear configuration, bidentate ligands more commonly occur in tetrahedral structure.

[5] C.M. Harris and R.L. Martin, *Proc. Chem. Soc.*, London 259, (1958).

The hydrate of copper(I) is unstable and disproportionates into copper(II) and metallic copper. However, in the presence of a suitable complexing agent, cuprous ion may be stabilised in aqueous solution and, in some cases, may even become more stable than cupric ion. Because of its lower charge density, copper(I) should be stabilised relative to copper(II) by decreasing the dielectric constant (ϵ) of the solvent at a specific temperature. Thus the reduction potential of copper(II) is observed to be lower in water (ϵ_{25} = 78.5) than in solvents such as acetonitrile (ϵ_{20} = 38.8), pyridine (ϵ_{25} = 12.3), or dioxane (ϵ_{25} = 2.2) at a specific temperature. This observed increase in stability is also in part due to coordination with the solvent.

The sharing of the electron pair of a ligand (known as the electron pair donor) by a metal ion (in this electron pair acceptor) may, in the Lewis sense, be considered as an acid-base reaction. Therefore, it is not surprising that the stability of coordination compounds generally increase in proportion to the basicity of the ligand. The nature of the donor atom also affects the stability of the metal complexes. Copper(II) belongs to a group of metal ions which exhibit the stability orders N > O > S and $F^- >> Cl^- > Br^- > I^-$, while copper(I) exhibits the orders N > S > O and $I^- > Br^- > Cl^- >> F^-$.

2.3 Oxidation-Reduction Reactions of Transition Metal Ions

2.3.1 Introduction

Redox reactions involve the transfer of charge from a reducing agent to an oxidizing reagent, together with a change in the oxidation state of both. These reactions are of great importance because both the chemical and physical properties of the element changes considerably when the oxidation state of the element changes. The $[Cr(H_2O)_6]^{2+}$ ion, for example, is quite labile in terms of a substitution reaction.[6] The half life of the water exchange between the aqua complex and the solvent is less than 10^{-9} seconds. When the $[Cr(H_2O)_6]^{2+}$ complex is oxidized to $[Cr(H_2O)_6]^{3+}$, the half life increases, in terms of the water exchange, to about 10^6 seconds. Thus, by taking one electron away from $[Cr(H_2O)_6]^{2+}$ the labile ion becomes stable.

[6] H. Taube, *J. Chem. Educ.*, **45**, 452, (1968).

In an oxidation–reduction sequence between metal ions in solution, two transition states for electron transfer are possible. Inorganic chemists describe these two transition states as outer-sphere and inner-sphere transition states.

2.3.2 Outer-Sphere Reactions

Outer-sphere reactions are known for the direct contact that the two metal complexes make during the transition stage, where the coordination shell of both complexes stays intact during the process of electron transfer. As a rule, outer-sphere reactions are also known as reactions that are both first order in respect of both reagents, and are further characterised by the fact that both reagents are inert in terms of substitution reactions. The rate of electron transfer is thus faster than the rate of substitution. The electron exchange between $[Fe(CN)_6]^{3-}$ and $[Fe(CN)_6]^{4-}$ from Eq 2.1 is a typical example of a reaction that, by direct electron transfer, proceeds via an outer-sphere activated complex. The rate of electron exchange, studied by means of isotope exchange, is quite fast ($k \approx 10^3\ M^{-1}\ s^{-1}$ at 4 ^{0}C).[7] Both the ferricyanide and the ferricyanide ion are unreactive in terms of the substitution reaction.

$$[Fe(CN)_6]^{4-} + [Fe(CN)_6]^{3-} \rightleftharpoons [Fe(CN)_6]^{3-} + [Fe(CN)_6]^{4-} \qquad \text{...Eq 2.1}$$

In the above mentioned reaction, rearrangement takes place.[8] When an electron is being transferred from $[Fe(CN)_6]^{4-}$ to $[Fe(CN)_6]^{3-}$ there is no change in the conformation of the atoms Fe, C or N. The normal bond length between Fe and C in $[Fe(CN)_6]^{3-}$ is shorter than in $[Fe(CN)_6]^{4-}$.[9] The Fe–C bond length in the newly formed $[Fe(CN)_6]^{3-}$ is longer than the equilibrium value, while in the product $[Fe(CN)_6]^{4-}$ the bond length is shorter than the equilibrium value. Electron transfer in outer-sphere reactions takes place after the change in electronic arrangement, as opposed to inner-sphere reactions where both the change in coordination shell and the electronic rearrangement take place before the electron transfer.

2.3.3 Inner-Sphere Reactions

As briefly mentioned above, with inner-sphere reactions, change in the coordination shell of one of the metal ions takes place before the electron transfer. The electron transfer takes place via a bridging group common to the coordination shells of both the metal ions. During inner-

---

[7] R.J. Campion, N. Purdie and N. Sutin, *Inorg. Chem.*, **3**, 1091, (1964).
[8] A.C. Wahl, *Z. Electrochem.*, **60**, 90, (1960).
[9] D. Benson, *Mechanisms of Inorganic Reactions in Solutions: An Introduction*, McGraw-Hill, London, 91, (1968).

sphere reactions a change in the coordination shells of both metal ions takes place during the formation of the activated transition state. Inner-sphere reactions take place in three different steps.[10] Eq 2.2 is a typical example of an inner-sphere reaction.[7,11]

$$Cr^{II}_{aq}{}^{2+} + [XCo^{III}(NH_3)_5]^{2+} + 5H^+ \rightarrow Cr^{III}X_{aq}{}^{2+} + Co^{II}_{aq}{}^{2+} + 5NH_4^+ \quad \text{...Eq 2.2}$$

a) A transition stage is formed by the insertion of one of the ligands of one of the metal complexes into the coordination sphere of the other metal complex.

The first step is the formation of the activated complex:

$$[XCo^{III}(NH_3)_5]^{2+} + [Cr^{II}(H_2O)_6]^{2+} \rightarrow [(NH_3)_5Co^{III}–X–Cr^{II}(H_2O)_5]^{4+} + H_2O \quad \text{...Eq 2.3}$$

b) Electron transfer from the reducing agent to the oxidizing agent takes place to yield the reaction product in the new oxidation state.

$$[(NH_3)_5Co^{III}–X–Cr^{II}(H_2O)_5]^{4+} \xrightarrow{\text{Electron transfer}} [(NH_3)_5Co^{II}–X–Cr^{III}(H_2O)_5]^{4+} \quad \text{...Eq 2.4}$$

c) The decomposition of the activated transition state by the exchange of ligands to yield the free reaction product:

$$[(NH_3)_5Co^{II}–X–Cr^{III}(H_2O)_5]^{4+} + 5H^+ \rightarrow Co^{II}_{aq}{}^{2+} + Cr^{III}X_{aq}{}^{2+} + 5NH_4^+ \quad \text{...Eq 2.5}$$

In a case where the ligand X is a chloride ion, and radioactive chloride is added to the solution, no activity is found in the formed $Cr^{III}Cl_{aq}{}^{2+}$. This shows that no substitution of the chloride ion takes place, but that the non-radioactive Cl^- is transferred from the Co-complex to the $Cr^{III}Cl_{aq}{}^{2+}$.[7,11]

2.4 Oxidation

2.4.1 Introduction

In inorganic chemistry, where ions are common, an oxidation is defined as the loss of one or more electrons by an atom. In organic chemistry, however, where polar covalent bonds are common, an oxidation is a reaction that results in a loss of electron density by carbon. This loss is often caused either by bond formation between carbon and a more electro-negative

[10] R.G. Wilkins, *The Study of Kinetics and Mechanisms of Reactions of Transition Metal Complexes*, Allyn and Bacon Inc., Boston, (1974).
[11] H. Taube, H. Myers and R.L. Rich, *J. Am. Chem. Soc.*, **75**, 4118, (1953).

atom (usually an oxygen, nitrogen or halogen atoms) or by bond breaking between carbon and a less electronegative atom (usually hydrogen).

One of the most valuable reactions of alcohols is their oxidation to yield carbonyl compounds -the opposite of the reduction of a carbonyl compound to yield an alcohol.

While primary alcohols yield aldehydes or carboxylic acids, and secondary alcohols yield ketones , tertiary alcohols do not normally react with most oxidizing agents (Scheme 2.3).

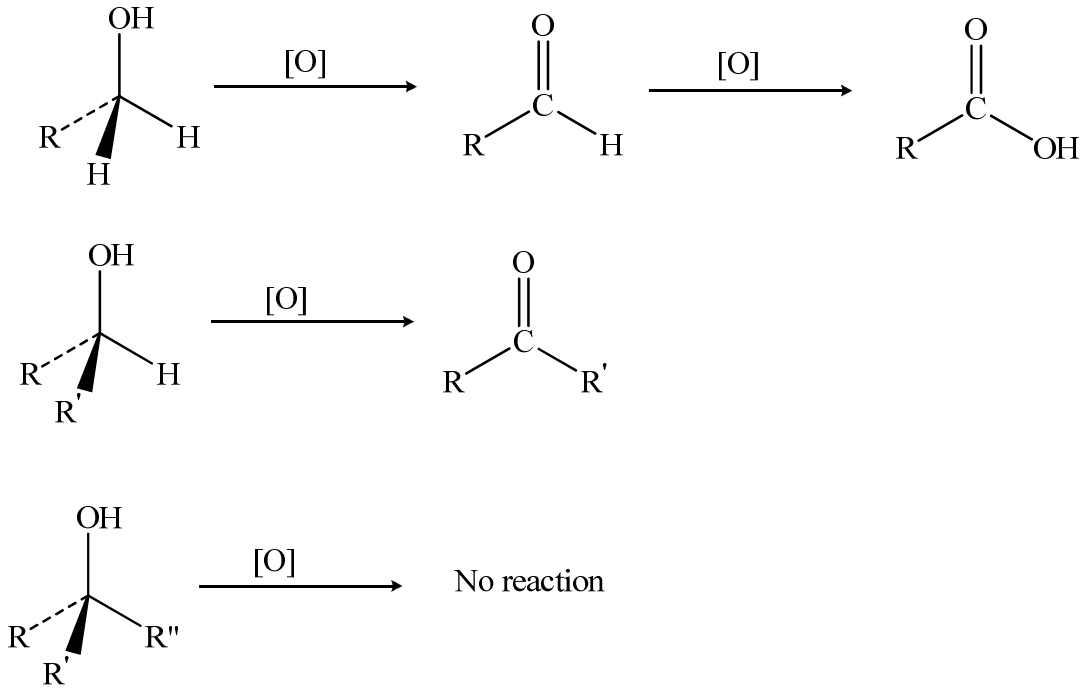

Scheme 2.3 The oxidation of primary, secondary and tertiary alcohols yielding their different products.

The oxidation of a primary or secondary alcohol can be accomplished by any of a large number of reagents, including $KMnO_4$, CrO_3 and $Na_2Cr_2O_7$. Which reagent is used in a specific case depends on such factors as cost, convenience, reaction yield and alcohol sensitivity. For example, the large-scale oxidation of a simple inexpensive alcohol such as cyclohexanol would best be done with a cheap oxidant such as $Na_2Cr_2O_7$. On the other hand, the small scale oxidation of a delicate and expensive polyfunctional alcohol would best be done with one of several mild and high-yielding reagents, regardless of cost.

Primary alcohols are oxidized either to carboxylic acids or aldehydes, depending on the reagent chosen and on the conditions used. One of the best methods for preparing an

aldehyde from a primary alcohol on laboratory scale (as opposed to an industrial scale) is to use pyridinium chlorochromate (PCC, $C_5H_6NCrO_3Cl$) in dichloromethane as solvent (Scheme 2.4).

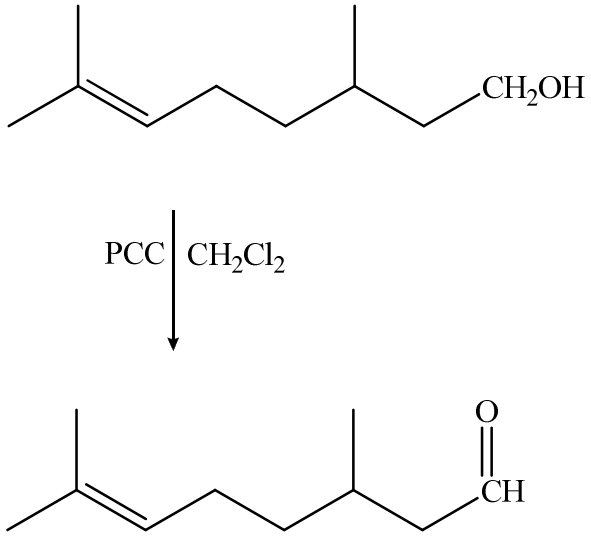

Scheme 2.4 Preparation of an aldehyde from a primary alcohol using pyridinium chlorochromate in dichloromethane.

Most other oxidizing agents, such as chromium trioxide (CrO_3) in aqueous acid, oxidize primary alcohols to carboxylic acids (Scheme 2.5). An aldehyde is involved as an intermediate in this reaction but can usually not be isolated because it is further oxidized too rapidly.

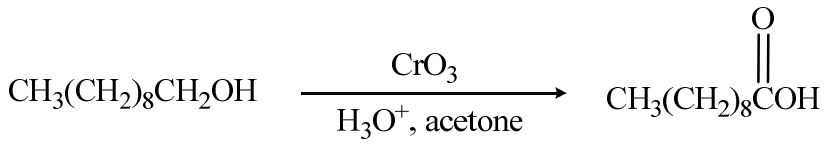

Scheme 2.5 The oxidation of a primary alcohol to a carboxylic acid by chromium trioxide.

Secondary alcohols are oxidized easily and in high yield to give the corresponding ketones. For large-scale oxidations, an inexpensive reagent such as $Na_2Cr_2O_7$ in aqueous acetic acid might be used (Scheme 2.6).

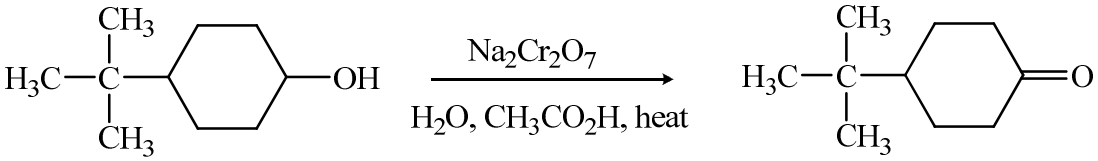

Scheme 2.6 Oxidation of a secondary alcohol by sodium dichromate in acetic acid to the ketone.

For more sensitive alcohols, pyridinium chlorochromate is often used because the reaction is milder and occurs at lower temperatures (Scheme 2.7).

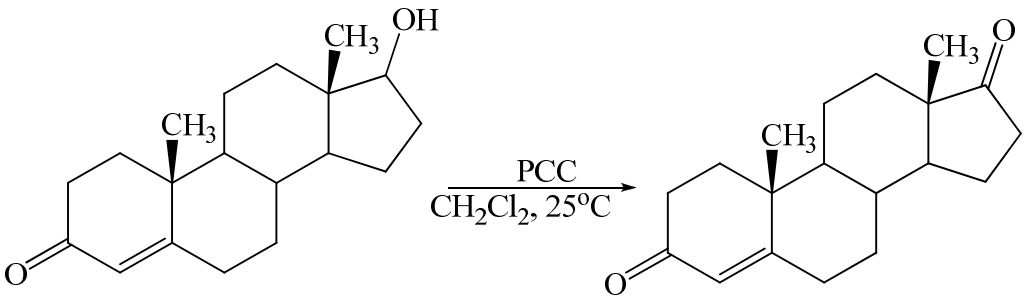

Scheme 2.7 Oxidation of a more sensitive alcohol by pyridinium chlorochromate under milder conditions.

All these oxidations occur by a pathway that is closely related to the E2 reaction (Scheme 2.8). The first step involves a reaction between the alcohol and a Cr(VI) reagent to form a chromate intermediate, which contains an O-Cr bond, then through bimolecular elimination with the expulsion of chromium as the leaving group, yields the carbonyl product.

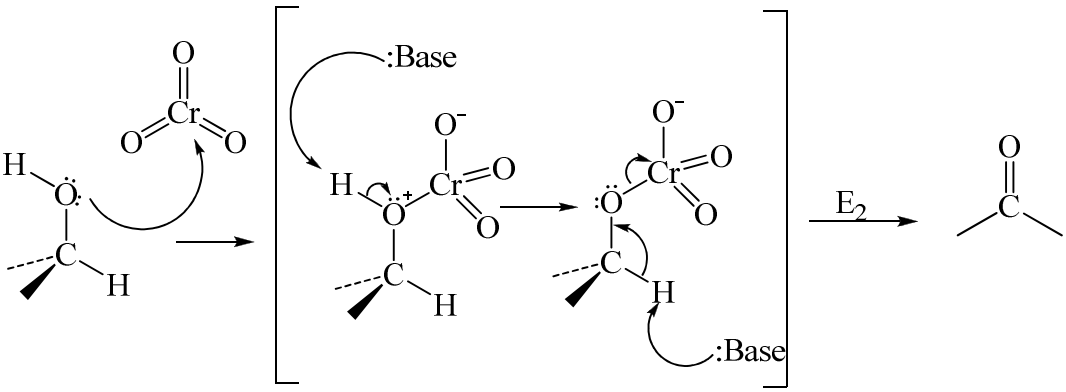

Scheme 2.8 The mechanism for the oxidation of alcohols by sodium dichromate.

Although we usually think of the E2 reaction as a means of generating a carbon-carbon double bond by elimination of a halide leaving group, the reaction is also useful for the generation of a carbon-oxygen double bond by elimination of a metal as the leaving group.

This is just one more example of how the same few fundamental mechanistic types keep reappearing in different variations.

2.4.2 Mechanisms of Oxidation

2.4.2.1 Wacker Oxidation

Since the oxidation of ethylene to acetaldehyde by $PdCl_2$ has been exploited industrially as the Wacker process[12], a wide variety of organic reactions using palladium has been developed. Of these, much attention has been given to the reaction of olefins with nucleophiles such as water, acetate, methanol, and amine in the presence of Pd(II). In reactions, such as Wacker-type reactions, the Pd(II) is reduced to Pd(0) and therefore the reaction is not catalytic. In catalytic reactions where Cu(II) and O_2 are used, the catalysis of these reactions has been frequently described (Eq 2.6 and Eq 2.7) as the reoxidation of Pd(0) by Cu(II).

$$Pd(0) + 2CuX_2 \rightarrow PdX_2 + 2CuX \qquad \text{...Eq 2.6}$$

$$2CuX + 2HX + {}^{1}/_{2}O_2 \rightarrow 2CuX_2 + H_2O \qquad \text{...Eq 2.7}$$

It has been widely believed that the oxidation state of palladium in the Wacker-type catalysis changes from Pd(II) → Pd(0) → Pd(II) (Scheme 2.9).

$$[PdCl_4]^{2-} + C_2H_4 + H_2O \longrightarrow CH_3CHO + Pd + 2HCl + 2Cl^-$$

$$Pd + 2CuCl_2 + 2Cl^- \longrightarrow [PdCl_4]^{2-} + 2CuCl$$

$$2CuCl + 1/2O_2 + 2HCl \longrightarrow 2CuCl_2 + H_2O$$

Scheme 2.9 Catalytic cycle of the Wacker oxidation process.[12]

2.4.2.2 Oxidation of Acetylenes

In 1896, Glazer reported the synthesis of 1,4-diphenylbutadiene, by passing air through a solution of cuprous chloride and phenylacetelene (Scheme 2.10).[13]

---

[12] J. Smidt, W. Hafner, R. Jira, J. Sedlmeier, R. Sieber, R. Rüttinger and H. Kojer, *Angew. Chem.*, **71**, 176, (1959).

[13] W.G. Nigh, *Oxidation by Cupric Ion* 11 Academic Press, New York, (1973).

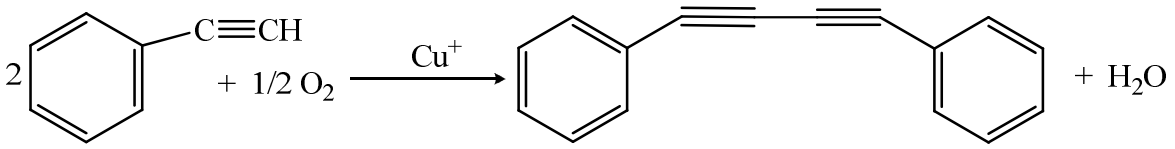

Scheme 2.10 The synthesis of 1,4-diphenylbutadiene by passing air through phenylacetelene in the presence of cuprous chloride.[13]

For many years the Glazer oxidative coupling of terminal acetylenes has been used with a great deal of success as a general method for the synthesis of 1,3-diynes. As a result of the mild oxidizing power of cupric ion, very few functional groups interfere with this reaction.[14] The oxidation has the further advantage of solvent versatility. Water, methanol, methyl cellosolve, acetone, pyridine, cyclohexylamine and toluene have all been used as a solvent for the reaction with nearly equal successes.[14] An aqueous or methanolic solution of cuprous chloride (or bromide) and ammonium chloride (buffered with HCl) at pH 3 appears to produce the highest yield of diyne in the shortest length of time.[15] For example, 1-hexyn-4-en-3-ol yields the expected dimer when treated with cuprous chloride and oxygen at pH 6.5. However, at pH 1 the reaction produces 5,7-dodecadiyne-3,9-diene-2,11-diol in high yield. [15]

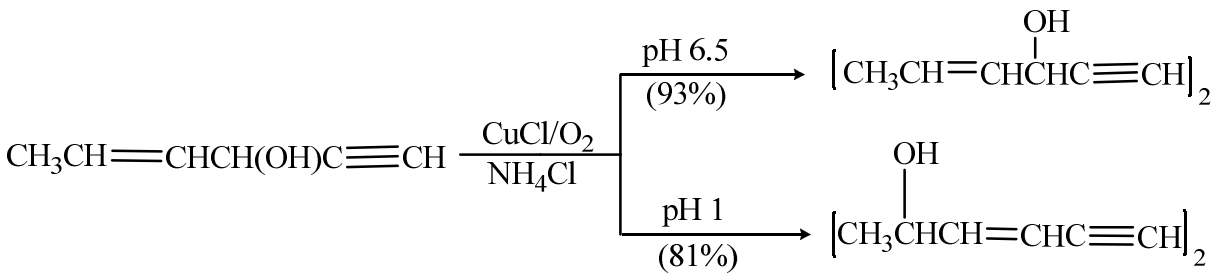

Scheme 2.11 Glazer oxidative coupling forming different products at different pH values.

The coupling reaction also occurs in both neutral and alkaline solutions. In fact, the rate of the homogeneous reaction increases with increasing pH.[16,17] Unfortunately, cuprous acetylides generally only begin to precipitate from a solution above pH 5, producing a decrease in the overall rate of oxidation. Although the yield of diyne is low, strongly alkaline

---

[14] J.E. Moses and A.D. Moorehouse, *J. Chem. Soc. Rev.*, **36**, 1249, (2007).
[15] J.B. Armitage, C.L. Cook, N. Entwistle, E.R.H. Jones and M.C. Whitting, *J. Chem. Soc.*, London 1998 (1952).
[16] A.L. Klebansky, I.V. Grachev and O.M. Kuznetsova, *J. Gen. Chem.* USSR, **27**, 3008, (1957).
[17] A.A. Clifford and W.A. Walters, *J. Chem. Soc.*, London 3056, (1963).

solutions of cupric ion have been used to couple water-soluble acetalenes such as sodium 4-pentynoate.[17]

These difficulties may be reduced somewhat by using amines such as ammonia, *tert*-butylamine, or cyclohexylamine, as both the base and the solvent. However, the best results have been achieved with tertiary amines[18]. Monodentate tertiary amines, such as pyridine, perform satisfactorily only at relative high concentrations of the base. On the other hand, bidentate tertiary amines, such as *N,N,N',N'*-tetramethylethylenediamine (TMED) are extremely effective even when used on an equimolar basis with catalytic amounts of copper(I). For example, the cuprous acetylide of propargyl alcohol is quantitatively precipitated from solutions of copper(I)-pyridine complexes, while the use of the copper(I)-TMED complexes allows the coupling reaction to proceed satisfactorily.[19] An interesting side reaction (see Scheme 2.12) occurs when dimethylamine is used in conjunction with molecular oxygen and cupric acetate to oxidize a benzene solution of phenylacetylene.[20] Although the expected diacetylene is obtained, the major product is an ynamine.

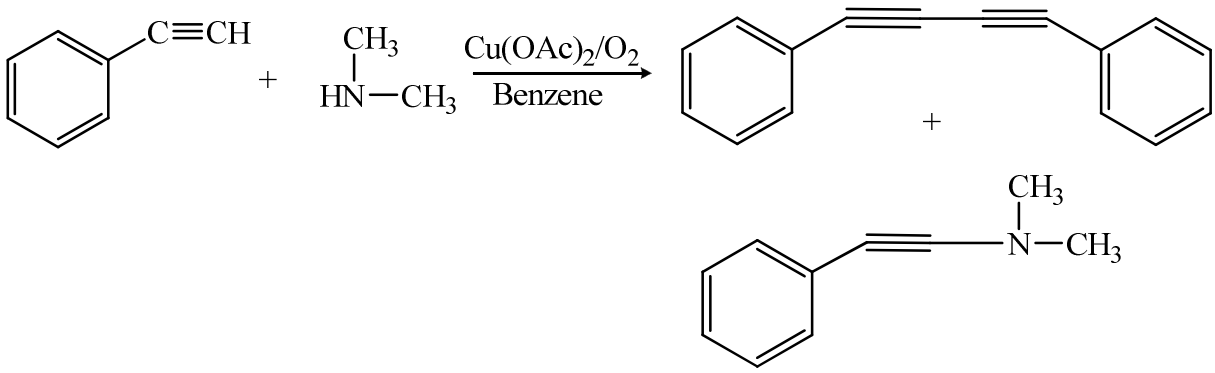

Scheme 2.12 Side reaction occurs when dimethylamine is used in conjunction with molecular oxygen and cupric acetate to oxidize benzene.

The ynamine is accounted for by the coupling of the phenylacetylide radical and the aminium radical, which is derived from the secondary amine.

---

[18] M. Verschoor-Kirss, J. Kreisz, W. Feighery, W.M. Reiff, C.M. Frommen and R.U. Kirss, *J. Organometal. Chem.*, **694**, 3262, (2009).
[19] A. S. Hay, *J. Org. Chem.*, **27**, 3320, (1962).
[20] L. I. Peterson, *Tetrahedron Lett. B.*, **53**, 57, (1968).

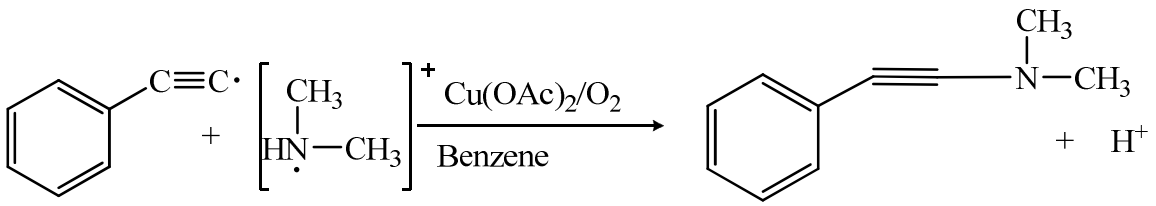

Scheme 2.13 Coupling of the phenylacetylide radical and the aminium radical.

The presence of at least trace quantities of copper salts is absolutely essential for the oxidative coupling of acetylenes. However, stoichiometric amounts of cupric salts may be used to effect the reaction directly without the need for molecular oxygen. The requirement for molecular oxygen is also eliminated by the use of ferric chloride or hydrogen peroxide[21] in combination with catalytic amounts of cuprous salts. In the absence of any other oxidizing agent, any compound containing an acetylenic hydrogen will react with an alkaline solution of copper(I) to produce a water-insoluble, shock-sensitive cuprous acetylide. Since this reaction is quite specific for terminal alkynes, it has been used extensively for both the qualitative and quantitative determination of these compounds.[22,23,24,25] This reaction has also been used successfully for the separation and purification of terminal acetylenes.[26]

Although the oxidative coupling of acetylenes is most successful when a single alkyne is used to prepare a symmetrical 1,3-diyne,[27,28,29] the reaction may also be used to synthesise unsymmetrical polyynes[30] and cyclic polyynes.[31,32,33] In the case of the cyclisation reaction, a pyridine solution of cupric acetate would appear to be the reagent of choice. Although high dilution techniques have usually been utilised to enhance the yield of cyclic products, it has been shown that this actually reduces the cyclic: acyclic product ratio in the case of the cupric

---

[21] N.A. Milas and O.L. Mageli, *J. Am. Chem. Soc.*, **75**, 5970, (1953).
[22] A.I. Vogel, *Practical Organic Chemistry*, 3rd ed., 245, Wiley, New York (1962).
[23] S. Siggia, *Quantitative Organic Analysis*, 3rd ed., 395, Wiley, New York (1963).
[24] Y. Chen, C.H. Cho, F. Shi and R.C. Larock, *J. Org. Chem.*, **74**, 6802, (2009).
[25] Y. Gao, G. Wang, L. Chen, P. Xu, Y. Zhao and L.B Han, *J. Am. Chem. Soc.*, **131**, 7956, (2009).
[26] L.F. Fieser and M. Fieser, *Organic Chemistry,* 3rd ed., 92, Heath, Boston (1956).
[27] J.B. Armitage, E.R.H. Jones and M.C. Whitting, *J. Chem. Soc.*, London, 2014, (1952).
[28] E.R.H. Jones, H.H. Lee and M.C. Whitting, *J. Chem. Soc.*, London, 341, (1960).
[29] T. Oishi, T. Katayama, K. Yamaguchi and N. Mizuno, *Chem. Eur. J.*, **15**, 7539, (2009).
[30] H. K. Black and B. C. L. Weedon, *J. Chem. Soc.*, London, 1785, (1953).
[31] F. Sondheimer and R. Wolovsky, *J. Am. Chem. Soc.*, **84**, 2846, (1962).
[32] F. Sondheimer and R. Wolovsky, *J. Am. Chem. Soc.*, **84**, 260, (1962).
[33] F. Sondheimer and R. Wolovsky, *J. Am. Chem. Soc.*, **87**, 5720, (1965).

acetate- pyridine oxidation of 1,7- octadiyne. High dilution, however, does increase the cyclic dimer: cyclic trimer ratio, as well as reducing the yield of polymerisation.[15]

2.4.2.3 Oxidation of Aldehydes

Alkaline solutions of copper(II) oxidize many aldehydes to their corresponding carboxylate anions. The synthetic utility of this reaction is quite limited, because of the occurrence of side reactions (e.g. aldol condensation). On the other hand, the reaction forms the basis of the well known Benedict`s and Felhing`s test for aliphatic aldehydes.[34]

With the exception of formaldehyde, other aldehydes which lack an enolisable α-hydrogen atom are not oxidized to carboxylic acids by copper(II).[35] Thus it would appear that the mechanism for this reaction involves the initial removal of an α proton and an enolate anion is formed which is subsequently oxidized by copper(II) via an electron transfer process.

The oxidation of RCHCHO can also lead to the α-hydroxyaldehyde by way of the carbonium ion RCHCHO. These α-aldols are easily oxidized by copper(II) and lead to a number of by products. In the presence of halide ions, the oxidation of the free-radical intermediate occurs through a ligand transfer process. Under these conditions, enolisable aldehydes are generally converted into α-halo aldehydes.[36] Cuprous oxide is the usual inorganic product of the copper(II) oxidation of aliphatic aldehydes. Formaldehyde, however, reduces alkaline solutions of cupric ion all the way to metallic copper. This unique behaviour of formaldehyde suggests the possibility of a mechanism involving a hydride abstraction by copper(II) (Scheme 2.14).

---

[34] R.L. Shringer, R.C. Fuson and D.V. Curtin, *The Systematic Identification of Organic Compounds*, 102. Wiley, New York (1956).

[35] W.A. Waters, *Mechanisms of Oxidation of Organic Compounds*, 89. Wiley, New York (1964).

[36] B. Moteiro, S. Gago, S.S. Balua, A.A. Valente, I.S. Goncalves and M. Pillinger, *J. Mol. Catal. A: Chem.*, **312**, 23, (2009).

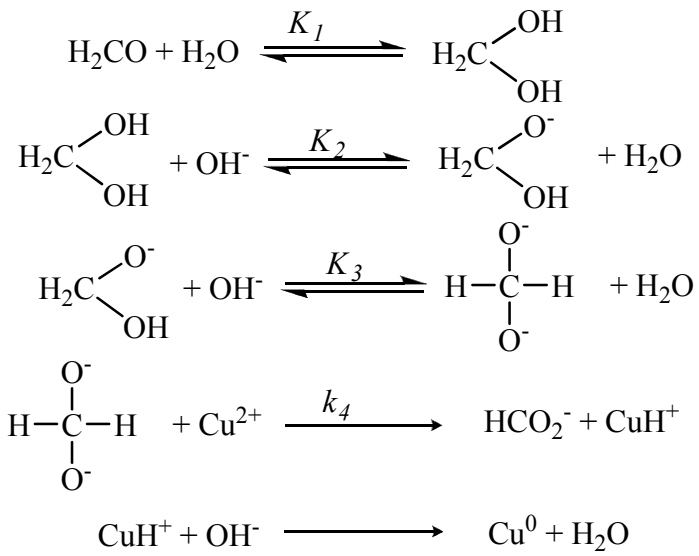

Scheme 2.14 Example of a hydride abstraction by Cu(II).

This is consistent with the ease with which formaldehyde undergoes hydrate formation and intermolecular hydride transfer.

2.4.2.4 Oxidation of Alcohols

Phenols are generally quite susceptible to oxidation. Thus, phenols are oxidized by copper(II) and oxygen to a mixture of quinones and oxidative coupling products.[37,38,39,40] The product distribution is dependent on the structure of the phenol and the reactions conditions. In contrast to phenols, aliphatic alcohols are generally resistant to oxidation by copper(II). However, in the presence of oxygen, ammonia and a strong base, cupric chloride oxidizes primary alcohols to the corresponding aldehydes.

Many substitution alcohols exhibit an increase in reactivity toward copper(II). For example, certain 1,2-diols are oxidized to the corresponding diketones by cupric ions. Thus hydroanision is oxidized to anisil by strong basic solutions of cupric tartrate (Scheme 2.15).[41]

The same type of reaction can also be done in glacial acetic acid.[42]

---

[37] W.W. Kaeding, *J. Org. Chem.*, **28**, 1063, (1963).
[38] E. Ochiai, *Tetrahedron.,* **20**, 1831, (1964).
[39] J. Mazur, A.M. Garcìa, C. Còrdova, O. Pizarro, V. Acuna and E. Spodine, *Polyhedron.*, **21**, 181, (2002).
[40] M.J. Schultz and M.S. Sigman, *Tetrahedron.*, **62**, 8227, (2006).
[41] E. Cattelain and P. Chabier, *Bull. Soc. Chim. Fr.,* **5,** 1103, (1947).
[42] I.A. Pearl, *J.Am. Chem. Soc.*, **74**, 4260, (1952).

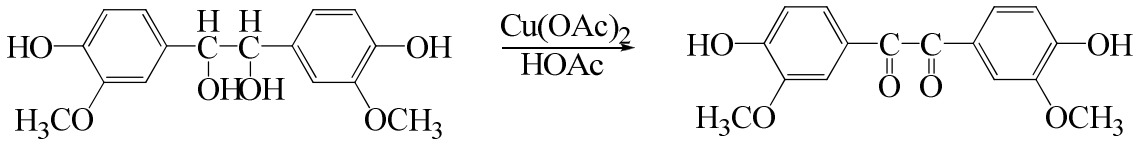

Scheme 2.15 Example where a hydroanision is oxidized by cupric tartrate to anisil in a basic solution.

By far the most reactive alcohols are those which are adjacent to a carbonyl group.[43] The best-known examples of this class of compounds are the reducing sugars. However, any primary or secondary α-hydroxy aldehyde or ketone is readily oxidized to the corresponding 1,2-dicarbonyl compound by copper(II). For example , D-xylose and α-hydroxyacetophenone are oxidized to the corresponding α-keto aldehyde by cupric acetate (Scheme 2.16).[44]

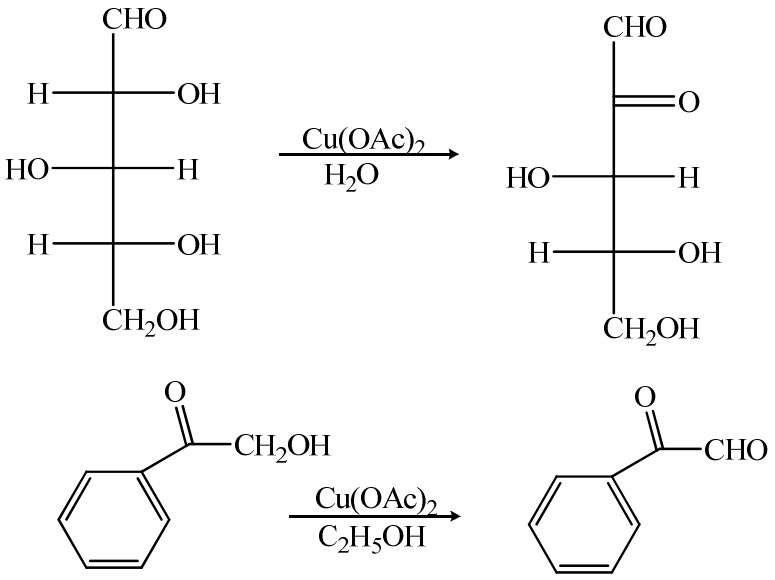

Scheme 2.16 Examples of the oxidation of D-xylose and hydroxyactophenone by cupric acetate to α-keto aldehyde.

The formation of α-keto aldehyde illustrates both the greater reactivity of the alcohol group and the stability of aldehydes which lack an enolisable α-proton. However, the initial oxidation product of D-xylose still possesses an α-hydroxy carbonyl group which is susceptible to further oxidation. Thus, reducing sugars are extensively oxidized by excess

[43] P.P. Hankare, P.D. Kamble, S.P. Maradur, M.R. Kadam, U.B. Sankpal, R.P. Patil, R.K. Nimat and P.D. Lokhande, *J. Alloys Compd.*, article in press (2009).
[44] J.K. Hamilton and F. Smith, *J. Am. Chem. Soc.*, **74**, 5162, (1952).

Fehling`s solution to a complex mixture of products, which includes carbon dioxide and oxalic acid.[45]

Although the copper(II) oxidation of aldols and ketols generally gives a high yield of the dicarbonyl product, there are a number of side reactions which may reduce the efficiency of the reaction. Under basic conditions, an α-keto aldehyde may undergo a hydride shift to form an α-hydroxyl carboxylic acid.[46]

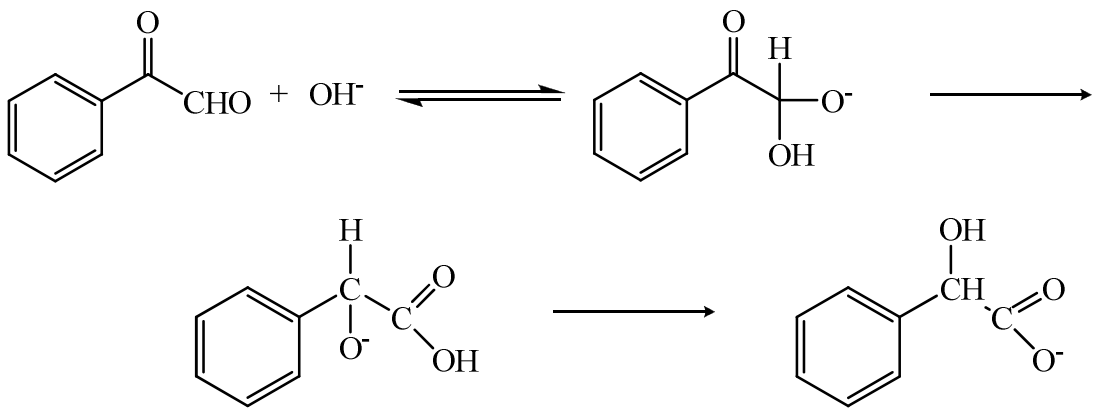

Scheme 2.17 Example of a side reaction during the oxidation of an α-keto aldehyde to form an α-hydroxyl carboxylic acid.

This reaction is quite similar to the benzilic acid rearrangement which involves the shift of an aryl group rather than a hydride.[47, 48]

Normally these rearrangements occur only under very alkaline conditions and, therefore, can only be significant in oxidation utilising a strong base. A side reaction involving the oxidative cleavage of the dicarbonyl product has been reported by Kinoshita.[49,50] Thus, an almost quantitative yield of benzoic acid was obtained when benzoin was oxidized with cuprous chloride and air, using pyridine as the solvent.

---

[45] A.F. McLeod, *J. Am. Chem.*, **37**, 20, (1906).
[46] E.R. Alexander, *J. Am. Chem. Soc.,* **69**, 289, (1947).
[47] F.H. Westheimer, *J. Am. Chem. Soc*., **58**, 2209, (1936).
[48] J. Fan, Y. Dai, Y. Li, N. Zheng, J. Guo, X. Yan and G.D. Stucky, *J. Am. Chem. Soc*., **131**, 15568, (2009).
[49] K. Kinoshita, *Bull. Chem. Soc. Jap*., **32**, 777, (1959).
[50] K. Kinoshita, *Bull. Chem. Soc. Jap*., **32,** 783, (1959).

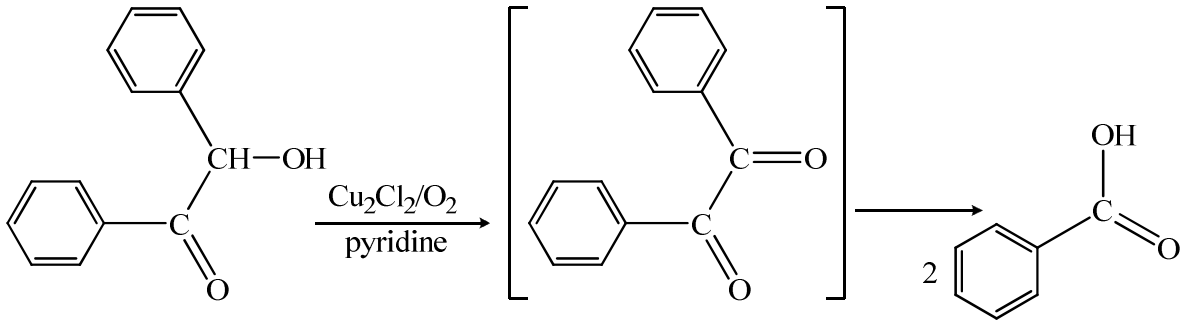

Scheme 2.18 Example of the oxidative cleavage of a dicarbonyl species by cuprous chloride in air.

On the other hand, benzil was the sole product of the oxidation of benzoin with cupric chloride and air in pyridine. Hydrobenzoin and α-methylbenzoin also undergoes a carbon-carbon bond cleavage with cuprous chloride and air in pyridine solvent.

The oxidative cleavage of benzoin, hydrobenzoin and α-methylbenzoin can also be affected by cupric chloride and air if a stoichiometric amount of potassium hydroxide is added to the reaction mixture.[50]

2.4.2.5 Oxidation of Amines

Although aliphatic amines are generally unreactive towards copper(II), α-amino ketones are readily oxidized to the corresponding dicarbonyl compounds by alkaline solutions of cupric ions. For example, α-aminodeoxybenzoin is oxidized to benzil by Fehling`s solution.[51]

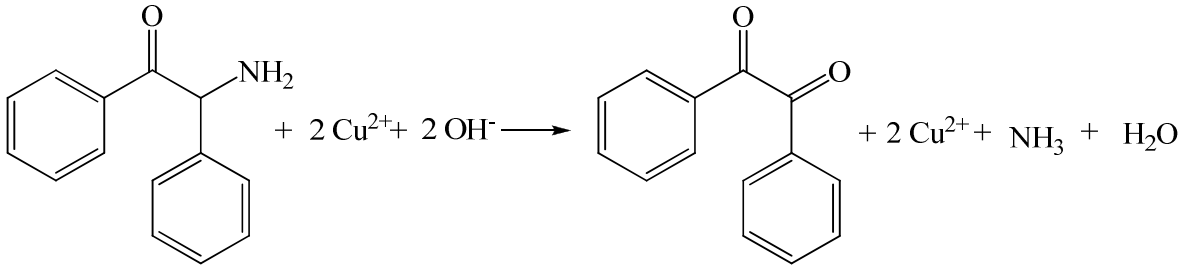

Scheme 2.19 Example of the oxidation of α-aminodeoxybenzoin by Feling`s solution to benzil.

The reaction apparently proceeds through a mechanism which is analogous to that which is operative in the oxidation of α-ketols. In the case of the amine, the initial product is presumably the α-imino ketone, which is rapidly hydrolysed to the diketone under the reaction conditions.

---

[51] T.H. James and A. Weissberger, *J. Am. Chem. Soc.*, **59**, 2040, (1937).

In contrast to the aliphatic case, primary aromatic amines are readily oxidized to azobenzenes by cuprous chloride and oxygen, when pyridine is used as the solvent.[49,50,52] Collidine and 2-picoline may be substituted for pyridine but with a resulting decrease in the rate of reaction. The oxidation fails, however, if alcohol, quinoline, dioxane, or 1,2-dichloroethane is used as solvent. Cuprous chloride is apparently unique in its ability to catalyze the oxidation of aniline. Thus, if acetate, bromide, or iodide is substituted for a chloride ion, copper(I) ceases to function as an oxidation catalyst. Ferrous, ferric, cobaltous, and cupric chloride also fail to bring about autoxidation of aniline. Since the aerial oxidation of copper(I) produces hydroxide ion as well as copper(II), it is not surprising that cupric chloride does affect the oxidation of analine if an equivalent amount of potassium hydroxide is added to the reaction mixture.[49] The hydroxide ion is consumed by the hydrogen ion which is liberated in the oxidation of aniline.

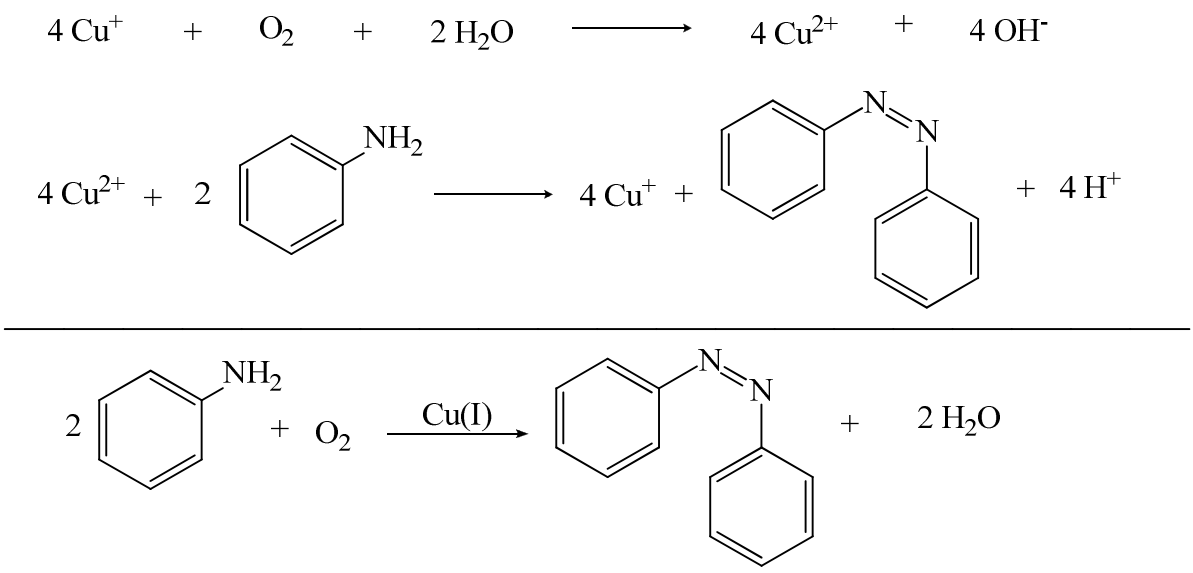

Scheme 2.20 Example of the oxidation of aniline by copper(I) in air.

The complete lack of a reaction in the presence of acetic acid further implicates hydroxide ions in the mechanism of the oxidation.

Kinoshita[49] has reported that the yield of azobenzene from the copper(II)-catalyzed autoxidation of aniline is drastically reduced by the addition of methanol. This is consistent with the observation of Engelsma and Havinga,[53] namely that a methanolic solution of aniline

[52] K. Muniz, A. Iglasias and Y. Fang, *Chem. Commun.*, 2551, (2009).
[53] G. Engelsma and E. Havinga, *Tetrahedron.,* **2**, 289, (1958).

is oxidized by cupric acetate and oxygen to a mixture of azobenzene (19%), 3-aminophenoxazone (5%), and 2-amino-5-anilinoquinone-4-anil (70%).

2.4.2.6 Oxidation of Organometallic Compounds

Organolithium and organomagnesium (Grignard reagents) compounds undergo oxidative coupling in the presence of copper(II).[54]

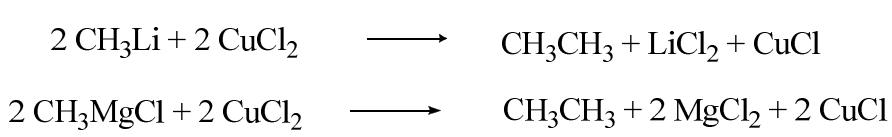

Scheme 2.21 Grignard reagents undergoing oxidative coupling in the presence of copper(II).

The cupric salt may be added either before or after the formation of the organometallic compound. Anhydrous cupric halides must be used due to the ease with which organometallic reagents are hydrolyzed. [55,56,57,58,59]

The oxidative coupling of organolithium and -magnesium compounds may also be accomplished with copper(I) and molecular oxygen.[55] The very nature of the reaction product suggests that copper(II) undergoes a one-electron transfer process to produce a free-radical intermediate. Although no oxidation-reduction processes are involved, there are several copper(I)-catalyzed reactions of organometallic compounds which are potentially useful for synthetic purposes. For example, cuprous halides react with organometallic substances to form organocopper(I) species which react readily with organohalides to form substitution products.[60,61,62,63]

---

[54] H. Gilman, R.G. Jones and L.A. Woods, *J. Am. Chem. Soc.*, **76**, 3615, (1954).
[55] G.M. Whitesides, J. San Filippo, Jr., C.P. Casey and E.J. Panek, *J. Am. Chem. Soc.*, **89**, 5302, (1967).
[56] H. Gilman and H.H. Parker, *J. Am. Chem. Soc.*, **46**, 2823, (1924).
[57] W.P. Norris and W.G. Finnegan, *J. Org. Chem.*, **31**, 3292, (1966).
[58] A. Kraak, A.K. Wiersma, P. Jordens and H. Wynberg, *Tetrahedron.,* **24**, 3381, (1968).
[59] H. Wynberg and A. Kraak, *J. Org. Chem.*, **29**, 2455, (1964).
[60] E.J. Corey and G.H. Posner, *J. Am. Chem. Soc.*, **89**, 3911, (1967).
[61] E.J. Corey, J.A. Katzenellenbogen and G.H. Posner, *J. Amer. Chem. Soc.*, **89**, 4245, (1967).
[62] E.J. Corey and G.H. Posner, *J. Am. Chem. Soc.*, **90**, 5615, (1968).
[63] G.M. Whitesides, W.F. Fischer, Jr., J. San Filippo, Jr., R.W. Bashe and H.O. House, *J. Am. Chem. Soc.*, **91**, 4871, (1969).

These organocopper species may also add to acetylenic bonds to yield substituted olefins or allenes.[64,65,66,67]

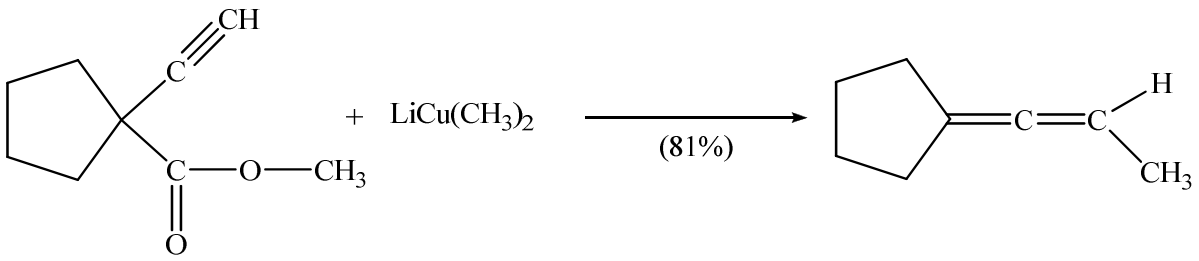

Scheme 2.22 Example of an organocopper that adds to an acetylenic bond to form an allene.

The aromatic boronic acids are also oxidized by copper(II). The organic product of this reaction, however, is quite dependent upon the anion associated with the metal ion. For example, cupric chloride yields the corresponding aryl chloride, while cupric acetate produces both the acetate and the biaryl coupling product.[68] The mechanism for the copper(II) oxidation of these organoboron compounds is apparently quite similar to that proposed for the more reactive organometallic compounds. That is, the boronic acid is first oxidized to the aryl radical, which subsequently either couples or is oxidized further by ligand transfer from copper(II).

$$ArB(OH)_2 + Cu^{2+} + H_2O \longrightarrow Ar\cdot + Cu^{+} + B(OH)_3 + H^{+}$$

$$2\,Ar\cdot \longrightarrow Ar_2$$

$$Ar\cdot + CuX_2 \longrightarrow ArX + CuX$$

Scheme 2.23 Example for the copper(II) oxidation of organoboron compound.

This latter process does not occur with the more reactive organolithium and -magnesium compounds. In contrast to its behaviour in an aqueous solution, cupric halide should exist in the diamagnetic dimeric form in a nonpolar solvent such as diethyl ether.

---

[64] E.J. Corey and J.A. Katzenellenbogen, *J. Am. Chem. Soc.*, **91**, 1851, (1969).
[65] P. Rona and P. Crabbe, *J. Am. Chem. Soc.*, **90**, 4733, (1968).
[66] P. Rona and P. Crabbe, *J. Am. Chem. Soc.*, **91**, 3289, (1969).
[67] K. Brown, S. Zolezzi, P. Aguirre, D. Venegas-Yazigi, V. Paredes-Garcia, R. Baggio, M.A. Novak and E. Spodine, *Dalton Trans.*, 1422, (2009).
[68] A.N. Nesmeyanov, V.A, Sazonova and V.N. Drozd, *Tetrahedron Lett.*, **17**, 13, (1959).

2.4.2.7 Oxidation of Carboxylic Acids

The copper(II) salts of aromatic carboxylic acids undergo an oxidative reaction when they are drastically heated. An example is the pyrolysis of solid cupric benzoate when heated in an aprotic solvent, and it produces benzoylsalicylic acid.[69, 70, 71,72]

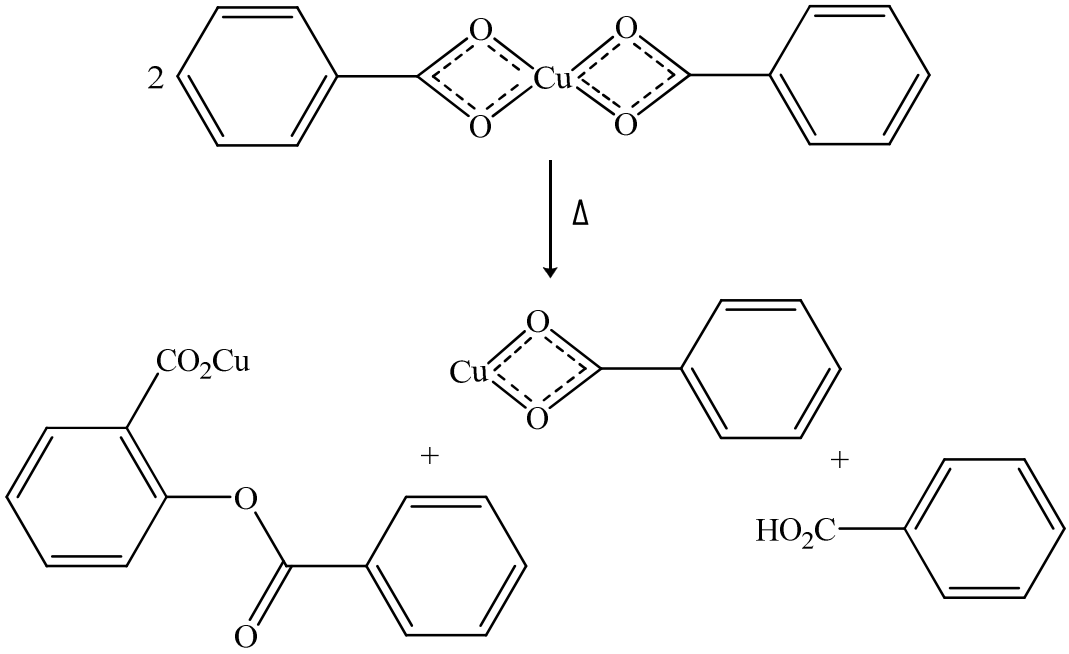

Scheme 2.24 An example of where Copper(II) salts of aromatic carboxylic acids can undergo an oxidative reaction.

When substituted benzoic acid is used in the reaction, the position of attack by the oxygen is always *ortho* to the carboxylic group.[73]

---

[69] W.G. Toland, *J. Am. Chem. Soc.*, **83**, 2507, (1961).
[70] W.W. Kaeding and G.R. Collins, *J. Org. Chem.*, **30**, 3750, (1965).
[71] W.W. Kaeding and A.T. Shulgin, *J. Org. Chem.*, **27**, 3551, (1962).
[72] O. Das, S. Paria and T.K. Paine, *Tetrahedron Lett.*, **49**, 5924, (2008).
[73] W.W. Kaeding, *J. Org. Chem.*, **26**, 3144, (1961).

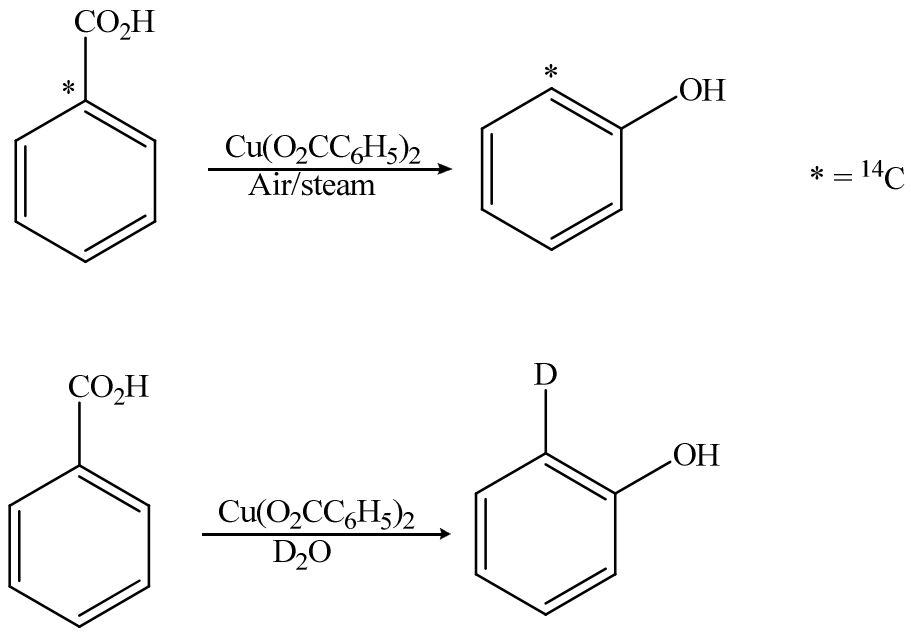

Scheme 2.25 Example of the ortho substitution on benzoic acid.

This behaviour suggests that an intermolecular cyclic mechanism is operative in this reaction.[74]

[74] W.W. Kaeding, H.O. Kerlinger and G.R. Collins, *J. Org. Chem.*, **30**, 3754, (1965).

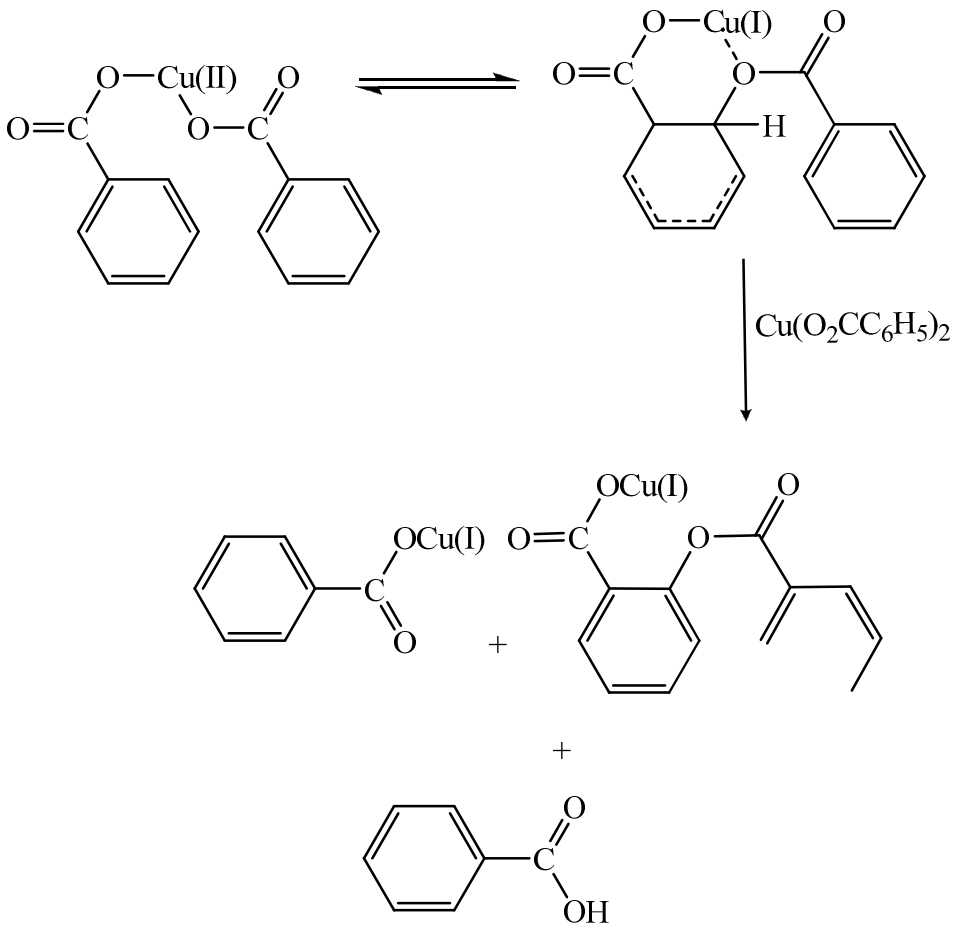

Scheme 2.26 Example of an intermolecular cyclic mechanism to produce benzoic acid.

The cyclic nature of this mechanism is supported by the observation that the basic cupric benzoate salt produces salicylic acid when heated in the aprotic solvent.[71,75] Since these basic salts decompose at lower temperatures than the corresponding normal salts, the former may very well be the active intermediate in Scheme 2.27.[71]

[75] P.K. Khanna, P. More, J. Jawalkar, Y. Patil and N.K. Rao, *J. Nanopart. Res.*, **11**, 793, (2009).

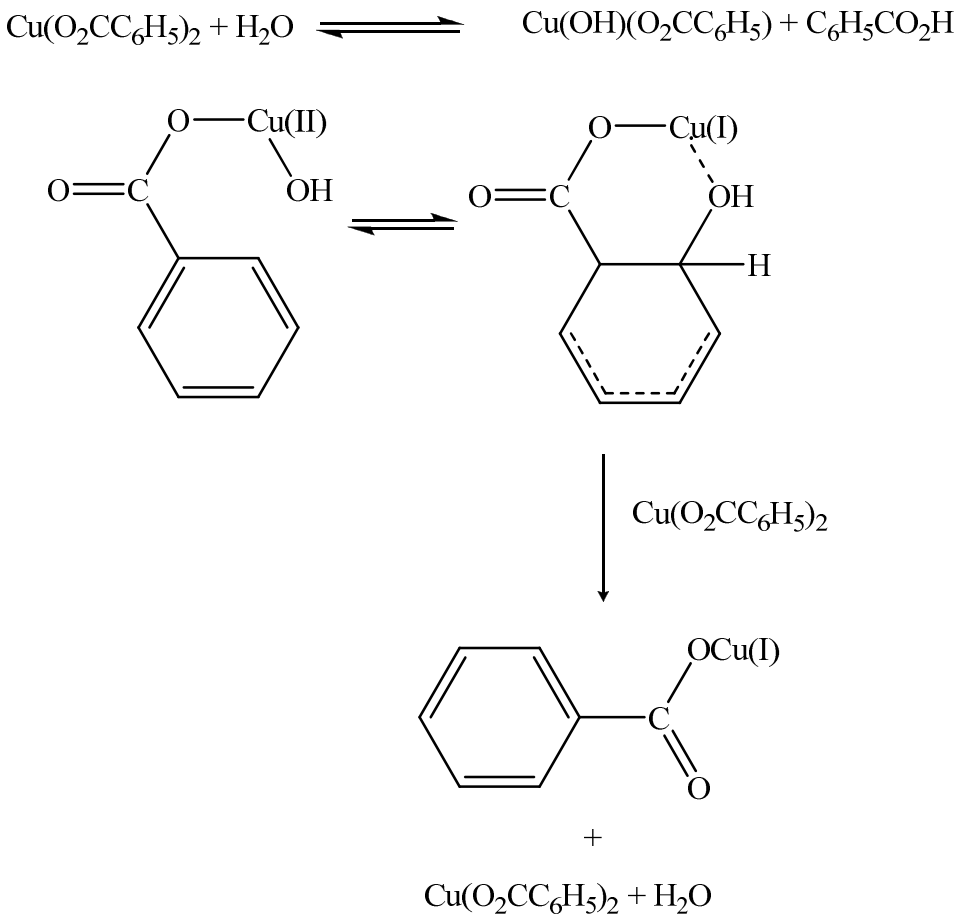

Scheme 2.27 Basic cupric benzoate salt produces salicylic acid when heated.

The use of two one-electron oxidations in this mechanism is based on the fact that copper(I) is the major inorganic species isolated in the reaction. Furthermore, in the absence of oxygen, the added metallic copper does not appear to dissolve in a solution of cupric benzoate in benzoic acid heated to 250 °C.[74] The free-radical nature of the reaction is supported by the competing intermolecular reaction of cupric benzoate with aprotic aromatic solvents. The product isolated and the isomer distribution suggests an attack by benzoyloxy radical.[74]

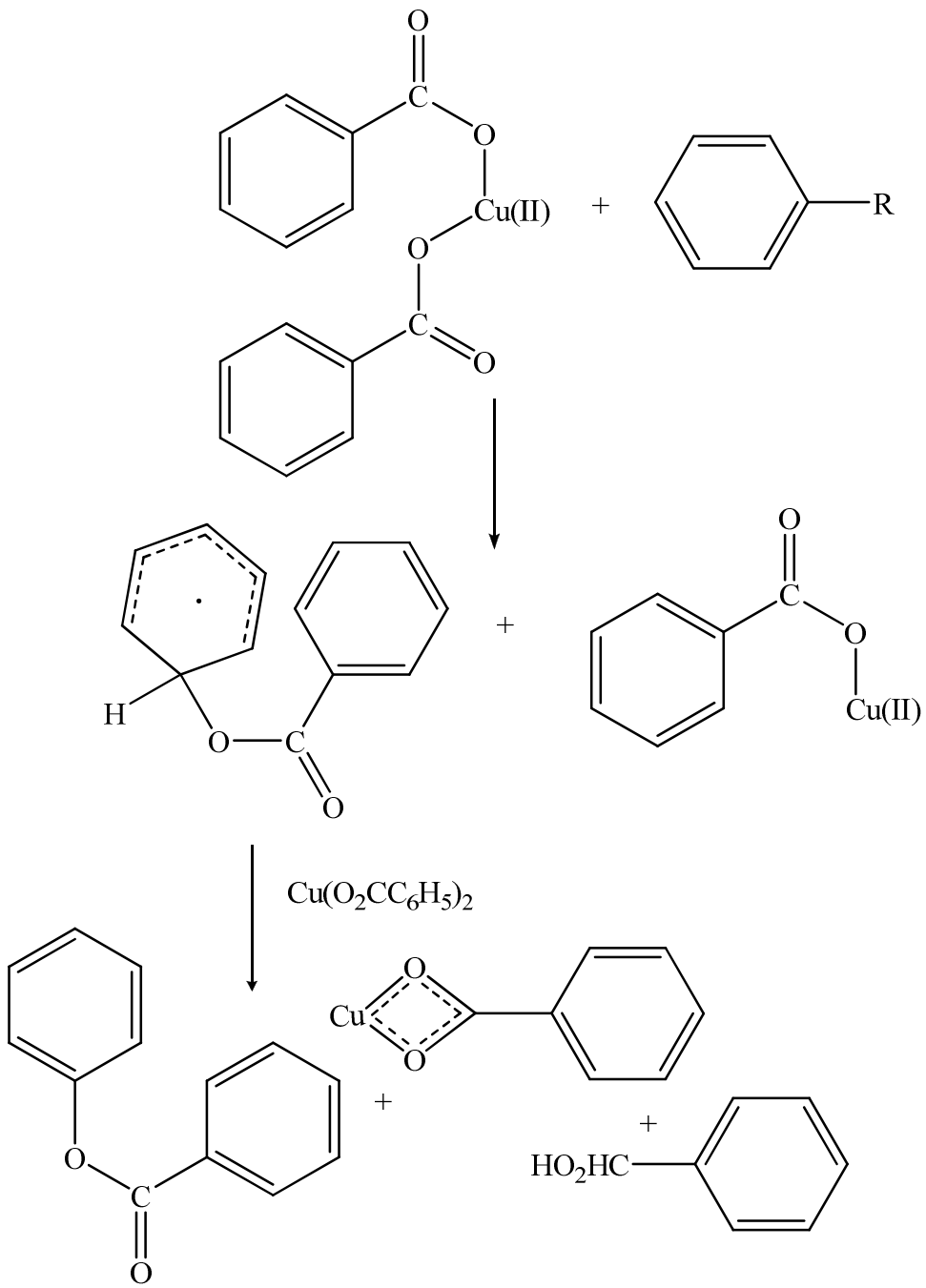

Scheme 2.28 An intermolecular reaction of cupric benzoate with aprotic aromatic solvents.

The course of the reaction is changed if protic solvents are used for the oxidative pyrolysis of copper(II) carboxylates. Under these conditions, the benzoylsalicylate salt is converted to salicylic acid which subsequently undergoes decarboxylation. For example, when benzoic acid is used as the solvent, the reaction product is phenylbenzoate.[76,75]

---

[76] W.W. Kaeding, *J. Org. Chem.*, **29**, 2556, (1964).

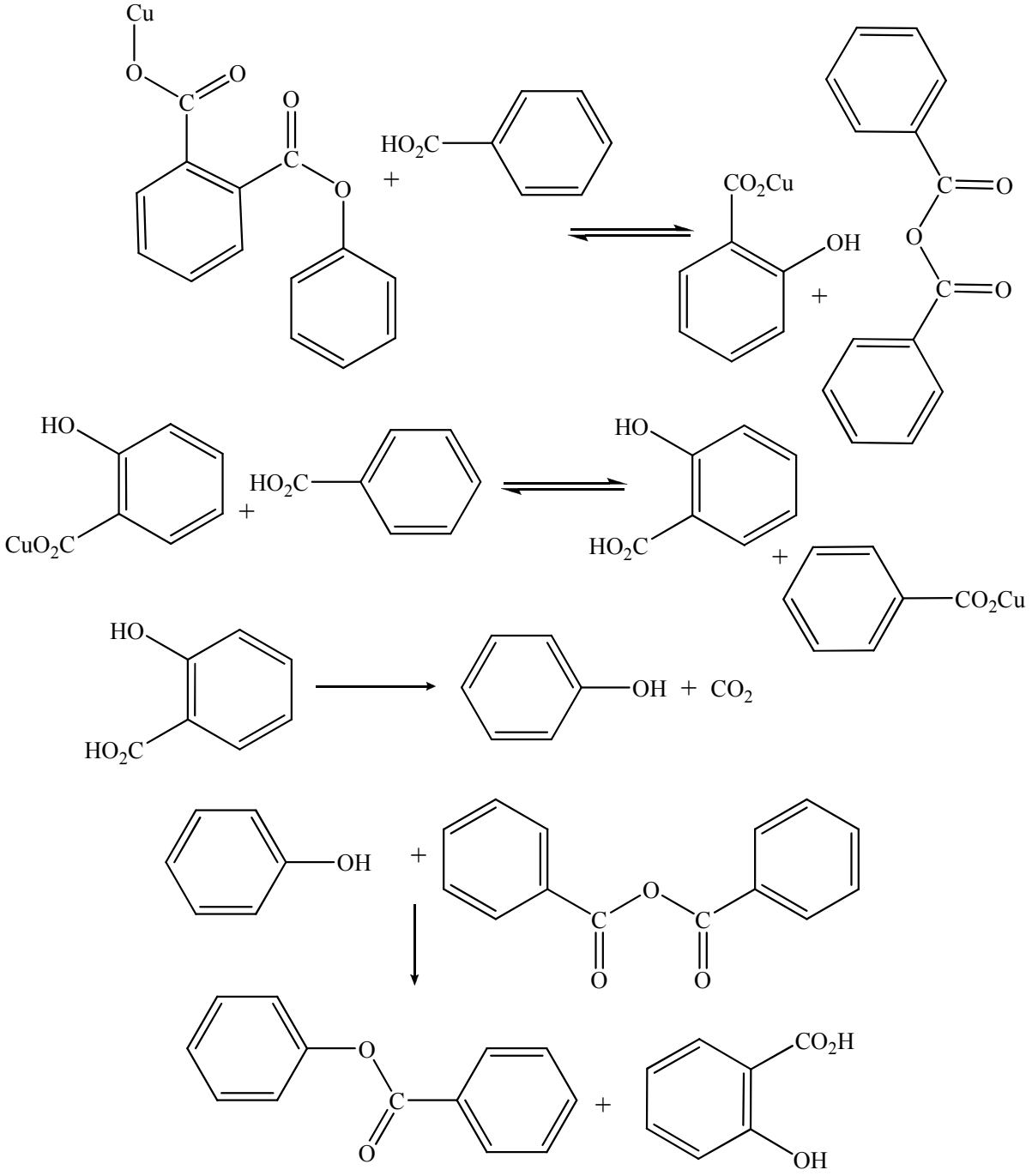

Scheme 2.29 Oxidative pyrolysis of copper(II) carboxylates.

If air is bubbled through the reaction mixtures, the copper(I) benzoate is reconverted to copper(II) benzoate and water. The water produced in this process, hydrolyzes the phenyl benzoate which liberates the phenol.

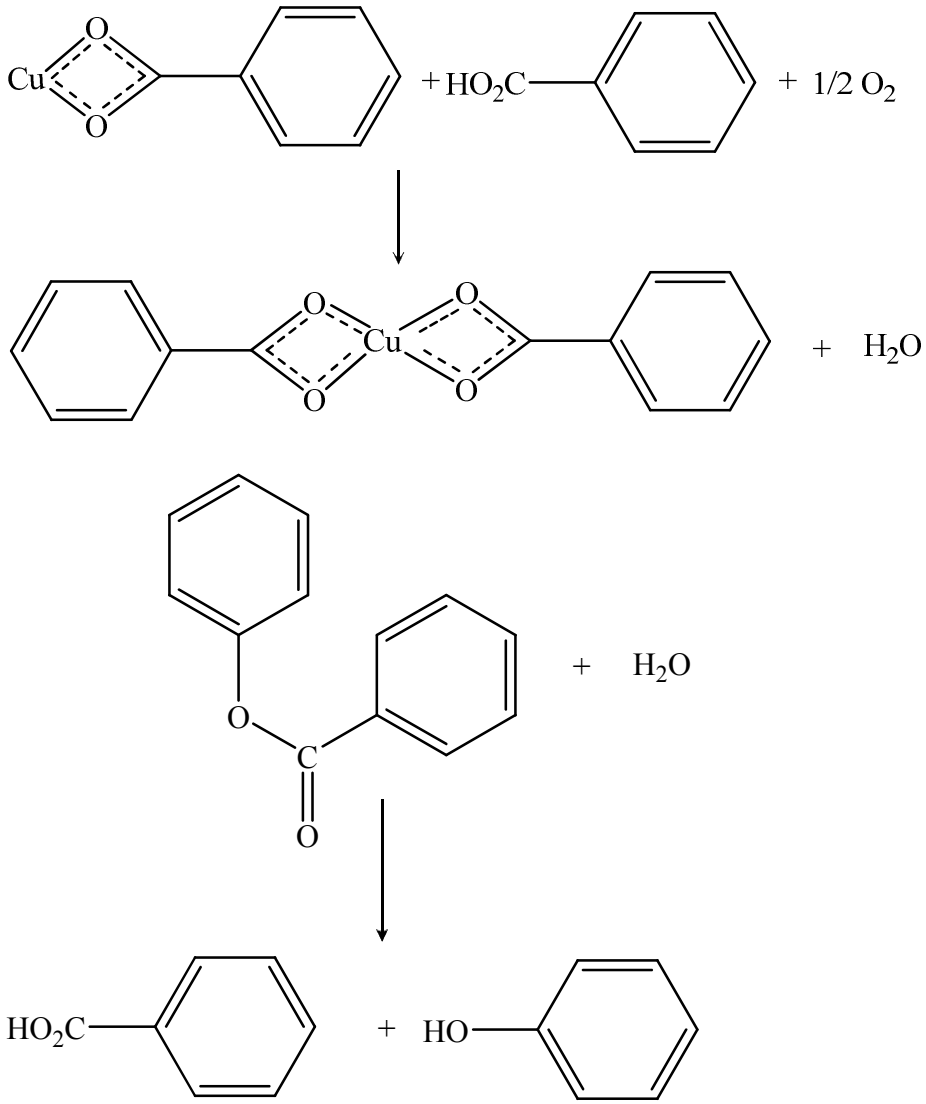

Scheme 2.30 Copper(I) benzoate is reconverted into copper(II) benzoate and water. The water hydrolyzes the phenyl benzoate, liberating the phenol.

The net result of this sequence is that benzoic acid is converted to phenol using only air, water, and a catalytic amount of copper(II). This reaction provides the basis for the Dow process and for the production of phenol from toluene via benzoic acid.

The necessity of preparing the cupric carboxylate salt separately may be avoided by the addition of either cupric carbonate or cupric oxide directly into the reaction mixture. The use of either cupric bromide or –chloride, however, should be avoided due to the possibility of competing nuclear halogenations.

The copper(II) salts of aliphatic carboxylic acids undergo simple decarboxylation and nonspecific oxidations. It would appear, however, that the cupric salts of substituted propiolic acids undergo oxidative decarboxylation to yield coupling products. For example, cupric 2-

chlorophenylpropiolate decomposes in refluxing pyridine to give bis(2-chlorophenyl)diacetylene and carbon dioxide.[77]

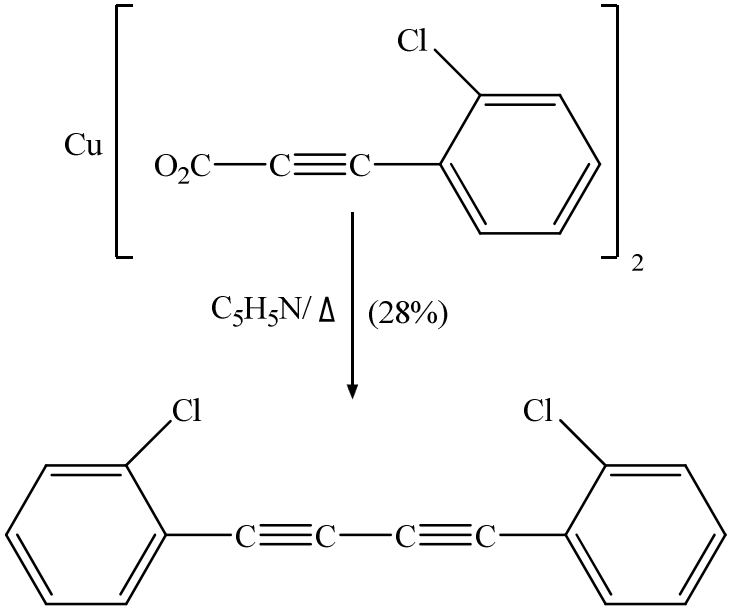

Scheme 2.31 Cupric 2-chlorophenylpropiolate decomposes in refluxing pyridine to give bis(2-chlorophenyl)diacetylene and carbon dioxide.

2.4.3 Factors Influencing Oxidation

While a consideration of the structure and relative stability of complexes involving cupric and cuprous ions is obviously quite useful in any discussion of the oxidation reaction of these ions, the more fundamental question concerns the actual mechanism of the oxidation step. By definition, the oxidation of an organic molecule by copper(II) must involve the net transfer of electrons from the substrate to the metal ion. In theory, this could be accomplished by the simultaneous transfer of two electrons with the resulting formation of metallic copper. Although the energy and probability factors involved in this type of processes are very large, they may not be altogether prohibitive. Indeed, this mechanism has been suggested for the oxidation of mercury(I) by thallium(III).[78,79]

At present, however, there is little evidence that this is anything other than a very rare oxidative pathway. The same net result can be achieved by the transfer of an atom or group, either with or without a pair of its valence electrons. The only known example (involving

[77] G.E. Coates, *J. Chem. Soc.*, London 838, (1946).
[78] A.M. Armstrong and J. Halpern, *Can. J. Chem.*, **35**, 1020, (1957).
[79] J. Halpern, *Can. J. Chem.*, **37**, 148, (1959).

cupric ions) of a two electron oxidation by ligand transfer appears to be the homogeneous reduction of copper(II) by hydrogen.[80,81,82,83]

A second possible oxidation mechanism might involve consecutive one electron transfers, again to produce metallic copper. However, copper(I) is generally obtained as the major inorganic product of the copper(II) oxidation of organic molecules. Although metallic copper is occasionally observed as a product in these reactions, it seems most likely that it is a result of the observation that copper(I) is a reasonably good reducing agent but gives little indication of functioning as an oxidant. Therefore, the available evidence suggests that cupric ion oxidations generally proceed by the one electron transfer mechanism.

The removal of a single electron from an organic molecule must result in the formation of a free-radical intermediate. In the case of copper(II) it would appear that the initial oxidation step is usually preceded by the removal of an acidic hydrogen from the organic substrate. The anion which is formed, is electro-statically attracted to the metal ion, thereby reducing the energy of the electron transfer step. Under suitable conditions the free-radical intermediate might be expected to dimerise rather than undergo further oxidation. Confirmation of this mechanism is found in the oxidative dimerisations of terminal alkynes, aromatic amines, and mercaptans. In these dimerisations the intermediate free radicals are unusually resistant to further oxidation. In the vast majority of cases, however, free radicals are found to react quite rapidly with paramagnetic copper(II). These subsequent oxidations are known to proceed by both electron and ligand transfer.[84, 85, 86]

Electron transfer oxidation occurs mainly with the oxy salts of copper(II), whereas ligand transfer oxidation predominates with the halide and *pseudo* halide salts. As expected, the singlet state of dimeric copper(II) is unreactive in electron transfer reactions. However, it has also been demonstrated that the triplet of the dimer is mostly inactive.[87] Therefore, only paramagnetic, monomeric copper(II) species function as electron transfer oxidizing agents for

---

[80] M. Calvin, *J. Am. Chem. Soc.*, **61**, 2230, (1939).
[81] M. Calvin and W.K. Wilmarth, *J. Am. Chem. Soc.*, **78**, 1301, (1956).
[82] W.K. Wilmarth and M.K. Barsh, *J. Am. Chem. Soc.*, **78**, 1305, (1956).
[83] W.K. Wilmarth and M.K. Barsh, *J. Am. Chem. Soc.*, **75**, 2237, (1953).
[84] J.K. Kochi, *J. Am. Chem. Soc.*, **84**, 774, (1962).
[85] J.K. Kochi, *J. Am. Chem. Soc.*, **84**, 1572, (1962).
[86] J.K. Kochi, *J. Am. Chem. Soc.*, **84**, 2785, (1962).
[87] J.K. Kochi and R.V. Subramanian, *J. Am. Chem. Soc.*, **87**, 4855, (1965).

alkyl radicals. Since electron transfer reactions involve only electronic motion, the second order rate constant for these process generally approach the diffusion-controlled limits.[87] Extensive coordination of the metal ion, however, significantly decreases its capacity to function as an electron transfer oxidant. The presence of electron withdrawing groups within the free radical also reduces the rate of electron transfer. For example, the 2-cyano-2-propyl radical is inert to oxidation by electron transfer, but is readily oxidized by ligand transfer.[88] The Sandmeyer and Meervein reactions are classic examples of ligand transfer oxidations.[89,90,91] In both cases of these reactions, free radicals of cupric ion are produced as intermediates in the copper(I)-catalyzed decomposition of diazonium salt.

2.4.3.1 Ligand Parameters

Providing that the steric requirements are not prohibitive, a ligand that possesses two or more donor groups may chelate to a single metal ion. Chelation generally results in a dramatic increase in the stability of the complex. For example, the bidentate ligand ethylenediamine forms a chelate with cupric ion, which is nearly a billion times more stable than the corresponding ammonia (monodentate) complex.[92]

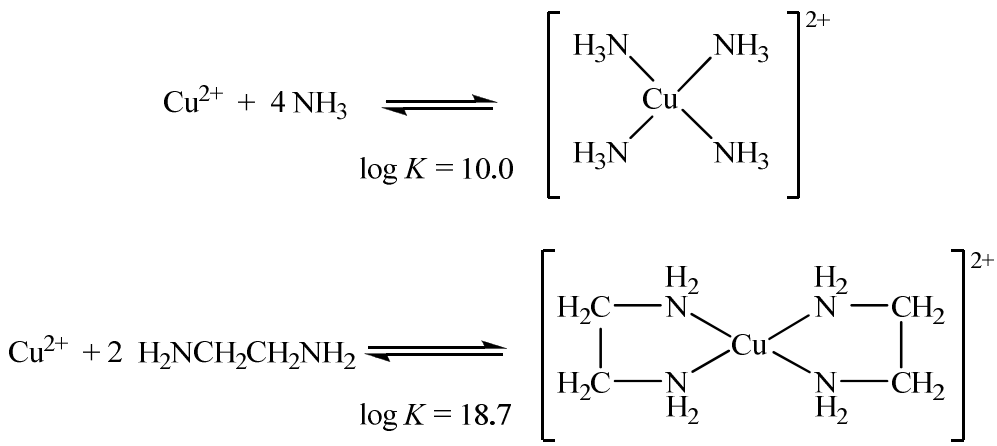

Scheme 2.32 Bidentate ligand ethylenediamine forms a chelate with cupric ion, which is usually more stable than the corresponding ammonia (monodentate) complex.

---

[88] J.K. Kochi and D.M. Mog, *J. Am. Chem. Soc.*, **87**, 522, (1965).
[89] W.A. Cowdrey and D.S. Davies, *J. Chem. Soc.*, London , 49, (1949).
[90] J.K. Kochi, *J. Am. Chem. Soc.*, **77**, 5090, (1955).
[91] J.K. Kochi, *J. Am. Chem. Soc.*, **78**, 1228, (1956).
[92] L.G. Sillen and A.E. Martell, *Chem. Soc., Spec.*, 17, (1964).

If the chelating agent is tri- or tetradentate, two or three interlocking rings may be formed, resulting in an even greater degree of stabilisation.[93]

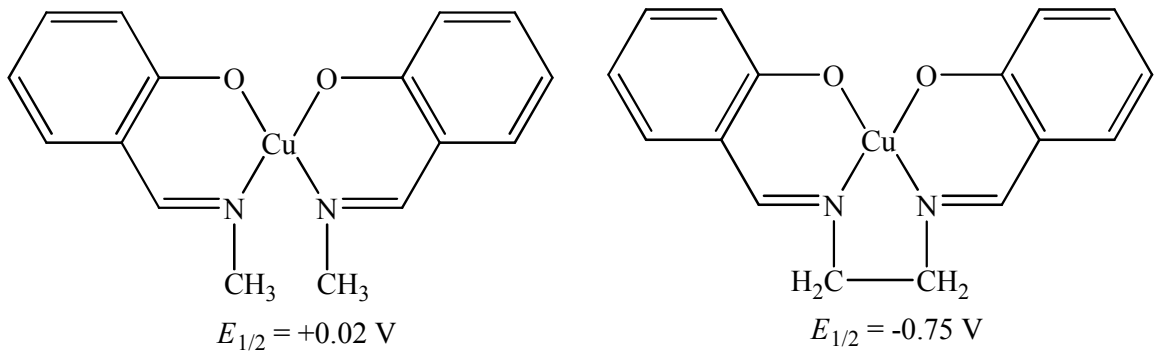

Scheme 2.33 Tri- or tetradentate chelating agents forming two or three interlocking rings.

In contrast to the behaviour of copper(II), the ethylenediamine complex of copper(I) does not exhibit any appreciable stabilisation relative to the ammonia (monodentate) complex.[94]

$$Cu^{+} + 2NH_3 \longleftrightarrow [Cu(NH_3)_2]^{+}$$
$$\log K = 10.6$$

$$Cu^{+} + 2\,H_2NCH_2CH_2NH_2 \longleftrightarrow [Cu(H_2NCH_2CH_2NH_2)_2]^{+}$$
$$\log K = 11.4$$

Scheme 2.34 Copper(I) does not exhibit any appreciable stabilisation between bidentate and monodentate.

This is a result of the formation of only a single coordinate bond between the diamine and the cuprous ion. The preferential stabilisation of copper(II) by ethylenediamine explains the unusual oxidation potentials as well as the unexpected disproportionation of cuprous chloride in the presence of ethylenediamine. In the absence of chelation effects, a ligand which possesses an amine donor group usually stabilises the cuprous state to such a degree that metallic copper is oxidized by cupric ion.

---

[93] M. Calvin and R.H. Bailes, *J. Am. Chem. Soc.*, **68**, 949, (1946).
[94] B.R. James and R.J.P. Williams, *J. Chem. Soc.*, London, 2007, (1961).

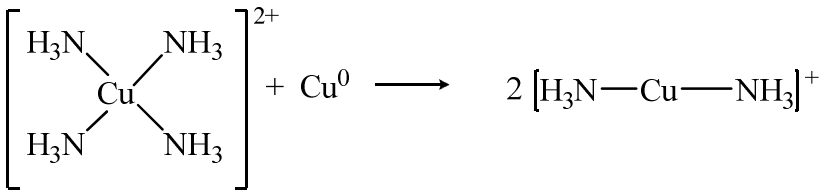

$$2\,CuCl + 2\,H_2NCH_2CH_2NH_2 \longrightarrow [Cu(EDA)_2]^{2+} + 2\,Cl^- + Cu^0$$

Scheme 2.35 An amine donor group usually stabilises the cuprous state to such a degree that a metallic copper is oxidized by cupric ion.

The most stable chelates, which can be formed with saturated bidentate ligands, such as the diamines, involve five-membered rings. Six-, seven-, eight-, and nine-membered chelate rings can be formed with copper(II). The stability of the chelate however decreases sharply with an increasing in ring size. If the chelate ring possesses two double bonds, it is the six-membered ring which is usually the more stable. Stable four-membered chelate rings can be formed between metal ions and bidentate ligands such as acetate, carbonate, and sulphate ions. In the case of copper(II), however, carbonate and carboxylate anions function as bridging units between two metal ions to form dimeric complexes. The dimeric structure of cupric acetate remains intact when dissolved in aprotic solvents or glacial acetic acid.[95,96,97] In the presence of water, acetate ion, or nitrogen-containing ligands the dimer dissociates. When pyridine is used as the solvent, cupric acetate is predominantly monomeric.[98] Although the chloroacetate salt of copper(II) is dimeric, even in an aqueous solution, cupric trichloroacetate is monomeric. The dichloroacetate salt is intermediate in its behaviour.

In addition to the entropy effect, chelate compounds may achieve additional stabilisation by means of a benzenoid resonance with certain types of ligands.[99]

---

[95] B.N. Figgs and R.L. Martin, *J. Chem. Soc.*, London, 3837, (1953).
[96] M. Kato, H.B. Jonassen and J.C. Fanning, *Chem. Rev.*, **64**, 99, (1964).
[97] J.K. Kochi and R.V. Subramanian, *Inorg. Chem.*, **4**, 1527, (1965).
[98] M. Kondo and M. Kubo, *J. Phys. Chem.*, **62**, 468, (1958).
[99] M. Calvin and K.W. Wilson, *J. Phys. Chem.*, **67**, 2003, (1945).

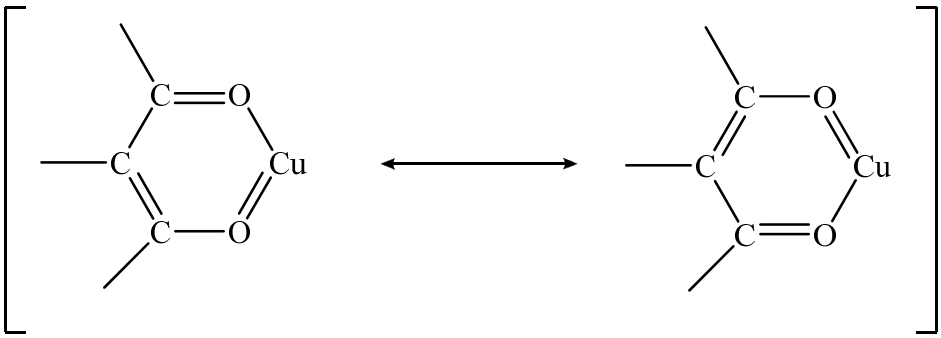

Scheme 2.36 Benzenoid resonance of the double bond causing additional stabilisation.

The stability of the copper(II) chelates thus decrease in the order acetylacetone, 2-hydroxyl-1-naphthaldehyde, salicylaldehyde, 2-hydroxy-3-naphthaldehyde, which is also the order of the decrease in double-bond character within the chelate ring. Similar resonance stabilisation is probably responsible, in part, for the extreme stability of copper(II) phthalocyanine.

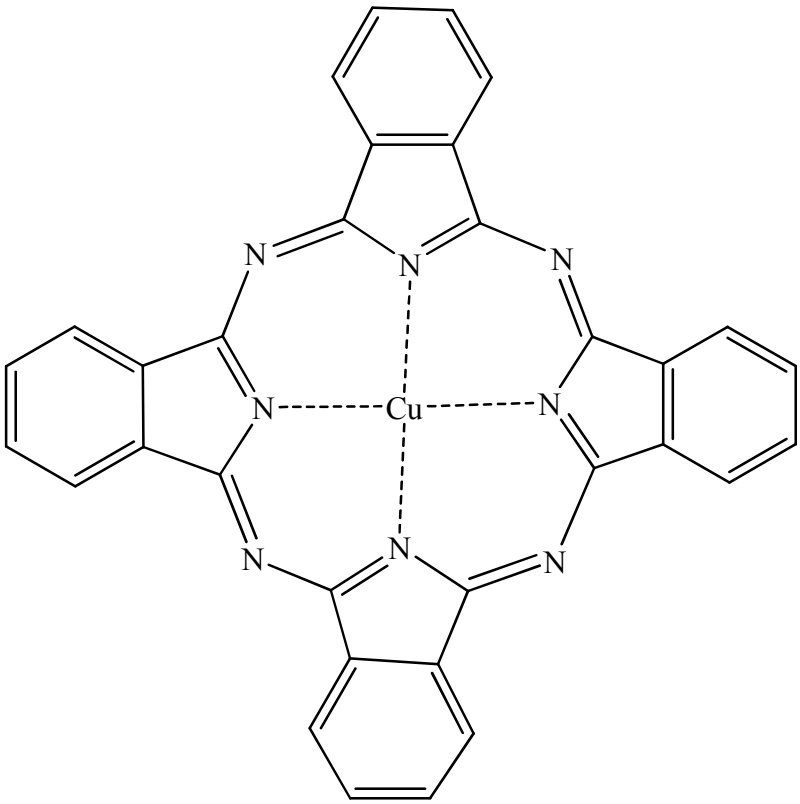

Figure 2.1 Example of a unsubstituted Copper(II) phthalocyanine which is stabilised by resonating double bonds.

This blue-green solid can be heated to 900 ^{o}C in a vacuum without suffering decomposition.[100] The formation of π-bonds between metal ions and their ligands has been postulated with a number of ligands e.g. carbon monoxide and cyanide ion.

A substitutional change on a ligand will have both an electrostatic and a steric effect on the stability of its complexes with metal ions.

a. The Electronic Parameter

Substituents which tend to decrease the electron density at the donor atom will decrease the basicity of the ligand and hence decrease the stability of its coordination compounds. This effect will be the same whether the ligand is mono- or polydentate.

b. The Steric Parameter

As a result of the rigid structural requirements of chelate compounds, substitution within polydentate ligands may produce very large steric effects. A particularly dramatic example is observed in the case of the biquinoline chelates of copper. In the copper(II) chelate the hydrogen atoms in the 8 and 8' positions of the ligand overlap with the corresponding hydrogen atoms on the second ligand owing to the favoured square-planer bond orientation of this valence state. On the other hand, copper(I) forms a very stable complex with biquinoline since steric hindrance is minimised in the tetrahedral structure of this complex. Therefore, there is a strong driving force for the conversion of the copper(II) complex to the corresponding copper(I) complex as demonstrated by the large oxidation potential.

2.5 Metal-Catalyzed Oxidations

2.5.1 Introduction

The oxidation of organic compounds by molecular oxygen has a long history stemming as it does from Lavoisier`s explanation of combustion, which also marked the beginning of the modern era of chemistry. Observations made in the nineteenth century linked the deterioration of many organic materials, such as rubber and natural oils and fats, to the absorption of dioxygen. Early investigators were mainly concerned with the inhibition of such oxidative degradations.

---

[100] E.A. Lawton, *J. Phys. Chem.*, **62**, 384, (1958).

Around the turn of the century, it was recognised that these oxidative processes involved the formation of organic peroxides. Subsequent mechanistic studies of the interaction of simple hydrocarbons with dioxygen, carried out in the 1940`s, provided the basic concepts for the development of the free radical chain theory of autoxidation.[101,102] Although autoxidation can be spontaneously initiated, it is more commonly prompted by metal species, often in trace quantities.

The control of autoxidation is desirable not only from the point of inhibiting the oxidative deterioration of plastics, gasoline, lubricating oils and rubber, but also for promoting the selective oxidation of petroleum hydrocarbon feedstock to a variety of industrial organic chemicals. Although autoxidation of organic compounds are generally highly exothermic reactions, they do not readily undergo spontaneous combustion in air, largely owing to the relatively high activation energies for the initiation process. In other words, aerial oxidation is usually difficult to initiate, but once underway, they are often difficult to interrupt short of the most thermodynamically stable products, namely carbon dioxide and water.

Catalysis by metal complexes plays an important role in the control of selective, partial oxidation of alkanes, olefins, and aromatic hydrocarbons to useful products.[103] If we are in the age of petroleum today, with 90% of organic chemicals derived from this raw material, it is also the age of catalysis.[104,105] Indeed, the majority of petrochemical processes are catalytic, the most important ones being catalytic oxidations.[106,107,108] The first observation of a catalytic oxidation can probably be attributed to Davy,[109] who showed in 1820 that ethanol is oxidized to acetic acid in the presence of platinum (Eq 2.8).

$$CH_2CH_2OH + O_2 \xrightarrow{[Pt]} CH_3CO_2H + H_2O \qquad \text{...Eq 2.8}$$

---

[101] J.L. Bolland, *Q. Rev. Chem. Soc.*, **3**, 1, (1949).
[102] L. Bateman, *Q. Rev. Chem. Soc.*, **8**, 147, (1954).

[103] K. Rakottyay and A. Kazonyi, *Appl. Catal.*, **A367**, 32, (2009).
[104] H.M. Stanley, *Chem. Ind.*, London, 681, (1949).
[105] J.D. Idol, *Chem. Ind.*, London, 272, (1979).
[106] M. Sitting, *Combine Hydrocarbons and Oxygen for profit*, Chem. Process Rev. No. 11. Noyes Dev. Co., Park Ridge, New Jersey, (1968).
[107] T. Dumas and W. Bulani, *Oxidation of Petrochemicals: Chemistry and Technology*. Appl. Sci. Publ., London, (1974).
[108] D.J. Hucknall, *Selective Oxidation of Hydrocarbons*. Academic Press, New York, (1974).
[109] E. Davy, *Philos. Trans. R. Soc.*, London, 108 (1820).

Although there were some industrial processes, such as the silver-catalyzed oxidation of ethylene to ethylene oxide, discovered in 1933, the field of metal-catalyzed oxidation assumed importance only in the 1940's; that is it coincided with the development of the theory of the free radical in the autoxidation. The following observation, made in 1945 by Sir Eric Rideal in his introductory remarks to the Faraday Society meeting; devoted to the subject of oxidation,[110] is indicative of the state of the art only 62 years ago.

Several important industrial processes were developed for the selective partial oxidation of hydrocarbons feedstock during the 1940's and 1950's. Initially, the majority of these processes involved vapour-phase oxidations over heterogeneous catalysts. The serious study and application of homogeneous catalysis of liquid-phase oxidation originates from the late 1950s. For example, the Mid-Century process, aptly named, for the production of terephthalic acid and the Wacker process for acetaldehyde, was both first reported in 1959.

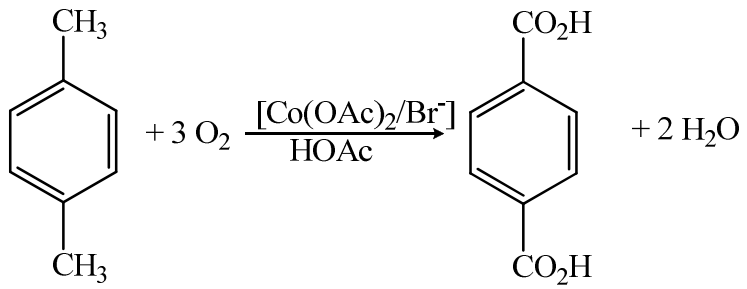

Scheme 2.37 Production of terephthalic acid.

$$2\ H_2C{=}CH_2 + O_2 \xrightarrow[H_2O]{[PdCl_2/CuCl_2]} 2\ CH_3CHO$$

Scheme 2.38 The Wacker process.

The Celanese process for the liquid-phase oxidation of *n*-butane to acetic acid was also developed in the 1950`s and is still in use today. In the last couple of decades, an efficient liquid-phase process for the epoxidation of olefins (such as propylene), which can`t be carried out with silver, has been developed in the following two steps.

[110] E. Rideal, *Trans. Faraday Soc*., **42**, 100, (1946).

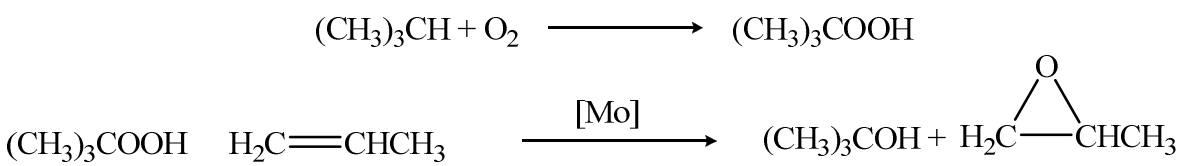

Scheme 2.39 Example of where the Celanese processes is used for epoxidation of olefins.

A variety of metal catalysed oxidations has also been developed for selective oxidations that can be carried out in laboratory-scale synthesis. The importance of metal catalysts is illustrated in the following transformations of olefins and acetylenes with *tert*-butyl hydroperoxide.[111]

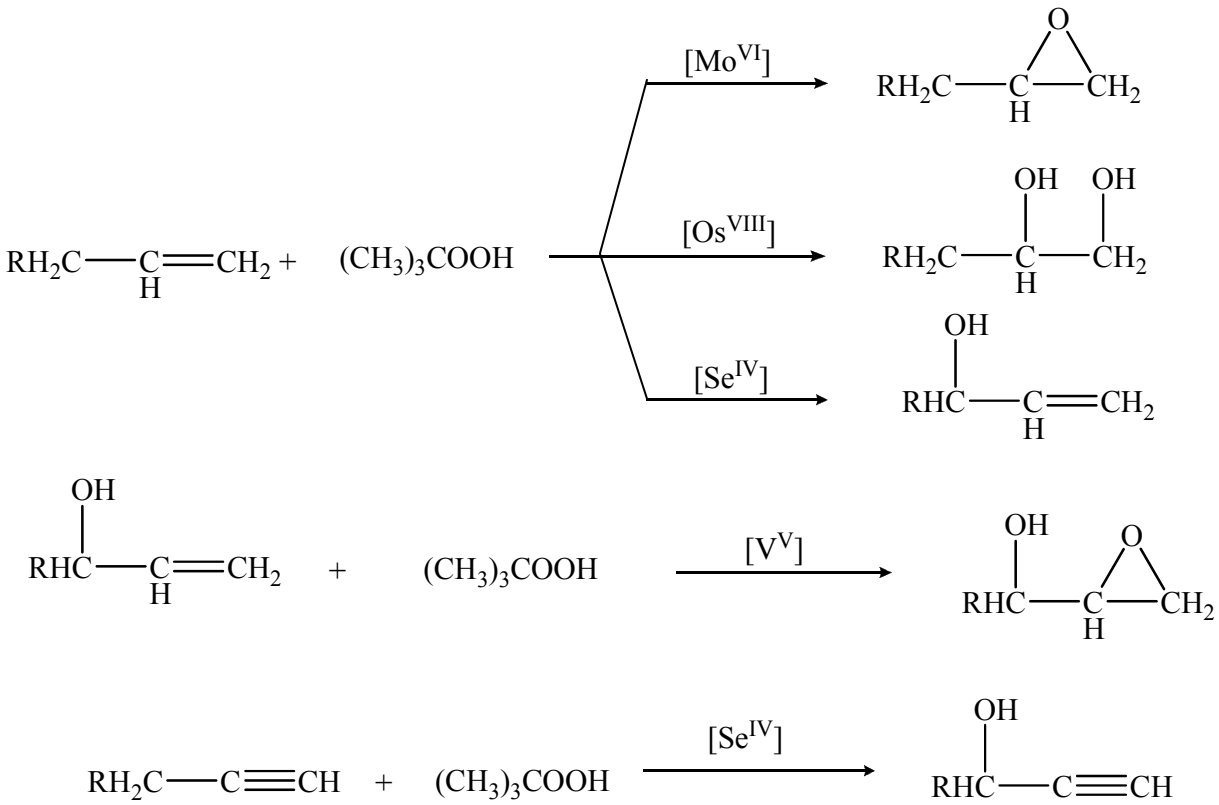

Scheme 2.40 Transformations of olefins and acetylenes with *tert*-butyl hydroperoxide.

The application of the Wacker oxidation in Eq 2.9 to a variety of higher terminal olefins affords methyl ketones selectively.

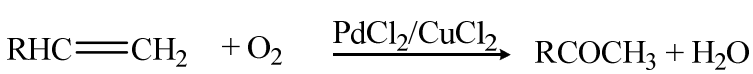

...Eq 2.9

[111] K.B. Sharpless and T.R. Verhoeven, *Aldrichimica Acta.,* **12**, 63, (1979).

Catalytic oxidation can be effectively employed in the synthesis of a variety of natural products.[112]

2.5.2 Mechanistic Principles of Metal-Catalyzed Oxidation

Metal–catalyzed oxidations may be conveniently divided into two types, which are arbitrarily designate as homolytic and heterolytic. The first type of catalysis usually involves soluble transition metal salts (homogeneous), such as the acetates or naphthenates of Co, Mn, Fe, Cu, etc., or the metal oxides (heterogeneous). Furthermore, homolytic catalysis necessitates the recycling of the metal species between several oxidation states by one-equivalent changes. Free radicals are formed as intermediates from the organic substrate. Heterolytic catalysis involves reactions of organic substrates which are coordinated to transition metals. It is characterised by the metal complex acting as a Lewis acid or formally undergoing two-equivalent changes. Free radicals are not intermediates. For example, consider the acyloxylation of benzene by trifluoroacetate (Scheme 2.41), which leads to the concomitant reduction of Pb(IV) to Pb(II). The same transformation can be effected by cobalt tristrifluoroacetate, which corresponds to a two-electron oxidation.[113] This oxidative substitution may be effected by lead tetrakistrifluoroacetate, leading to the concomitant reduction of 2 Co(III) to 2 Co(II).

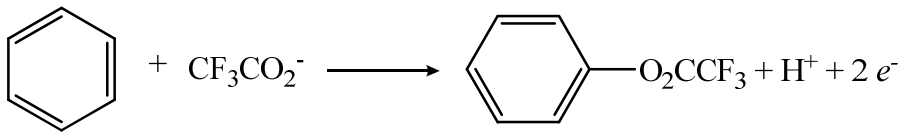

Scheme 2.41 Acyloxylation of benzene by trifluoroacetate.

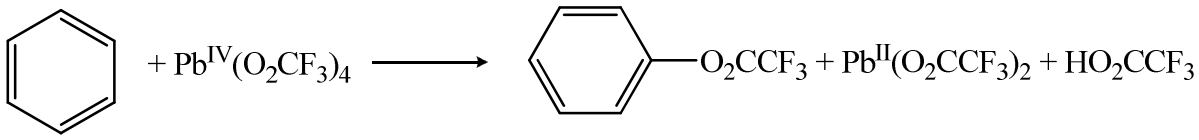

Scheme 2.42 Oxidative substitution by lead tetrakistrifluoroacetate.

---

[112] J. Tsuji, *Pure Appl. Chem.*, **51**, 1235, (1979).
[113] R.A. Sheldon and J.K. Kochi, *Adv. Catal.*, **25**, 272, (1976).

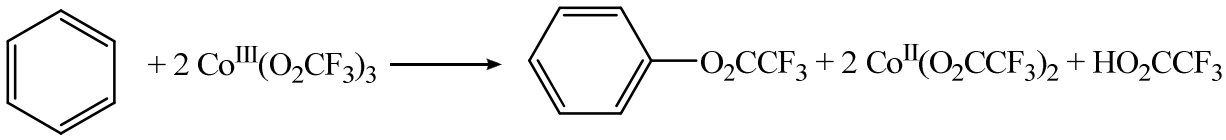

Scheme 2.43 Oxidative substitution cobalt tristrifluoroacetate.

It can be shown that the oxidative substitution promoted by Pb(IV) proceeds via the heterolytic process in Scheme 2.44.

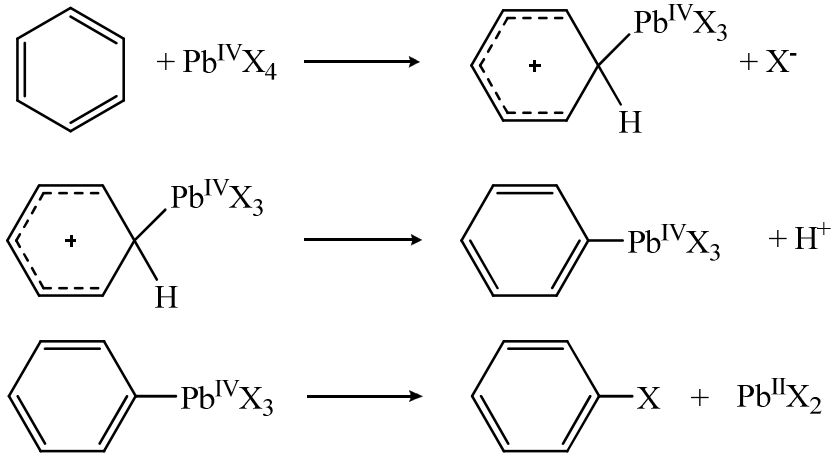

Scheme 2.44 Oxidative substitution promoted by Pb(IV) proceeds via the heterolytic process.

According to this mechanism, an electrophilic attack by Pb(IV) is rate-limiting and is followed by reductive elimination of Pb(II). On the other hand, the oxidative substitution of benzene promoted by Co(III) proceeds via a homolytic mechanism in Scheme 2.45.[114]

[114] J.K. Kochi, R.T. Tang and T. Bernath, *J. Am. Chem. Soc.*, **95**, 7114, (1973).

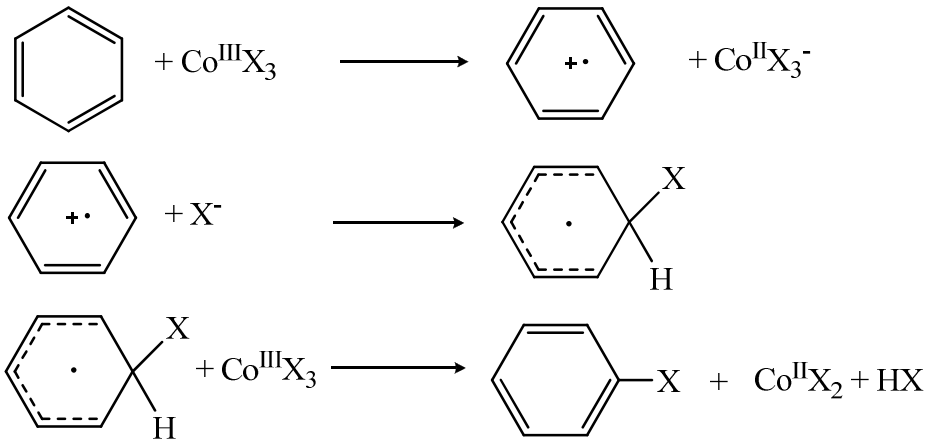

Scheme 2.45 The oxidative substitution of benzene promoted by Co(III) proceeds via a homolytic mechanism.

Electron transfer is rate-limiting, and all the subsequent reactions are fast. The successive one-electron transfer corresponds to the formation of benzene cation-radicals and the destruction of cyclohexadienyl radicals, respectively.

Catalytic processes may also be devised which correspond to the recycling of the metal species by heterolytic and homolytic mechanisms. These two types of catalytic processes will be treated separately in the ensuing discussion, although the distinction is not always clear since there are transition metal complexes that are capable of participating in both types of catalysis. Homolytic catalysis and heterolytic catalysis also fall into the categories that have been described as “hard” and “soft” processes, respectively.[115]

Historically, the homolytic type of catalysis has been known and studied for a long time. The heterolytic catalysts represent a relatively recent innovation, but nevertheless includes such important developments as the Wacker process for the oxidation of olefins. Regardless of the mechanism involved, the most important characteristics of metal catalysts for effecting oxidation are the accessibility of several oxidation states, as well as the accommodation of various coordination numbers, both of which are properties of transition metal complexes.

Homolytic processes are intimately involved in classical autoxidation processes which are catalysed by cobalt, manganese, iron and copper complexes, as in the commercially important conversion of *p*-xylene to terephtalic acid. Heterolytic processes include the industrial epoxidation of olefins with alkyl hydroperoxides in the presence of molybdenum, vanadium, tungsten and titanium catalysts.

---

[115] R. Ugo, *Chim. Ind.*, Milan **51**, 1319, (1969).

The activation of dioxygen by transition metal complexes includes the reactions of the various types of peroxometal complexes, involving both homolytic and heterolytic processes. The considerable effort devoted to this subject in the last couple of decades has been spurred by the hope that the activation of dioxygen by transition metal complexes would lead to selective oxidations of hydrocarbons under mild conditions.[116,117] The results of this research have been generally disappointing, except for the demonstration[118] that terminal olefins can be selectively oxidized to methyl ketones in the presence of rhodium complexes:

$$2\ RHC{=}CH_2 + O_2 \xrightarrow{[Rh]} 2\ RCOCH_3 \qquad \text{...Eq 2.10}$$

2.5.3 Homogeneous and Heterogeneous Catalysis

Catalytic reactions play an important role in the industrial production of liquid fuels and bulk chemicals. Many organic chemicals, which are produced in bulk quantities, are derived from natural gas or petroleum, usually by converting these hydrocarbons into olefins. A catalyst is defined as: "A substrate that increases the rate of a chemical reaction without itself undergoing any permanent chemical change".[119] By definition, a catalyst works by lowering the activation energy of the chemical reaction because it provides an alternative pathway by which the reaction can proceed. It increases the rate at which a reaction comes to equilibrium, without altering the position of the equilibrium. Although a catalyst takes part in the reaction, formally it does not experience any permanent chemical change and therefore should be recovered chemically unchanged at the end of the reaction. It can however be physically changed, e.g. converted to a powder.

Homogeneous and heterogeneous catalysis in the liquid and vapour-phase processes can be considered on the basis of common mechanistic principles. Although these two areas of catalysis have tended to develop independently in the past, it has become increasingly evident in recent years that the fundamental chemical steps are essentially the same, whether the oxidation occurs in the coordination sphere of a soluble metal complex or on the absorbed metal-containing surface.

---

[116] J. Lyons, *Fundamental Research in Homogeneous Catalysis*, Vol. 3, (M. Tsutsui and R. Ugo, eds.), Plenum, New York, (1977).
[117] J. Lyons, *Aspects Homogeneous Catal.*, **3**, 1, (1977).
[118] H. Mimoun, M.M Perez Machirant and I. Sèrèe de Roch, *J. Am. Chem. Soc.*, **100**, 5437, (1978).
[119] Oxford University Press, *Dictionary of Science*, London: Market House Books Ltd., (1999).

Heterogeneous catalysts, where the catalyst exists in a different phase from the reacting species e.g. a solid catalyst in contact with a gaseous or liquid solution of reactants,[119] are practically advantageous from an industrial point of view because the products can be easily separated from the excess reactants and from the catalyst.[120] Homogeneous catalysts, where the catalyst is in the same phase as the reacting species, have been of great interest to industry because of higher selectivity in reactions, operating under milder conditions of temperature and pressure to name just a few advantages. A comparison of homogeneous and heterogeneous catalysis is listed in Table 2.1.

Table 2.1 Advantages and disadvantages of homogeneous and heterogeneous catalysis.[121]

	Homogeneous	Heterogeneous
Efficiency of catalyst use	All metal centres active	Only surface site active
Experimental conditions	Generally mild	Often high temperatures and/or high pressure
Separation of catalyst from product	Difficult	Generally easy
Catalyst recovery	Difficult	Easy
Establishment of reaction mechanism	Kinetic studies and rate laws usually informative	Often difficult

2.6 Oxidation of 3,5-di-*tert*-butylcatechol

2.6.1 Introduction

The oxidation of organic substrates with molecular oxygen under mild conditions is of great interest for industrial and synthetic processes, both from an economical and environmental point of view. The synthesis and investigation of functional model complexes for

[120] F.A. Cotton, G. Wilkinson, *Advanced Inorganic Chemistry*, 4th Ed., London: John Wiley & Sons, Inc., (1980).
[121] M.L. Tobe and J. Burgess, *Inorganic Reaction Mechanisms*, England: Addison Wesley Longman Ltd., (1999).

metalloenzymes with catechol oxygenase or catechol oxidase activity is therefore of great promise for the development of new and efficient catalysts for oxidation reactions.[122] Most functional mimics of catechol oxidase are mono- or dinuclear Cu(II) complexes.[123,124]

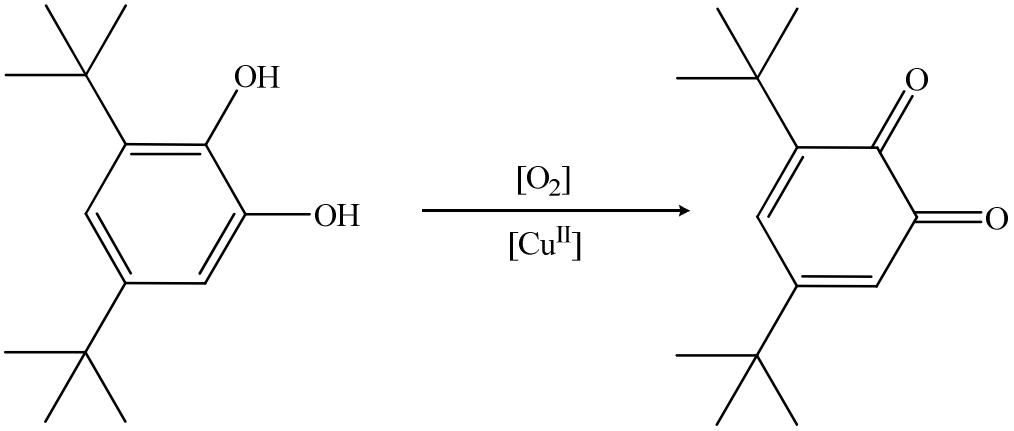

Scheme 2.46 The oxidation of 3,5-di-*tert*-butylcatechol to 3,5-di-*tert*-1,2-benzoquinone by Cu^{II} in the presence of molecular oxygen.

2.6.2 Factors Influencing the Oxidation

In general, 3,5-di-*tert*-butylcatechol is used as substrate to investigate the oxidation capability of copper complexes due to its low redox potential, which makes it easy to oxidize to 3,5-di-*tert*-butylquinone, as well as the presence of bulky, non-polar substituents, which prevent further oxidation reactions such as ring opening reactions and cyclization/tautomerization reactions.[125] Among the mononuclear copper(II) complexes, compounds possessing intermediate geometry between trigonal bipyramidal and square pyramidal[124], are considered to be potential models due to its biological relevance in the geometrical rearrangment[126] during the tyrosinase substrate binding reaction. Kida and co-workers[127] have studied a number of copper(II) complexes and have shown that dinuclear complexes catalyze the reaction while the mononuclear species are either not as efficient or inactive, depending on

---

[122] P. Gentschev, N.Möller and B. Krebs, *Inorg. Chim. Acta*, **442**, 300, (2000).
[123] K. Selmeczi, M. Règlier, M. Giorgi and G. Spier, *Coord. Chem. Rev.*, **245**, 191, (2003).
[124] A.C.D. Midoes, P.E. Aranha, M.P. dos Santos, E. Tozzo, S. Romera, R.H. de A. Santos and E.R. Dockal, *Polyhedron*, **27**, 59, (2008).
[125] M. Gullotti, L. Santagostini, R. Pagliarin, A. Granata and L. Casella, *J. Mol. Catal. A: Chem.*, **164**, 1, (2000).
[126] C.H. Kao H.H. Wei, Y.H. Liu, G.H. Lee, Y. Wang and C.J. Lee, *J. Inorg. Biochem.*, **84**, 171, (2001).
[127] N. Oishi, Y. Nishida, K. Ida and S. Kida, *Bull. Chem. Soc. Jpn.*, **53**, 2847, (1980).

the steric demand of the ligands. Neves and co-workers[128] studied the mononuclear and binuclear copper(II) complexes of the unsymmetrical binucleating ligand, N,N,N-tris-(2-pyridylmethyl)-1,3-diaminopropan-2-ol, as models for the active site in catechol oxidase. The mononuclear complex was inactive in this oxidation reaction, while the binuclear complex is a potential model for the dinuclear copper site in catechol oxides.

2.6.3 Mechanistic Investigation

The oxidation of catechol and in particular, 3,5-di-*tert*-butylcatechol, using copper(II) complexes as catalysts, has been studied widely as a model reaction. The reaction mechanism proposed by several authors includes an initial step leading to the formation of a reduced copper(I) complex as the active species towards molecular oxygen. The copper-oxygen adduct then would react with the catechol to give the quinone, or be oxidized to copper(II), which in turn reacts with the catechol in a ping-pong mechanism, giving the corresponding quinone.[129] In this way the properties of the copper(I) complex should be as important as those of the copper(II) complex, to determine the catalytic activity, which is dependent on the rate-determining step.[39]

Turnover rates ranging from 3.2 to 41.3 h^{-1} have been observed for oxidation reactions by Bhardwaj et al.[130] These are comparable to those reported by Reim *et al.*[131,132] and Fernandes *et al.*[128] and to an order of two or three times more than those reported by Neves *et al.*[133] but

---

[128] C. Fernandes, A. Neves, A.J. Bortoluzzi, A.S. Mangrich, E. Rentschler, B. Szpoganicz and E. Schwingel, *Inorg. Chim. Acta*, **320**, 12, (2001).
[129] J.P. Chyn and F.L. Urbach, *Inorg. Chim. Acta*, **189**, 157, (1991).
[130] V.K. Bhardway, N. Aliaga-Alcalde, M. Corbella and G. Hundal, *Inorg. Chim. Acta*, article in press (2009).
[131] J. Reim and B. Krebs, J. *Chem Soc., Dalton Trans*., 3793, (1997).
[132] J. Reim, R. Werner, W. Hasse and B. Krebs, *Chem. Eur. J*., **4**, 289, (1998).
[133] A. Neves, L.M. Rossi, A.J. Bortoluzzi, B. Szpoganicz, C. Wiezbicki, E. Schwingel, W. Haase and S. Ostrovsky, *Inorg Chem.*, **41**, 1788, (2002).

are significantly lower than those reported by Krebs and coworkers.[134,135], Monzani et al.[136] and Vittal and coworkers.[137,138]

2.7 Conclusion

In this chapter, various aspects of copper chemistry were discussed in terms of general copper(II) oxidation reactions, factors affecting oxidation and various homogeneous catalytic processes.

It is important to understand the details of a catalytic cycle in order for progress to be made. Advances in homogeneous catalysis can occur by alternating and understanding the effects that various metal centres can have on a specific catalytic system. Furthermore, the choice of an appropriate ligand can significantly alter the final result. Ligand modification is an important part of industrial process design. Manipulation of the electronic and steric properties of a specific ligand will affect factors such as rate, selectivity, stability, lifetime etc., all of which must be considered and understood.

In order to achieve specific objectives, it is important to characterise the catalyst and understand the reactivity of the complex in light of a catalytic reaction. In view of this objective, the following two chapters deal with the characterisation of the chosen copper complexes and the investigation of their catalytic properties.

---

[134] F. Zippel, F. Ahlers, R.Werner, W. Haase, H.F. Nolting and B. Krebs, *Inorg. Chem.*, **35**, 3409, (1996).
[135] P. Gentschev, N. Möller and B. Krebs, *Inorg. Chem. Acta*, **300**, 442, (2000).
[136] E. Monzani, L.Quinti, A. Perrotti, L. Cassella, M. Gulloti, L. Randaccio, S. Germia, G. Nardin, P. Faleschini and G. Tabbi, *Inorg. Chem.*, **37**, 553, (1998).
[137] C.T. Yang, M. Vetrichelvan, X. Yang, B. Moubaraki, K.S. Murray and J.J Vittal, *Dalton Trans.*, 113, (2004).
[138] X. Wang, J. Ding and J.J. Vittal, *Inorg. Chim. Acta*, **359**, 3481, (2006).

3. Synthesis and Characterisation of Copper Complexes

3.1. Introduction

The synthesis and characterisation of a range of Cu(II) complexes will be discussed in this chapter. Complex characterisation was performed using various techniques, including nuclear magnetic resonance (NMR), infrared (IR) and ultraviolet-visible (UV-Vis) spectroscopy. Brief overviews of the theory of these characterisation techniques are included in the following sections.

The synthesised complexes were also characterised by X-ray crystallography as far as possible. As X-ray crystallography is such a powerful identification tool for the characterisation of complexes in the solid state, the theoretical aspects of this technique, as well as a detailed discussion of two crystal structures, are presented.

3.2. Spectroscopic Techniques

3.2.1 Infrared Spectroscopy

Infrared (IR) spectroscopy is a powerful analytical tool which can be used by chemist to qualitatively and quantitatively identify a complex.[1] Almost all organic and inorganic compounds containing covalent bonds, with the exception of a few homonuclear molecules such as H_2, N_2 and Cl_2, absorb infrared radiation. Each molecular species, with the exception of molecules differing only with regard to its chirality in the crystalline state, has a unique infrared spectrum.

The infrared region in the electromagnetic spectrum consists of a wavelength range that varies from approximately 100 μm to 1000 nm. The near-IR wavelength range is from 0.78-2.5 μm,

[1] D.A. Skoog, D.M. West, F.J. Holler and S.R. Crouch, *Fundamentals of Analytical Chemistry*, 8th Ed., California, Thomson Brooks/Cole, (2004).

while the mid-IR wavelength range is from 2.5-50 μm.[1] The energy of IR radiation can excite vibrational and rotational transitions, but has insufficient energy to induce electronic transitions. Changes in rotational energy can split the peak for each vibrational state. In liquid and solid state, this rotation is often hindered or prevented, so the effects of these small energy differences are not detected. Therefore typical IR spectra originate from transitions between two vibrational levels of the molecule in the electronic ground state and are usually observed as absorption spectra.

As with other types of energy absorption, molecules are excited into a higher energy state when they absorb quanta of infrared radiation. The absorption of IR radiation corresponds to energy changes in the order of 8-40 kJ/mole. Molecules can only absorb the energy of infrared radiation if it corresponds to the natural stretching and bending vibrational frequencies of the molecule. The absorbed energy serves to increase the amplitude of the vibrational motions of the bonds in the molecule.[2] Only bonds that have a dipole moment, which changes as a function of time, are capable of absorbing infrared radiation. Symmetrical bonds, such as H_2 or Cl_2, do not absorb infrared radiation. A bond must have an electrical dipole that changes at the same frequency as the entering radiation in order for energy to be transferred. Only then can the changing electrical dipole of the bond couple with the sinusoidal electromagnetic field of the incoming radiation. Every type of bond has a different natural frequency of vibration, and although two different compounds may have the same type of bond, the bonds will experience two slightly different environments, and therefore cannot give the same infrared absorption pattern, and thus an infrared spectrum of each different molecule is unique and can be used to identify different compounds.

Another important use of IR spectroscopy is to determine structural information about molecules. The absorption of each type of bond (N-H, C-O, C=O, O-H, C≡N etc.) is regularly found only in certain sections of the vibrational infrared region. For each bond type, a small range of absorption can be defined. Outside of this range, absorptions are generally due to different types of bonds.

The carbonyl group is permanently polarised due to the difference in electro-negativity between the carbon and the oxygen atom; therefore any vibrational stretching of this bond will

[2] K. Nakamoto, *Infrared Spectra of Inorganic and Coordination Compounds*. 2nd Ed., New York, John Wiley & Sons, Inc., (1970).

affect the dipole moment. For these reasons, the carbonyl group is often used for complex characterisation, since the carbonyl stretching produces a distinct absorption peak.[3]

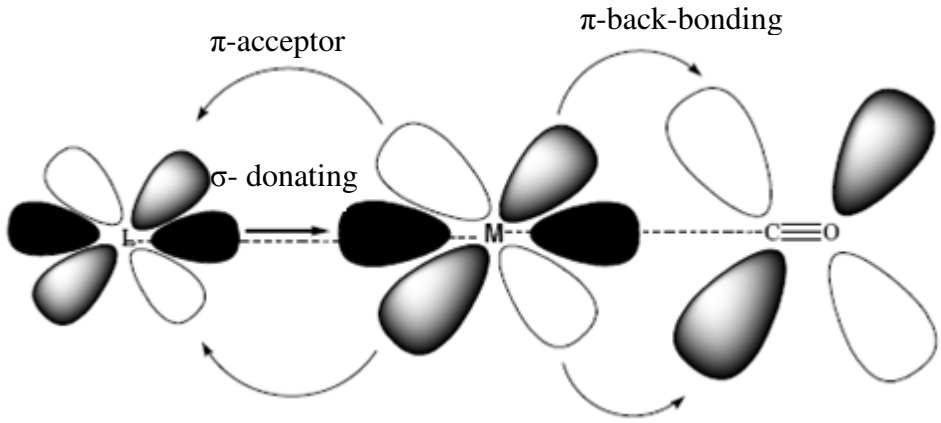

Figure 3.1 A stronger σ-donor ligand will increases the metal-carbonyl bond strength because of CO π-back-bonding.

General CO stretching and bending frequencies have a range from between 2360 to 1080 cm^{-1}. However, characteristic stretching frequencies[2] of metal carbonyl complexes (M-CO) have a range from between 2200 to 1700 cm^{-1}. Abel *et al.*[4] have found that the CO stretching frequency of the $[M(CO)_3L_3]$ type compounds (M = Cr, Mo or W; L = pyridine, PPh_3, $AsPh_3$, etc.) are in the region from between 2100 to 1700 cm^{-1}. The carbonyl stretching frequency, ν_{CO}, is very sensitive to the groups bonded to the M atom. The effect of the group 15 donor ligands can be used as an example, where the electron donating capability of the group 15 donor ligands decreases (from Sb to P), with a corresponding decrease in the electron density on the metal. Therefore, less electron density is available to the C≡O moiety via π-back-bonding into the carbon anti-bonding orbital[5] (Figure 3.1). This results in a weaker M-CO bond, a stronger C≡O bond and thus an increase in ν_{CO}, for example 1971, 1975 and 1979 cm^{-1} for *trans*-$[Rh(CO)(Cl)(SbPh_3)_2]$, *trans*-$[Rh(CO)(Cl)(AsPh_3)_2]$ and *trans*-$[Rh(CO)(Cl)(PPh_3)_2]$.[6]

3.2.2 Ultraviolet- Visible Spectroscopy

Ultraviolet (UV) and visible (Vis) light forms part of the electromagnetic spectrum with wavelengths that range between 190 to 800 nm. The technique of UV-Vis spectroscopy is

[3] B. Stuart, *Modern Infrared Spectroscopy*, Editor. D.J. Ando, England: John Wiley & Sons, Ltd., (1996).
[4] E.W. Abel, M.A. Bennet and G. Wilkinson, *J. Chem. Soc.*, 2323, (1959).
[5] C. Elschenbroich and A. Salzer, *Organometallics: A Concise Introduction*, New York: VCH Publishers, (1989).
[6] A. Roodt, S. Otto and G. Steyl, *Coord. Chem. Rev.*, **121**, 245, (2003).

based on the absorption of energy. As a result of energy absorption, atoms or molecules pass from a state of low energy (ground state) to a state of higher energy (the excited state). The electromagnetic radiation that is absorbed consists of energy exactly equal to the energy difference between the excited and ground state (Figure 3.2).[7]

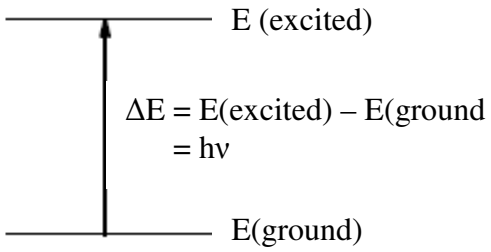

Figure 3.2 The excitation process where electrons pass from the ground state to the excited state when they absorb energy.

In ultraviolet and visible spectroscopy, the absorption of electromagnetic radiation causes the transitions between electronic energy levels. As a molecule absorbs energy, an electron is promoted from a **highest occupied molecular orbital (HOMO)** to the **lowest unoccupied molecular orbital (LUMO)** (Figure 3.3).

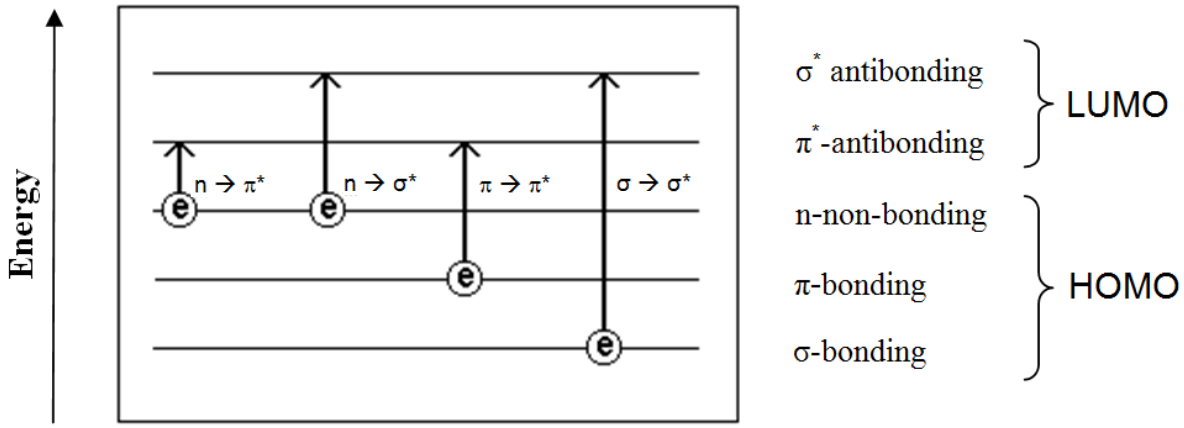

Figure 3.3 Energy of orbitals and the electronic transitions between the respective orbitals.

The absorption of energy by molecules in the UV-Vis region results from interactions between photons and electrons that either participate directly in bond formation or are localised about atoms such as oxygen, sulphur and halogens. The wavelength that the molecules absorb depends on how tightly its electrons are bound. Electrons involved in double and triple bonds

[7] D.L. Pavia, G.M. Lampman and G.S. Kriz, *Introduction to Spectroscopy*, 3rd Ed., USA: Thomson Learning, Inc., (2001).

are not strongly held and are easily excited by radiation and therefore generally exhibit useful absorption peaks. Unsaturated organic functional groups that absorb in the ultraviolet and visible regions are known as chromophores. In general, the ions and complexes of inorganic elements in the first two transition series absorb broad bands of visible radiation in at least one of their oxidation states. The absorption involves transitions between filled and unfilled d-orbitals, with energies that depend on the ligands bonded to the metal ions. The energy differences between the d-orbitals depend on the position of the element in the periodic table, its oxidation state and the nature of the ligands bonded to it.[1]

Ultraviolet and visible spectroscopy has many uses, but is primarily used for quantitative analysis and following reaction profiles corresponding to the formation or disappearance of different coloured reaction complexes.[8] UV-Vis spectra, however, do not always provide sufficient fine structure data to permit unambiguous identification of a molecule. Therefore other analytical techniques, such as infrared and nuclear magnetic resonance spectroscopy, as well as X-ray crystal diffraction, are required to support the information that UV-Vis spectroscopy produces.

3.2.3 Nuclear Magnetic Resonance Spectroscopy

Nuclear Magnetic Resonance (NMR) spectroscopy is one of the most powerful tools available to modern science. The use of NMR has spread to include a wide range of fields such as chemistry, physics, biology and even to living biological material for medical diagnosis (magnetic resonance imaging: MRI). Unlike IR spectroscopy, which reveals the type of functional groups present in a molecule, NMR gives information about the number of magnetically distinct atoms of a specific type that is being studied.

NMR makes use of the intrinsic magnetic character of an atom`s nucleus. Magnetic nuclei have an intrinsic angular momentum known as spin. The spin quantum number I can have one of the following values:

$$I = 0, 1/2, 1, 3/2, 2, ...$$

where quantum numbers greater than 4 are not that abundant.

[8] C.N.R. Rao, *Ultra-Violet & Visible Spectroscopy: Chemical Applications*, 2nd Ed., England: Butterworth & Co. (publishers) Ltd., (1967).

In order for a nucleus to be observed by NMR, the spin: I, must have a non-zero value. The most common spin quantum number is I = 1/2, with common nuclides such as ^{1}H, ^{13}C, ^{15}N, ^{19}F, ^{29}Si and ^{31}P. Nuclei with spin quantum numbers greater than 1/2 generally give broad NMR lines.[9]

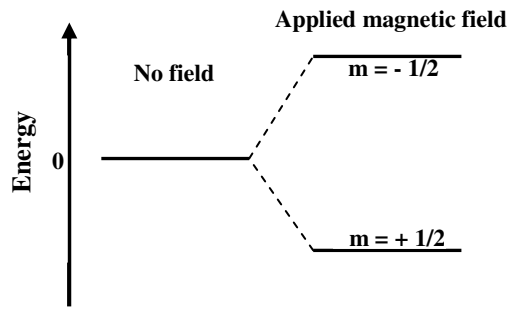

Figure 3.4 Energy levels for a nucleus with a quantum number 1/2.

When a magnetic nucleus is placed in a magnetic field, it can adopt a limited amount of permissible orientations of different energy. A hydrogen nucleus only has two permitted orientations: a clockwise spin (+1/2) with the magnetic moment aligned with the magnetic field, or a counter clockwise spin (-1/2) with the magnetic moment pointing in the opposite direction to the induced magnetic field (Figure 3.5).

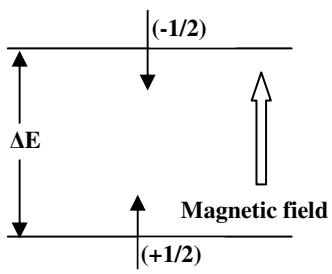

Figure 3.5 Energy levels of a hydrogen nucleus in a magnetic field.[9]

The spin state +1/2 has the lowest energy because it is aligned with the applied field, while the alternate spin state -1/2 has higher energy because it is opposed to the applied field. The two states are separated by an energy difference, ΔE, which depends on the size of the nuclear magnetic moment and the strength of the magnetic field. ΔE may be measured by applying electromagnetic radiation of frequency, ν, which causes the nuclei to flip from the lower energy level to the higher level (the resonance condition $\Delta E = h\nu$ must be satisfied). This interaction is termed nuclear magnetic resonance.[7]

[9] P.J. Hore, *Nuclear Magnetic Resonance*, New York: Oxford University Press, Inc. (1995).

The NMR spectrum is produced by the protons in a molecule that exist in slightly different chemical, and hence electronic, environments from one another and therefore absorb different frequencies. The protons are shielded by the surrounding valence-shell electrons which vary from hydrogen to hydrogen atom, and cause the effective magnetic field that is felt by the proton to be less than the applied magnetic field. These varying resonance frequencies result in different signals known as chemical shifts, δ. Factors such as hydrogen bonding, polar functionality groups, stereochemistry and geometry can affect the shielding of the proton and alter the chemical shift.

A proton can be affected by the magnetic field of a nearby proton. This results in magnetic interactions between nuclei, an effect called *spin-spin coupling*, whereby the resonance frequency of the first proton is split by the presence of the second proton. The difference between the peaks of the split frequency is indicated by the *coupling constant, J,* and it measured by how much a nucleus is affected by the spin states of its neighbour.[7]

The values of chemical shifts and *spin-spin coupling*, also from a long range of non-hydrogen atoms, can provide valuable information on the position, environment and forces which are experienced by atoms in different chemical species.

3.3. Theoretical Aspects of X-Ray Crystallography

3.3.1. Introduction

Mineralogy, the study of naturally occurring chemical compounds, gave birth to the scientific field of crystallography. With their clean regular morphology, crystals have fascinated people from ancient times. The name *crystal* originated from the Greek term *krystallos*, meaning ice. This term has been applied to quartz, as it was believed the mineral was water that had crystallised at high pressure deep inside the earth.[10]

3.3.2. X-Ray Diffraction

Although X-rays had been discovered in 1895 by C.W. Röntgen, it was only in 1912 that Max von Laue discovered the diffraction of X-rays by crystals. This discovery allowed the absolute configuration of a previously unknown chemical compound to be determined. The general

[10] H.R. Wenk and A. Bulakh, *Minerals: Their Constitution and Origin*, UK: Cambridge University Press, (2004).

procedure[11] for determining the crystal structure of a chemical compound is summarised below:

- Select a suitable crystal and mount it for an X-ray study
- Obtain unit cell geometry and preliminary symmetry information
- Measure intensity data
- Data reduction
- Solve the structure by:
    - Patterson methods
    - Direct methods
    - Other methods
- Complete the structure and find all the atoms: Fourier and difference Fourier synthesis
- Refine the structure model and determine a least squares model fit
- Interpret the results

Analytic instruments, such as NMR and IR spectroscopy, give information on the structure of a molecule according to the manner which in it absorbs or emits radiation. X-ray crystallography measures the variation of intensity with direction, in other words the scattering of monochromatic radiation. The scattered electromagnetic radiation waves can add constructively or deconstructively, depending on the direction of the diffracted beam and the atomic positions, because each atom is able to scatter X-rays.[12] Diffraction or interference effects cause these intensity variations, and this creates a complex scattering pattern which can then be analysed quantitatively. From measurements of the diffraction pattern, it is possible to determine the positions of the atoms in the sample.[11]

A crystal structure can be simplified by representing each molecule by a single point which results in a regular array of points. The *lattice* of the structure is known as the array of

[11] W. Clegg, *Crystal Structure Determination*, New York: Oxford University Press, Inc., (1998).
[12] M.F.C. Ladd and R.A. Palmer, *Structure Determination by X-ray Crystallography*, New York: Plenum Press, (1977).

identical points which are equivalent to each other by translation symmetry. A *unit cell* is the characteristic portion of the crystal, from which the whole part of the crystal can be reproduced, if it is repeated indefinitely in the direction of the crystal axes.[13] The lattice is therefore built up from many unit cells, and a unit cell consists of three sides (*a, b, c*) and three angles (α, β, γ). By placing certain restrictions on the unit cell, crystal symmetry can loosely be divided into the seven *crystal systems*. It has been shown that there are 230 possible three-dimensional patterns or *space groups* which arise when lattices are combined with the appropriate point and translational symmetry elements. These space groups are described in the *International Tables for Crystallography*.[14] A shorthand notation is used to describe the directions and planes in a crystal lattice, known as the plane index or *Miller index* (*hkl*) from which the reciprocal lattice is defined.

X-rays are scattered by each atom in a crystal to contribute to an overall scattering pattern. A complete pattern can only be recorded by rotating the crystal in the X-ray beam. The diffraction consists of a pattern of spots of varied intensity and has three properties which correspond to three properties of the crystal structure. The three properties are:

- The pattern has a particular geometry which is related to the lattice and unit cell geometry of the crystal structure.
- The pattern has symmetry which is related to the symmetry of the unit cell of the crystal structure.
- The pattern has varied intensities. The intensities reveal information about the position of the atoms in the unit cell.[11]

Max von Laue envisaged crystals in terms of a three-dimensional network of rows of atoms and based his analysis on the idea that a crystal behaves as a three-dimensional diffraction grating. This led to the development of the three Laue equations:[15]

$$a\,(\cos\alpha_n - \cos\alpha_0) = a\cdot(s - s_0) = n_x\lambda \qquad \text{… Eq 3.1}$$

[13] D.W.A. Sharpe, *The Penguin Dictionary of Chemistry*, 3rd Ed., London: Penguin Books Ltd., (2003).
[14] *International Tables for Crystallography, Volume A*, 5th Ed., The Netherlands: Kluwer Academic Publishers, (2002).
[15] C. Hammond, *The Basics of Crystallography and Diffraction*, 2nd Ed., New York: Oxford University Press, Inc., (2001).

where a is the one-dimensional lattice, spacing along the x-axis; α_n and α_0 are the angles between the diffracted and incident beams to the x-axis; n_x is an integer, s and s_0 are the unit vectors along the directions of the diffracted and incident beams and a is the translation vector from one lattice point to the next.

The other two Laue equations are for atoms along the y-axis and z-axis and are given by Eq 3.2 and Eq 3.3,

$$b\,(\cos\beta_n - \cos\beta_0) = \mathbf{b}\cdot(\mathbf{s} - \mathbf{s}_0) = n_y\lambda \qquad \text{… Eq 3.2}$$

$$c\,(\cos\gamma_n - \cos\gamma_0) = \mathbf{c}\cdot(\mathbf{s} - \mathbf{s}_0) = n_z\lambda \qquad \text{… Eq 3.3}$$

Although von Laue's equations are accurate, they are complicated to calculate. In order for constructive interference to occur simultaneously from all three atom rows, all three Laue equations must be satisfied simultaneously. An alternative and much simpler equation was derived by W.L. Bragg in 1912 and is known as Bragg's Law.[12]

3.3.3. Bragg's Law

Bragg assumed that when X-rays are diffracted by crystals, they act as though they were reflected by "atomic mirror planes" within the crystal. However, parts of the X-ray beam may not be reflected at the given crystal plane, but can penetrate deeper into the crystal and undergo a similar process at a deeper level in the crystal. All X-rays that are reflected from a given plane remain in phase after reflection. The two X-rays that are reflected from neighbouring planes are in general out of phase after reflection because they have travelled different path lengths. Bragg's law is used to correct these differences in phase.[12]

Bragg's law defined for rays reflected by two adjacent planes is given in Eq 3.4,

$$n\lambda = 2d_{hkl}\sin\theta \qquad \text{… Eq 3.4}$$

In Eq 3.4 n is an integer, λ is the wavelength, d_{hkl} is the distance between the successive parallel crystal planes and θ is the angle of incidence and reflection of the reflected X-ray beam.

In Figure 3.6, the Bragg reflection of two parallel rays reflected at A and C is illustrated.

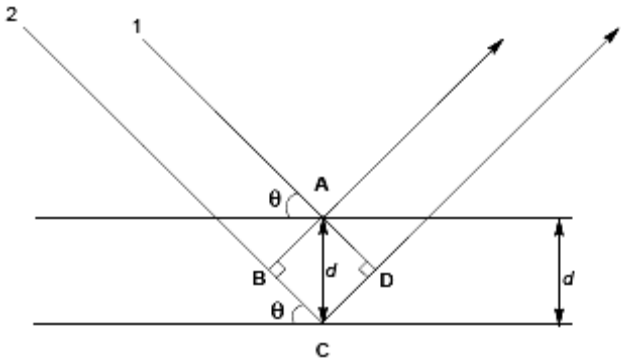

Figure 3.6 X-ray scattering according to Bragg's law.

$$BC + CD = 2d_{hkl} \sin \theta \qquad \text{… Eq 3.5}$$

Bragg's law is the basis of all methods for obtaining unit cell geometry from the measured geometry of the diffraction pattern. The exact application depends on the experimental setup used to obtain the diffraction pattern.

3.3.4. Structure Factor

Two numerical values can be associated with each reflection in a crystal diffraction pattern, namely the *amplitude* |F(*hkl*)| and the *phase* Φ of the diffracted wave. The amplitude |F(*hkl*)| is represented by the height of the wave and is measured in electrons and the phase by the horizontal shift relative to some chosen origin.

The structure factor, F(*hkl*), is related to the square root of the intensity of the reflected beam $\sqrt{I_{hkl}}$ which expresses the combined scattering of all atoms (*j*) and in the unit cell, compared to that of a single electron.

The resultant wave for the unit cell is therefore:[12]

$$F(hkl) = \sum_{j=1}^{N} g_j \exp(i\phi_j) = \sum_{j=1}^{N} g_j \exp[i2\pi(hx_j + ky_j + lz_j)] \qquad \text{… Eq 3.6}$$

Where g_j is the temperature-corrected atomic scattering factor ($g_j = f_j$, T_j; f_j = atomic scattering factor and T_j = temperature). Eq 3.6 indicates that the structure factor magnitude depends only on the relative disposition of the N atoms in the unit cell and on the atomic scattering factors. Each term in Eq 3.6 represents a wavelet with an amplitude g_j and a phase $\emptyset_j = 2\pi(hx_j +$

$ky_j + lz_j$) which expresses the path length for each scattered wavelength. The structure factor F(hkl) is then simply the resultant of the wavelets scattered by the *N* atoms in a unit cell.[16]

Eq 3.6 can also be written in the following format:

$$\mathbf{F(hkl)} = \sum_{j=1}^{N} \mathbf{g_j}\left[\cos 2\pi\left(\mathbf{hx_j} + \mathbf{ky_j} + \mathbf{lz_j}\right) + \mathbf{i}\sin 2\pi\left(\mathbf{hx_j} + \mathbf{ky_j} + \mathbf{lz_j}\right)\right] \quad \text{…Eq 3.7}$$

The energy associated with a cosine wave is proportional to the square of the amplitude of the wave. In X-ray diffraction it is expressed in terms of the intensity of the scattered wave from the unit, $I_o(hkl)$ where subscript *o* signifies an experimentally observed quantity. Since the amplitude of the structure factor is $|F(hkl)|$, the symbol $I(hkl)$ can be used to represent $|F(hkl)|^2$, which is sometimes called the ideal intensity. Therefore:

$$I_o(hkl) \propto |F_o(hkl)|^2 \quad \text{… Eq 3.8}$$

Eq 3.8 forms the basis of X-ray structure analysis, which allows the experimental quantities of $I_o(hkl)$ to be directly related to the structure through $|F(hkl)|$.

The image or X-ray diffraction pattern created when X-rays are scattered by the electrons associated with the atoms in a crystal can be used to determine the crystal structure. Atoms with high atomic numbers provide a greater concentration of electrons than do atoms of low atomic numbers. This concentration of electrons and its distribution around the atom is called the electron density, ρ. The units of electron density are measured in electrons per cubic angstrom, $e\text{Å}^{-3}$. In general, since it is a function of position, it can be specified at a point X, Y, Z as ρ(X, Y, Z).

The electron density can be expressed in terms of the structured factor F(*hkl*) in Eq 3.9 where Vc is the unit cell volume[17]:

$$\rho(x, y, z) = \frac{1}{Vc}\sum_{h}\sum_{k}\sum_{l} F(hkl)e^{-i2\pi(hx+ky+lz)} \quad \text{… Eq 3.9}$$

[16] L.V. Azároff, *Elements of X-ray Crystallography*, New York: McGraw-Hill, Inc., (1968).
[17] G.H. Stout, L.H. Jensen, *X-ray Structure Determination: A Practical Guide*, London: the Macmillan Company, (1968).

3.3.5. The 'Phase Problem'

The determination of a crystal structure cannot proceed directly from the observed intensity data. Analysis of the crystal structure is severely hampered in an X-ray diffraction experiment by the inability to determine the complete vectorial structure factor. The modulus |F(*hkl*)| can be obtained from the intensity data (Eq 3.8), but the corresponding phase $\phi(hkl)$ is not directly measurable. However to determine the structure, both amplitude and phase must be known. This inability to determine the phase is known as the 'Phase Problem'; and it can be overcome by using a number of means. The most common methods includes the Patterson function and direct methods.

3.3.5.1 Direct Methods

Direct methods attempt to determine the approximate reflection phases from the measured X-ray intensities using mathematical formulae. Direct methods are particularly useful in determining good phase information for structures consisting only of light atoms. The Patterson function is best used for molecules which contain only one atom or a small number of atoms with significantly more electrons than the rest.[12]

3.3.5.2 The Patterson Function

The Fourier transforms of the observed diffracted beam amplitudes $|F_o(hkl)|$, gives the correct electron density, but requires the position of the phase to determine the structure factor F(*hkl*). However the Fourier transforms of the squared amplitudes $|F_o(hkl)|^2$ with all the phases set equal to zero produces the Patterson Function or Patterson Map.

$$\rho(x,y,z) = \frac{1}{Vc}\sum_h\sum_k\sum_l |F_0(hkl)|^2 e^{-i2\pi(hx+ky+lz)} \qquad \text{… Eq 3.10}$$

The Patterson Function looks like an electron density map with peaks of positive electron density in various positions. These are not the positions of atoms in the structure. The Patterson Function is a map of vectors between pairs of atoms in the structure. For each peak seen in the map, found at point (*u, v, w*), there are two atoms in the structure whose *x* coordinates differ by *u,* the *y* coordinates differ by *v* and the *z* coordinates differ by *w*. The Patterson peaks show where atoms lie relative to each other, but not where they lie relative to the unit cell origin. The Patterson peaks are also proportional in size to the product of the atomic numbers of the two atoms involved.[11]

3.3.6. Least-Squares Refinement

Once it is believed that the correct crystal structure has been found, a calculated diffraction pattern can be made. If the atoms of the model structure are in the approximate correct positions, then there should be a degree of resemblance between the calculated diffraction pattern and the observed one. The least-squares refinement compares the calculated structure factor $|F_c|$ to the experimental data and the observed structure factor $|F_o|$. This comparison is described in terms of the *residual index* or R-*factor*, Eq 3.11, defined as

$$R = \frac{\sum \big| |F_0| - |F_c| \big|}{\sum |F_0|} \qquad \text{… Eq 3.11}$$

The value of the R-factor for a correct and complete crystal structure determined from well measured experimental data is around 0.02-0.07.

A variation on Eq 3.11 uses F^2 values instead of |F| values, squaring the differences, and/or incorporating different weighting factors multiplying different reflections that are based on their standard uncertainties and therefore incorporating information on the relative reliability of different measurements. A residual factor which is widely used for crystal structure determination is:

$$wR2 = \sqrt{\frac{\sum w(F_0^2 - F_c^2)^2}{\sum w(F_0^2)^2}} \qquad \text{… Eq 3.12}$$

where each reflection has its own weight *w*, Eq 3.12 is more meaningful from a statistical viewpoint than the basic *R* factor.[11]

3.4. Synthesis and Spectroscopic Characterisation of Compounds

3.4.1. Chemicals and Instrumentation

All reagents used for synthesis and characterisation were of analytical grade. If nothing else is stated, all commercially available reagents were used as received from Sigma-Aldrich. All organic solvents were dried and distilled before use.

All infrared spectra were recorded as neat samples on a Bruker Tensor Standard System spectrophotometer with a laser range of 4000 – 370 cm^{-1} and reported in cm^{-1}. The UV-Vis

spectra were collected on a Varian Carey 50 Conc Spectrometer equipped with a Julabo F12-mV temperature cell regulator (accurate to within 0.1 ^{o}C) in a 1.00 cm quartz cuvette cell. The ^{1}H NMR spectra were obtained in $CDCl_3$ solutions on a 300 MHz Bruker spectrometer. ^{1}H chemical shifts are reported relative to TMS using the $CDCl_3$ peak (7.24 ppm). All chemical shifts are reported in ppm and coupling constants in Hz.

3.4.2. Synthesis of Compounds

3.4.2.1 Synthesis of Bis(tropolonato)copper(II) ([Cu(Trop)$_2$])

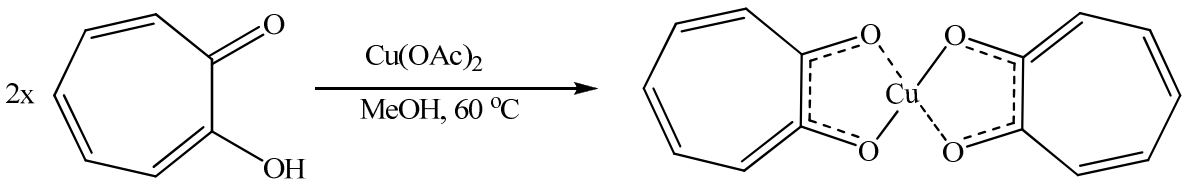

Scheme 3.1 Reaction scheme of the formation of bis(tropolonato)copper(II).

Bis(tropolonato)copper(II) was prepared by dissolving troplone (3.0 mmol; 0.366 g) in methanol (15 ml) and the mixture was heated to 60.0 ^{o}C while stirring. After the addition of copper acetate (1.5 mmol; 0.300 g) to the mixture, it was stirred for 4 hours at 60.0 ^{o}C. The solution was left to cool to room temperature, and a green precipitate appeared that was filtered. The filtrate was washed with cold ethanol and dried. Yield: 0.38 g, 84 %. Anal. Calcd. for $CuO_4C_{14}H_{10}$: C, 54.99 %; H, 3.30 %; O, 20.93 %; Cu, 20.78 %. Found: C, 55.21 %; H, 3.35 %; O, 20.70 %; Cu, 20.74 %. IR: υ(C=O) 1621, 1589; υ(C=C) 1512; υ(C-O) 1274.

3.4.2.2 Synthesis of Bis(tri-bromotropolonato)copper(II) ([Cu(TropBr$_3$)$_2$])

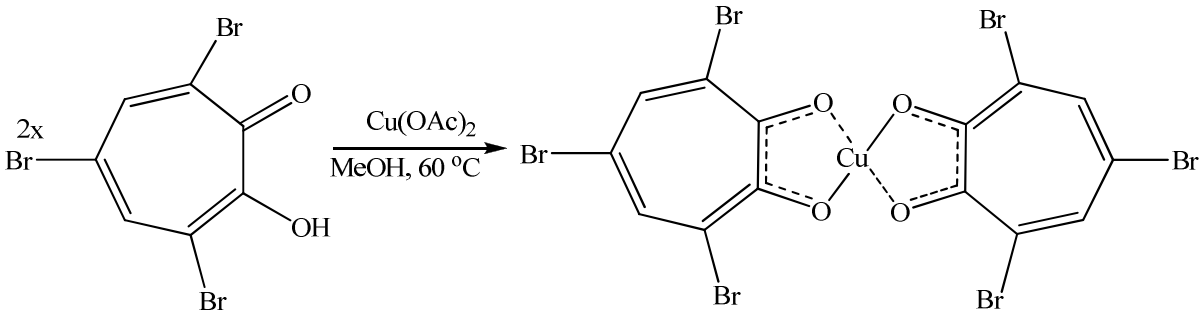

Scheme 3.2 Reaction scheme of the formation of bis(tri-bromotropolonato)copper(II).

Bis(tri-bromotropolonato)copper(II) was prepared by dissolving tri-bromotroplone (3.0 mmol; 1.076 g) in methanol (15 ml) and the mixture was heated to 60.0 ^{o}C while stirring. After the addition of copper acetate (1.5 mmol; 0.300 g) to the mixture, it was stirred for 4 hours at 60.0

^{o}C. The solution was left to cool to room temperature, and a yellow-green precipitate appeared that was filtered. The filtrate was washed with cold ethanol and dried. Yield: 1.02 g, 86 %. Anal. Calcd. for $CuO_5C_{14}H_6Br_3$: C, 21.09 %; H, 0.52 %; O, 8.21 %; Cu, 8.16 %; Br, 61.53 %. Found: C, 21.58 %; H, 0.96 %; O, 10.89 %; Cu, 7.74 %; Br, 60.01 %. IR υ(C=O) 1630, 1599; υ(C=C) 1513; υ(C-O) 1273. Physical measurements were conducted on this polycrystalline powder. For single crystals, 0.2 g of $[Cu(TropBr_3)_2]$ was dissolved in DMSO (20 ml). Yellow plate-like crystals of bis(tri-bromotropolonato DMSO)copper(II) begins to form at ambient temperature after one month.

3.4.2.3 Synthesis of Bis(2-methyl-3-hydroxy-4-pyrone)copper(II) ($[Cu(Memal)_2]$)

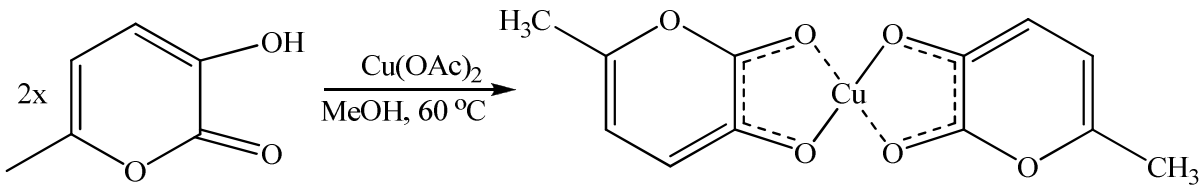

Scheme 3.3 Reaction scheme of the formation of bis(2-methyl-3-hydroxy-4-pyrone)copper(II).

Bis(2-methyl-3-hydroxy-4-pyrone)copper(II) was prepared by dissolving 2-methyl-3-hydroxy-4-pyrone (3,0 mmol; 0.378 g) in methanol (15 ml) and the mixture was heated to 60.0 ^{o}C while stirring. Copper acetate (1.5 mmol; 0.300 g) was added to the mixture and it was stirred for 4 hours at 60.0 ^{o}C. The solution was left to cool down to room temperature, and a light green precipitate formed that was filtered. The filtrate was washed with cold ethanol and dried. Yield: 0.42 g, 90 %. Anal. Calcd. for $CuO_6C_{12}H_{10}$: C, 45.94 %; H, 3.21 %; O, 30.60 %; Cu, 20.25 %. Found: C, 46.51 %; H, 3.25 %; O, 30.06 %; Cu, 20.18 %. IR υ(C=O) 1599, 1555; υ(C=C) 1508; υ(C-O) 1275.

3.4.2.4 Synthesis of Bis(2-ethyl-3-hydroxy-4-pyrone)copper(II) ([Cu(Etmal)$_2$])

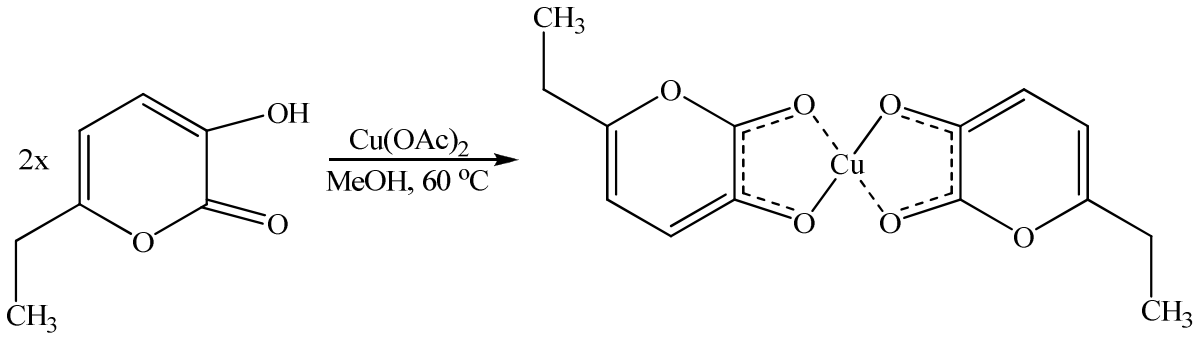

Scheme 3.4 Reaction scheme of the formation of bis(2-ethyl-3-hydroxy-4-pyrone)copper(II).

Bis(2-ethyl-3-hydroxy-4-pyrone)copper(II) was prepared by dissolving 2-ethyl-3-hydroxy-4-pyrone (3,0 mmol; 0.421 g) in methanol (15 ml) and the mixture was heated to 60.0 ^{o}C while stirring. Copper acetate (1.5 mmol; 0.300 g) was added to the mixture and it was stirred for 4 hours at 60.0 ^{o}C. The solution was left to cool down to room temperature, and a white-green precipitate formed that was filtered. The filtrate was washed with cold ethanol and dried. Yield: 0.45 g, 87 %. Anal Calcd for $CuO_6C_{14}H_{14}$: C, 49.19 %; H, 4.13 %; O, 28.09 %; Cu, 18.59 %. Found: C, 49.52 %; H, 4.16 %; O, 27.99 %; Cu, 18.33 %. IR υ(C=O) 1563, 1610; υ(C=C) 1509; υ(C-O) 1276.

3.5. Crystal Structure Determination of Bis(tri-bromotropolonato)Bis(dimethylsulphoxide)Copper(II) Complex and 3,5-di-*tert*-butylcatechol

The complex, bis(tri-bromotropolonato) bis(dimethylsulphoxide) Copper(II) ([Cu(TropBr$_3$)$_2$(DMSO)$_2$]), and 3,5-di-*tert*-butylcatechol investigated in this study were characterised by means of X-ray crystallography and the instruments and procedures involved are described below.

3.5.1 Experimental

The reflection data was collected on a Bruker X8 ApexII 4K diffractometer[18] using graphite monochromated Mo *K*α radiation with ω-and-φ-scans at 100K. COSMO[19] was utilised for

[18] Bruker, APEX2 (Version 1.0-27), Bruker AXS Inc., Madison, Wisconsin, USA, (2005).
[19] Bruker, COSMO, (Version 1.48), Bruker AXS Inc., Madison, Wisconsin, USA, (2003).

optimum collection of more than a hemisphere of reciprocal space. After a complete collection, the first 50 frames were repeated to check for any decomposition, but all the crystals remained stable throughout the collection. The frames were integrated using a narrow-frame integration algorithm and reduced with Bruker SAINT-Plus[20] and XPREP[20] software packages, respectively. Data was corrected for absorption effects using the multi-scan technique SADABS.[21] The structures were solved by direct methods package SIR97[22] and refined using the software package WinGX,[23] incorporating SHELXL.[24] The program DIAMOND[25] was used for all graphic representations of the crystal structures. All structures are shown with thermal ellipsoid drawn at 50% probability level.

All non-hydrogen atoms were refined anisotropically, while the methyl and aromatic H atoms were placed in geometrically idealised positions and constrained to ride on their parent atoms, with δ C-H = 0.95, 0.98 Å and U_{iso}(H) = 1.5U_{eq}(C), 1.2U_{eq}(C), respectively.

A summary of the general crystal data and refinement parameters is given in Table 3.1 for the bis(tri-bromotropolonato)bis(dimethylsulphoxide)Copper(II) complex and 3,5-di-*tert*-butylcatechol. Supplementary data for the atomic coordinates, bond distances, angles and anisotropic displacement parameters are given in the Appendix, Table A and B for [Cu(TropBr$_3$)$_2$(DMSO)$_2$] and 3,5-di-*tert*-butylcatechol respectively.

[20] Bruker, SAINT-Plus (Version 7.12) (Including XPREP), Bruker AXS Inc., Madison, Wisconsin, USA, (2004).
[21] Bruker, SADABS, (Version2004/1), Bruker AXS Inc., Madison, Wisconsin, USA, (1998).
[22] A. Altomare, M.C. Burla, M. Camalli, G.L. Cascarano, C. Giacovazzo, A. Guagliardi, A.G.G. Moliterni, G. Polidori and R. Spagna, *J. Appl. Cryst*., **32**, 115, (1999).
[23] L.J. Farrugia, *J. Appl. Cryst*., **32**, 837, (1999).
[24] G.M. Sheldrick, SHELXL97, *Program for Solving Crystal Structures*, University of Göttigen, Germany, (1997).
[25] K. Brandenburg and H. Putz, DIAMOND, Release 3.0c, Crystal Impact GbR, Bonn, Germany, (2005).

Table 3.1 General X-ray crystallographic data and refinement parameters for bis(tri-bromotropolonato)bis(dimethylsulphoxide)copper(II) and 3,5-di-*tert*-butylcatechol.

Compound	**$[Cu(TropBr_3)_2(DMSO)_2]^a$**	**3,5-di-*tert*-butylcatechol**
Empirical formula	C18 H16 Br6 Cu O6 S2	C28 H44 O4
Formula weight	935.43	444.64
Temperature (K)	100.0(2)	100.0(2)
Wavelength (Å)	0.71073	0.71073
Crystal system	Monoclinic	Triclinic
Space Group	C2/c	P-1
Unit cell dimensions		
a (Å)	18.002(7)	9.101(5)
b (Å)	20.351(7)	11.394(5)
c (Å)	7.578(3)	13.203(5)
α (°)	90	83.653(5)
β (°)	108.331(2)	79.601(5)
γ (°)	90	85.091(5)
Volume ($Å^3$)	2635.4(17)	1335.3(11)
Z	4	4
Calculated density ($g.cm^{-1}$)	2.358	1.106
Absorption coefficient μ (mm^{-1})	10.117	0.072
F(000)	1772	488
Crystal Colour	yellow	colourless
Crystal Morphology	plate	cuboid
Crystal size (mm)	0.23 x 0.11 x 0.03	0.19 x 0.25 x 0.41
Theta range (°)	1.56 to 26.99	2.28 to 27.00
Completeness	100.0 %	97.3 %
Limiting indices	h = -22 to 22	h = -11 to 11
	k = -25 to 25	k = -14 to 9
	l = -9 to 9	l = -16 to 16
Reflections collected	13497	14423
Unique reflections	2873	5675
R_{int}	0.0556	0.0514
Refinement method	Full-matrix least-squares on F^2	Full-matrix least-squares on F^2
Data / restraints / parameters	2873 / 0 / 151	5675 / 0 / 321
Goodness-of-fit on F^2	1.062	1.384
Final R indices [I>2sigma(I)]	R1 = 0.0320	R1 = 0.1245
	wR2 = 0.0571	wR2 = 0.3548
R indices (all data)	R1 = 0.0474	R1 = 0.1475
	wR2 = 0.0676	wR2 = 0.3727

a = bis(tri-bromotropolonato)bis(dimethylsulphoxid)copper(II)

3.5.2 Crystal Structure of Bis(tri-bromotropolonato)-Bis(dimethylsulphoxide)Copper(II)

Yellow crystals of the title compound were synthesised as described in Section 3.4.2.2. The $[Cu(TropBr_3)_2(DMSO)_2]$ complex crystallised in a centrosymetric, monoclinic space group C2/c, with four molecules per unit cell. The structure and numbering scheme of $[Cu(TropBr_3)_2(DMSO)_2]$ is illustrated in Figure 3.7, while the most important bond distances and angles are reported in Table 3.2 and Table 3.3, respectively. The positional and thermal parameters are given in Table 1.A and a complete list of bond distances and angles are given in Table 2.A.

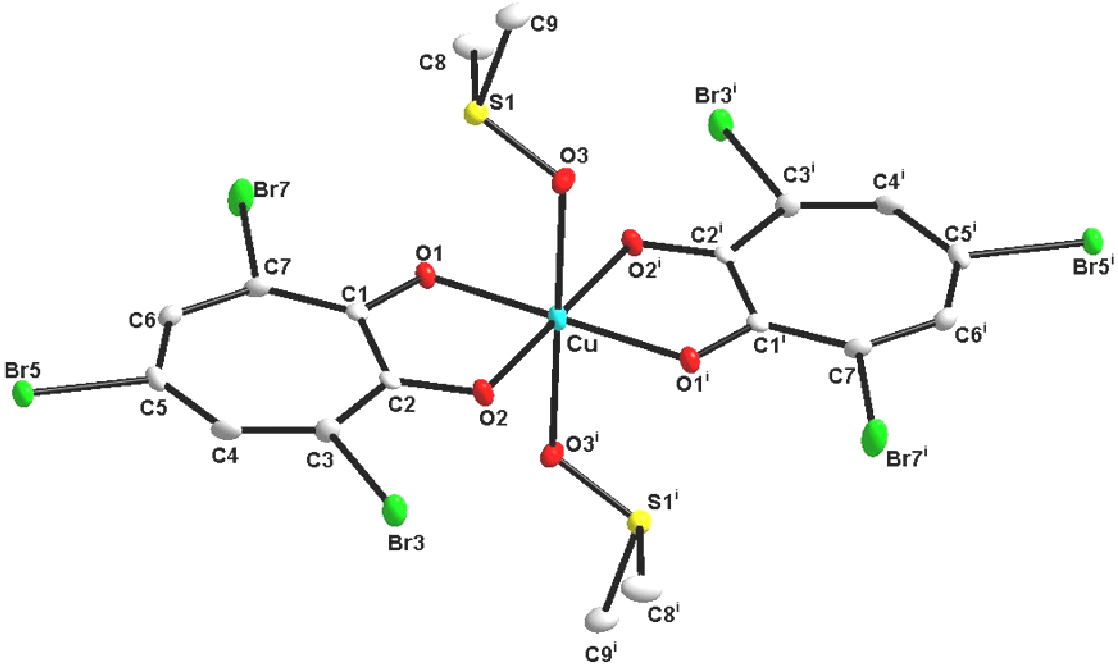

Figure 3.7 Thermal ellipsoid structure of $[Cu(TropBr_3)_2(DMSO)_2]$ showing the atom numbering system. Hydrogen atoms have been omitted for clarity. Thermal ellipsoid probability set at 50 %. [i = 1.5 – x, 0.5 – y, 1 – z]

The molecular structure of $[Cu(TropBr_3)_2(DMSO)_2]$ consists of a Cu(II) metal centre which is coordinated to four virtually equivalent oxygen atoms of the two tri-bromotropolonato bidentate ligands, and coordinated by two oxygen atoms each from a dimethylsulphoxide molecule.[26] The Cu(II) atom resides on a two-fold rotation axis. The tri-bromotropolonato bidentate ligands consist of a tropolone ring with three rotational bromine atoms bonded at the 3-, 5- and 7- positions.

[26] M. Kawahara, K. Kabir, K. Yamada, K. Adachi, H. Kumagai, Y. Narumi, K. Kindo, S. Kitagawa and S. Kawata, *Inorg. Chem. Acta.*, **24**, 92, (2004).

Table 3.2 Selected bond lengths for [Cu(TropBr$_3$)$_2$(DMSO)$_2$].

Selected bond lengths			
Atoms	**Bond length (Å)**	**Atoms**	**Bond length (Å)**
Br 5-C5	1.909(4)	C7-C6	1.382(6)
Br3-C3	1.901(5)	C7-C1	1.426(6)
Br7-C7	1.900(5)	C4-C3	1.382(6)
Cu-O2	1.951(3)	C4-C5	1.388(6)
Cu-O1	1.957(3)	C6-C5	1.379(6)
Cu-O3	2.392(3)	C2-C3	1.419(6)
O1-C1	1.274(5)	C2-C1	1.480(6)
O2-C2	1.277(5)	S1-C9	1.784(5)
O3-S1	1.503(3)	S1-C8	1.785(5)

i = 1.5 – x, 0.5 – y, 1 – z

Table 3.3 Selected bond angles for [Cu(TropBr$_3$)$_2$(DMSO)$_2$].

Selected bond Angles			
Atoms	**Bond angles (°)**	**Atoms**	**Bond angles (°)**
O(2^i)-Cu-O(1^i)	82.08(13)	O(2)-C(2)-C(3)	119.7(4)
O(2)-Cu-O(1^i)	97.92(13)	O(2)-C(2)-C(1)	114.7(4)
O(1^i)-Cu-O(1)	180	C(3)-C(2)-C(1)	125.6(4)
O(2^i)-Cu-O(3)	89.88(12)	O(1)-C(1)-C(7)	119.3(4)
O(2)-Cu-O(3)	90.12(12)	O(1)-C(1)-C(2)	115.7(4)
O(1^i)-Cu-O(3)	91.72(12)	C(7)-C(1)-C(2)	125.0(4)
O(1)-Cu-O(3)	88.28(12)	C(6)-C(5)-C(4)	128.9(4)
C(1)-O(1)-Cu	113.4(3)	C(6)-C(5)-Br(5)	115.1(3)
C(2)-O(2)-Cu	114.1(3)	C(4)-C(5)-Br(5)	116.1(3)
C(6)-C(7)-C(1)	131.7(4)	C(4)-C(3)-C(2)	131.4(4)
C(6)-C(7)-Br(7)	113.9(3)	C(4)-C(3)-Br(3)	114.3(3)
C(1)-C(7)-Br(7)	114.5(3)	C(2)-C(3)-Br(3)	114.3(3)
C(3)-C(4)-C(5)	128.8(4)	S(1)-O(3)-Cu	119.79(17)
C(5)-C(6)-C(7)	128.7(4)	O(3)-S(1)-C(9)	105.7(2)
O(3)-S(1)-C(8)	105.3(2)	C(9)-S(1)-C(8)	99.2(2)

i = 1.5 – x, 0.5 – y, 1 – z

The molecular structure of [Cu(TropBr$_3$)$_2$(DMSO)$_2$] displays an octahedral geometry. The distorted octahedral geometry around the Cu(II) centre is supported by the small bidentate bite angle (82.08(13) °) O(1)-Cu-O(2) of the tribromotropolonato moiety. This bite angle is significantly smaller than the average 5-member ring O-Cu-O bidentate bite angles.[27] The bite angles of bis O,O$^{'}$ ligand, with a 5-membered ring system bonded to copper, has an average of 82.71 (32) °[27], this is smaller than the average bis O,O$^{'}$ bidentate ligand with a 6-member ring

[27] Cambridge Structural Database, Version 5.30, Cambridge Crystallographic Data Centre, Cambridge UK, Nov, (2008).

system, which has an average of 90.956(79) ° .[27] The closest example to this system is trans-bis(6-isopropyltropolonato-O,O')-(pyridine)-copper(II) which comprises of a bite angle of 82.34(14) °.[28] The O(2)-Cu-O(1^i) bond angle is 97.92(13) ° for $[Cu(TropBr_3)_2(DMSO)_2]$ and it is significantly larger than the average bis O,O ligand, 5-member ring system bonded to copper(II).[27]

The Cu-O bonds in the equatorial plane of $[Cu(TropBr_3)_2(DMSO)_2]$ are 1.96(3) Å and 1.95(3) Å respectively. These are shorter than the average Cu-O bond length (2.03(14) Å.)[27] of $[Cu(O,O\text{-}Bid)_2]$ complexes forming 5-membered ring systems. The Cu-O bond lengths of $[Cu(Hin)_2Py]$[28] are 1.97(3) Å and 1.93(3) Å, which is the closest correlation to $[Cu(TropBr_3)_2(DMSO)_2]$. The Cu-O bond lengths of copper tropolonato ($[Cu(Trop)_2]$)[29] and trans-bis(4-isopropyltropolonato-O,O)-copper(II) ($[Cu(Hin)_2]$)[28] are 1.913(3), 1.915(3) Å and 1.904(3), 1.900(2) Å, respectively, which are all shorter than $[Cu(TropBr_3)_2(DMSO)_2]$ (Table 3.4). The C-O bond lengths are 1.274(5) Å and 1.277(5) Å, respectively. With regards to $[Cu(Hin)_2]$[28] and $[Cu(trop)_2]$[29] found in literature, the C-O bonds (1.293(5), 1.296(5) Å and 1.302(4), 1.286(4) Å) are relatively longer in comparison to $[Cu(TropBr_3)_2(DMSO)_2]$ but compare relatively well to the C-O bonds of $[Cu(Hin)_2Py]$[28] (1.287(5), 1.278(6) Å). All the C-Br bond lengths are about 1.900(5) Å, which also compares well with literature.[27]

The Jahn-Teller effect describes the lengthening of the Cu-O bonds in the axial position and the shortening of the Cu-O bonds in the equatorial positions.[30] Octahedral copper(II) complexes usually exhibit a Jahn-Teller distortion (Section 2.2.2). According to Persson *et al.*[30] the Cu-O_{eq} bonds lengths are around 1.95(1) Å and the Cu-O_{ax} bonds are around 2.29(3) Å. DMSO is well known for its coordination ability[26,31,33,32] and can coordinate through either the S or O atom.[33] Kawahara *et al.*[26] also suggested that DMSO coordinates to the copper.[26] The Cu-O3 bond for $[Cu(TropBr_3)_2(DMSO)_2]$ is 2.392(2) Å, which relates well to the bond length suggested by Persson *et al.*[30] and that found by Kawahara *et al.*[26]. The work done by

[28] M.C. Barret, M.F. Mahon, K.C. Molloy, P. Wright and J.E. Creeth, *Polyhedron.*, **21**, 1761, (2002).
[29] M. Hasegawa, Y. Inomaki, T. Inayoshi, T. Hoshi and M. Kobayashi, *Inorg. Chim. Acta.*, **257**, 259, (1997).
[30] I. Persson, P. Perrson, M. Sandström and S.S. Ullström, *J. Chem.Soc., Dalton Trans.*, 1256, (2002).
[31] J. Jacob, G. Lente, I.A. Guzei and J.H. Espenson, *Inorg, Chem.*, **38**, 3762, (1999).
[32] C.P Rao, A. Sreedhara, P.V. Rao, M.B. Verghese, K. Rissanen, E. Kolehmainen, N.K. Lokanath, M.A. Sridhar and J.S. Prasad, *J. Chem. Soc., Dalton Trans.*, 2383, (1998).
[33] E. Alessio, B. Serli, E. Zangrando, M. Calligaris and N.S. Panina, *Eur. J. Inorg. Chem.*, 3160, (2003).

Kawahara *et al.*[26] was specifically on DMSO coordination to copper. Djedouani *et al.*[34] found that the Cu-O bond length for DMSO in [Cu(O,O'-Bid)$_2$] complexes to be *ca.* 2.46 Å, which was due to the Jahn-Teller effect and even longer than that of [Cu(TropBr$_3$)$_2$(DMSO)$_2$]. The Cu-O bond lengths of [Cu(TropBr$_3$)$_2$(DMSO)$_2$] are longer than the bond lengths of the 4-coordinated oxygen atoms in the plane of [Cu(O,O-Bid)$_2$], which further suggests the presence of an octahedral complex rather than a 4-coordinated species. The S-O bond lengths of [Cu(TropBr$_3$)$_2$(DMSO)$_2$] are 1.503(3) Å and this correlates well to the S-O bond lengths found by Alessio *et al.*[33] which range between 1.451(7) and 1.539(6) Å for coordinated DMSO.

Table 3.4 Summary of crystallographic data of four [Cu(O,O-Bid)$_2$] complexes.

	[Cu(O,O-Bid)$_2$] systems			
	[Cu(TropBr$_3$)$_2$(DMSO)$_2$]	**[Cu(Trop)$_2$]**[29]	**[Cu(Hin)$_2$Py]**[28]	**[Cu(Hin)$_2$]**[28]
Crystal system	Monoclinic	Monoclinic	Monoclinic	Monoclinic
Space group	C2/c	P2$_1$/c	P2$_1$/n	P2$_1$/c
Z	4	2	4	2
Volume (Å^3)	2635.4(17)	608.113	2237.545	941.155
ρ_{calc} (g.cm^{-1})	2.358	1.669	1.392	1.376
Cu-O1 (Å)	1.957(3)	1.913(3)	1.965(3)	1.904(3)
Cu-O2 Å)	1.951(3)	1.915(3)	1.933(3)	1.900(2)
O1-Cu-O2 (°)	82.08(13)	83.80(10)	82.34(14)	83.84(13)
O1-Cu-O2^i (°)	97.92(13)^a	95.26(4)^b	94.30(2)	96.16(13)^c
O1-Cu-O1^i(°)	180.000^a	180.00^b	155.20(2)	180.00^c

[Cu(trop)$_2$] = Copper tropolonato[29]
[Cu(Hin)$_2$Py] = *Trans*-bis(6-isopropyltropolonato-O,O')-(pyridine)-copper(II)[28]
[Cu(Hin)$_2$] = *Trans*-bis(4-isopropyltropolonato-O,O')-copper(II)[28]
a = 1.5 – x, 0.5 – y, 1 – z
b = 2 - x, 1 – y, 2 – z
c = - x, - y, - z

The cell volume of the four complexes shown in Table 3.4 indicates that [Cu(TropBr$_3$)$_2$(DMSO)$_2$] has the biggest unit cell dimensions in this set. The O1-Cu-O1^i bond angle is 180 ° for [Cu(TropBr$_3$)$_2$(DMSO)$_2$], [Cu(Trop)$_2$] and [Cu(Hin)$_2$], as would be expected from square planer or octrahedral systems for which Cu^{II} is well known (Section 2.2.2). This is not the case for [Cu(Hin)$_2$Py], which has a O2-Cu-O3 angle of only 155.19 °, which leads to

[34] A. Djedouani, A. Bendaas, S. Bouacida, A. Beghidja and T. Douadi, *Acta. Cryst.*, **E62**, m133, (2006).

less obvious square-pyramidal complexes of copper(II) (Section 2.2.2.). This is due to the steric demand of the pyridine that is coordinated to the Cu centre.

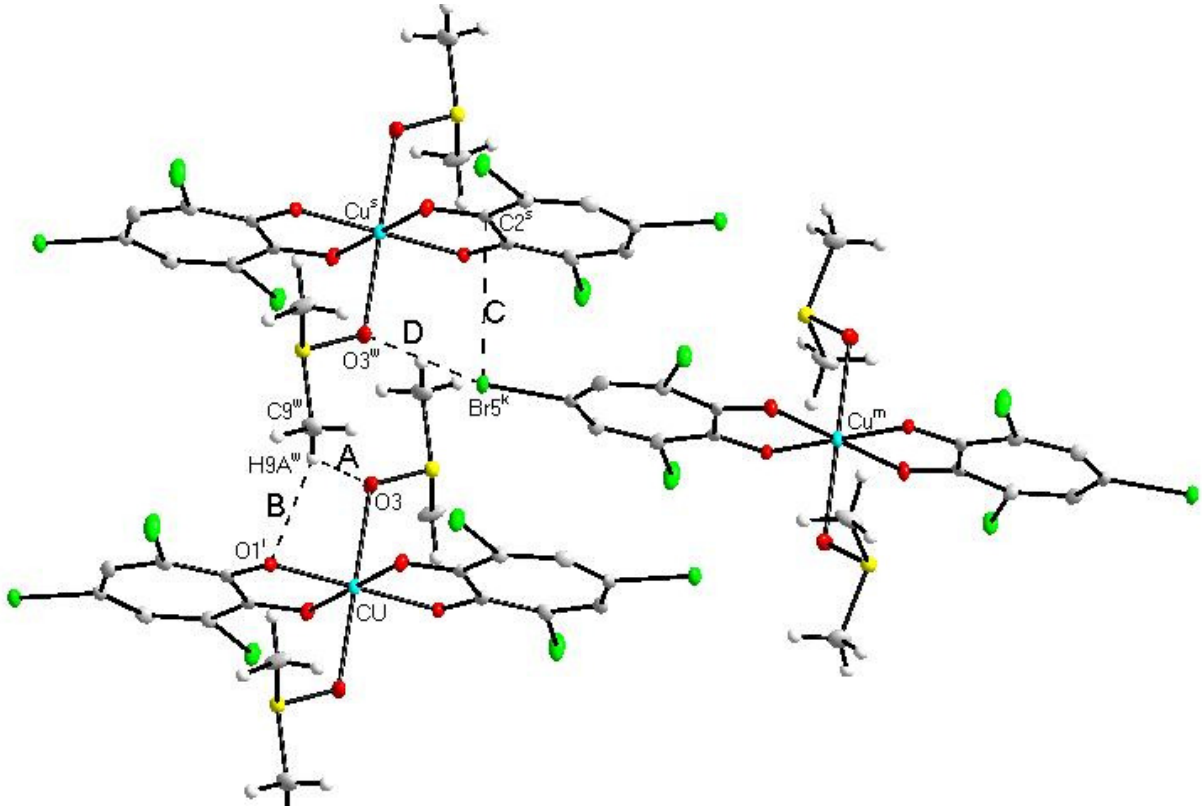

Figure 3.8 Inter and intramolecular hydrogen interactions and other short contacts found between [Cu(TropBr3)$_2$(DMSO)$_2$] molecules. [i = 1.5 - x, 0.5 - y, 1 – z; w = 1.5 – x, 0.5 – y, 2 – z; k = x, - y, 0.5 + z; s = x, y, 1 + z; m = 1.5 – x, -0.5 + y, 1.5 – z]

The packing of this molecule is stabilised by weak intermolecular C-Br(5)···O(3^i) bonds and weak hydrogen bonds between the hydrogen on the DMSO methyl groups and the tropolone oxygen atoms around the Cu(II) centre, which forms a three dimensional network. The Br and O interaction distance is 2.86 Å, while the sum of the Van der Waals radii of bromine and oxygen are 3.35 Å. There is reason to believe that O···Br interactions are energetically comparable to a strong hydrogen bond.[35]

[35] H.A Bent, *Chem Rev.*, **68**, 587, (1968).

Table 3.5 Hydrogen interactions and other short contacts for $[Cu(TropBr_3)_2(DMSO)_2]$.

Interaction	D-H...A	D-H (Å)	H...A (Å)	D----A (Å)	D-H...A (°)
A	$C9^z$ $H9A^z$ O3	0.98	2.538(9)	3.365(1)	142.10(2)
B	$C9^z$ $H9A^z$ $O1^i$	0.98	2.511(8)	3.326(9)	140.40(2)
C	$C2^x$ $Br5^k$			3.585(1)	
D	$O3^z$ $Br5^k$			2.858(9)	

i = 1.5 - x, 0.5 - y, 1 – z
k = x, - y, 0.5 + z
x = x, y, 1 + z
z = 1.5 – x, 0.5 – y, 2 – z

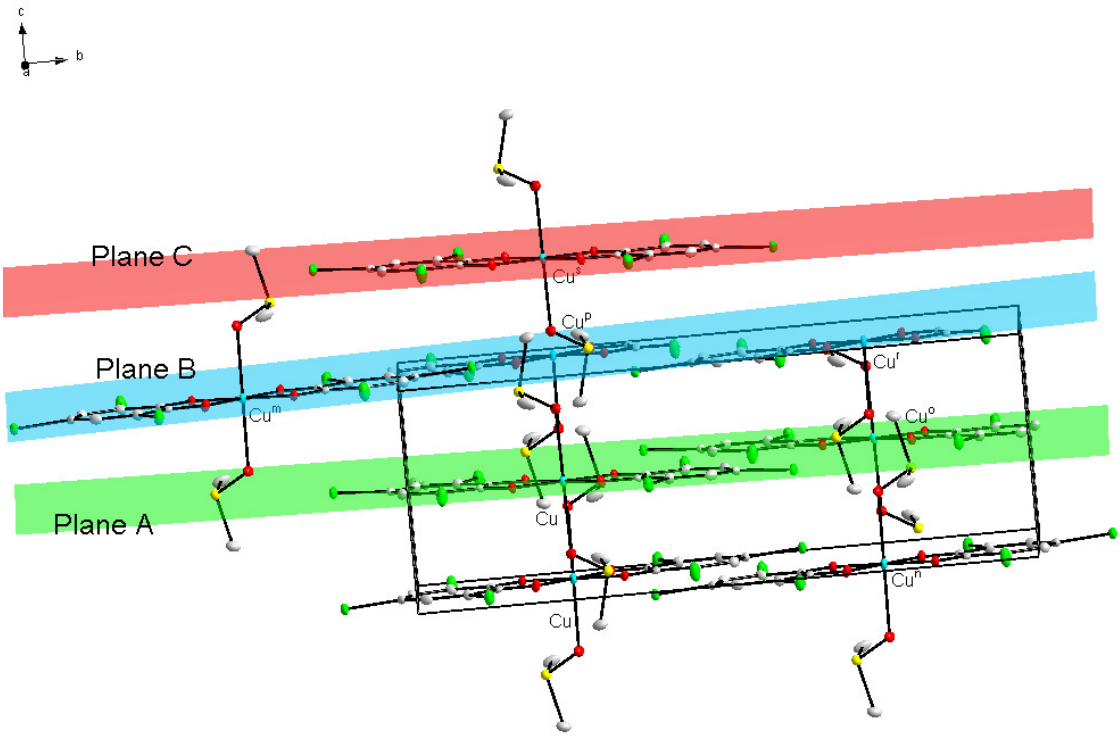

Figure 3.9 A view along the a-axis of $[Cu(TropBr3)_2(DMSO)_2]$ planes that forms the sheet-like packing. [m = 1.5 – x, -0.5 + y, 1.5 – z; n = 1.5 – x, 0.5 + y, 0.5 –z; o = -0.5 + x, 0.5 + y, z; p = 1 – x, y, 1.5 – z; r = 1.5 – x, 0.5 + y, 1.5 – z; s = x, y, 1 + z]

The packing of the unit cell is in a sheet-like fashion along the a-axis. The distance from Cu to plane B is 3.387Å and planes A and B are at angles of 1.94 ° to each other, while planes A and C are parallel to each other. The packing is in a head-to-head staggered fashion along the c-axis.

3.5.3 Crystal Structure of 3,5-di-*tert*-butylcatechol

Yellow crystals of the title compound were recrystallised from methanol at room temperature and after about 24 hours, single crystals were collected. The 3,5-di-*tert*-butylcatechol crystallised in a centrosymmetric space group, P-1, with 4 molecules per unit cell. The structure and numbering scheme of 3,5-di-*tert*-butylcatechol is illustrated in Figure 3.10, while

the most important bond distances and angles are reported in Table 3.6 and Table 3.7 respectively. The positional and thermal parameters are given in Table 1.B and a complete list of all bond distances and angles are given in Table 2.B of the Appendix.

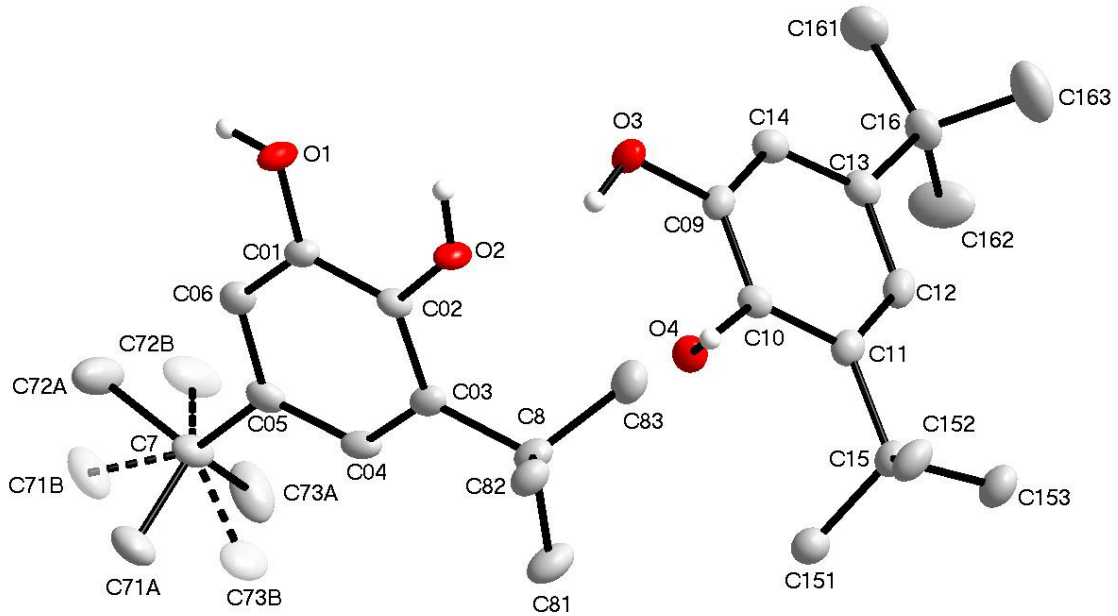

Figure 3.10 Thermal ellipsoid structure of 3,5-di-*tert*-butylcatechol, showing the atom numbering system. Hydrogen atoms have been omitted for clarity except the hydroxyl hydrogen atoms. Thermal ellipsoid probability set at 50 %.

The molecular structure of 3,5-di-*tert*-butylcatechol consists of a benzene ring with two hydroxyl groups bonded in the 1st and 2nd positions. On the 3rd and 5th positions, two *tert*-butyl groups are connected to the benzene ring. The *tert*-butyl group on the 5 position is distorted in 45 % to 55 %. The wR improved by 6 % when the disorder was included in the refinement.

Table 3.6 Selected bond lengths for 3,5-di-*tert*-butylcatechol.

Selected bond lengths			
Atoms	**Bond lengths (Å)**	**Atoms**	**Bond length (Å)**
O(2)-C(02)	1.386(4)	C(7)-C(71B)	1.422(10)
O(1)-C(01)	1.378(4)	C(7)-C(73A)	1.464(8)
C(01)-C(02)	1.381(5)	C(7)-C(72B)	1.553(9)
C(01)-C(06)	1.383(5)	C(7)-C(71A)	1.571(8)
C(02)-C(03)	1.401(4)	C(7)-C(72A)	1.581(8)
C(03)-C(04)	1.396(5)	C(7)-C(73B)	1.585(9)
C(03)-C(8)	1.534(5)	C(8)-C(81)	1.535(4)
C(04)-C(05)	1.399(5)	C(8)-C(82)	1.537(5)
C(05)-C(06)	1.392(4)	C(8)-C(83)	1.539(5)
C(05)-C(7)	1.529(5)		

Table 3.7 Selected bond angles for 3,5-di-*tert*-butylcatechol.

Selected bond Angles			
Atoms	**Bond angles (°)**	**Atoms**	**Bond angles (°)**
O(1)-C(01)-C(02)	116.0(3)	C(71B)-C(7)-C(72B)	114.5(6)
O(1)-C(01)-C(06)	122.2(3)	C(05)-C(7)-C(72B)	106.5(4)
C(02)-C(01)-C(06)	121.8(3)	C(73A)-C(7)-C(71A)	110.1(5)
C(01)-C(02)-O(2)	118.6(3)	C(05)-C(7)-C(71A)	107.2(4)
C(01)-C(02)-C(03)	120.5(3)	C(73A)-C(7)-C(72A)	109.2(5)
O(2)-C(02)-C(03)	120.9(3)	C(05)-C(7)-C(72A)	113.1(4)
C(04)-C(03)-C(02)	116.4(3)	C(71A)-C(7)-C(72A)	103.7(5)
C(04)-C(03)-C(8)	122.4(3)	C(71B)-C(7)-C(73B)	108.8(6)
C(02)-C(03)-C(8)	121.1(3)	C(05)-C(7)-C(73B)	111.0(4)
C(03)-C(04)-C(05)	124.0(3)	C(72B)-C(7)-C(73B)	104.5(6)
C(06)-C(05)-C(04)	117.4(3)	C(03)-C(8)-C(81)	111.7(3)
C(06)-C(05)-C(7)	120.8(3)	C(03)-C(8)-C(82)	109.9(3)
C(04)-C(05)-C(7)	121.8(3)	C(81)-C(8)-C(82)	107.3(3)
C(01)-C(06)-C(05)	119.9(3)	C(03)-C(8)-C(83)	109.7(3)
C(71B)-C(7)-C(05)	111.4(4)	C(81)-C(8)-C(83)	108.1(3)
C(73A)-C(7)-C(05)	113.1(4)	C(82)-C(8)-C(83)	110.1(3)

The C1-O1 and C2-O2 bond lengths are 1.378(4) Å and 1.386(4) Å, respectively. These bonds are obviously longer than that of the 3,5-di-*tert*-butyl-1,2-benzoquinone[36], which has C1-O1 and C2-O2 bond lengths of 1.217(3) Å and 1.214(3) Å, respectively, and also longer than that of 3,5-di-*tert*-butyl-1,2-benzoquinone coordinated to a copper complex in which instance the C1-O1 and C2-O2 bond lengths are 1.293(7) Å and 1.304(7) Å, respectively.[37] The C1-C2-C3

[36] D.N. Horng, J.P. Chyn, K.J. Shieh, J.L. Chou and Y.S. Wen, *Acta Cryst. C*, **55**, 652, (1999).
[37] J.S. Thomson and J.C. Calabrese, *Inorg. Chem.*, **24**, 3167, (1985).

and C2-C1-C6 bond angles are 120.5(3) ° and 121.8(3) °, respectively. This compares well with 3,5-di-*tert*-butyl-1,2-benzoquinone coordinated to a copper complex which has C1-C2-C3 and C2-C1-C6 bond angles of 120.2(6) ° and 120.5(6) °, respectively. The bond angles of 3,5-di-*tert*-butyl-1,2-benzoquinone for C1-C2-C3 and C2-C1-C6 are 118.3(2) ° and 118.7(2) °, respectively, and these are smaller than that of 3,5-di-*tert*-butylcatechol. All the bond lengths within the 6-member ring are between 1.381(5) Å and 1.401(4) Å, with no significant difference between the bond lengths, but with 3,5-di-*tert*-butyl-1,2-benzoquinone and copper(II)-3,5-di-*tert*-butyl-1,2-benzoquinone complexes, the bond lengths C3-C4 and C5-C6 [1.340(3) Å and 1.344(4) Å, respectively in 3,5-di-*tert*-butyl-1,2-benzoquinone; 1.362(8) Å and 1.361(9) Å respectively, in copper(II)-3,5-di-*tert*-butyl-1,2-benzoquinone complex] are always shorter than those of any other C-C bonds [1.439(4) Å-1.554(5) in 3,5-di-*tert*-butyl-1,2-benzoquinone and 1.407(9) Å -1.446(9) Å in copper(II)-3,5-di-*tert*-butyl-1,2-benzoquinone complex], on account of their double-bond character.[36]

Table 3.8 Summary of crystallographic data of three quinone complexes.

	Catechol[a]	Quinone[b]	Copper semiquinone[c]
Crystal system	Triclinic	Monoclinic	Triclinic
Space group	P-1	$P2_1/n$	P-1
Z	4	4	4
Volume ($Å^3$)	1335.3(11)	1344.7(4)	2708
ρ_{calc} ($g.cm^{-1}$)	1.106	1.088	
C1-O1 Å	1.378(4)	1.217(3)	1.293(7)
C2-O2 Å	1.386(4)	1.214(3)	1.304(7)
C3-C4 Å	1.396(5)	1.340(3)	1.362(8)
C5-C6 Å	1.392(4)	1.344(4)	1.361(9)
C1-C2-C3 °	120.5(3)	118.3(2)	120.2(6)
C2-C1-C6 °	121.8(3)	118.7(2)	120.5(6)

a = 3,5-di-*tert*-buylcatechol
b = quinone = 3,5-Di-*tert*-butyl-1,2-benzoquinone[36]
c = Copper semiquinone = Copper(II)-3,5-Di-*tert*-butyl-1,2-semiquinone[37]

The cell volumes of the two organic compounds are comparable, which indicates that the cell dimensions are almost the same. The Z of all four complexes are 4 and the density of the two organic compounds are comparable.

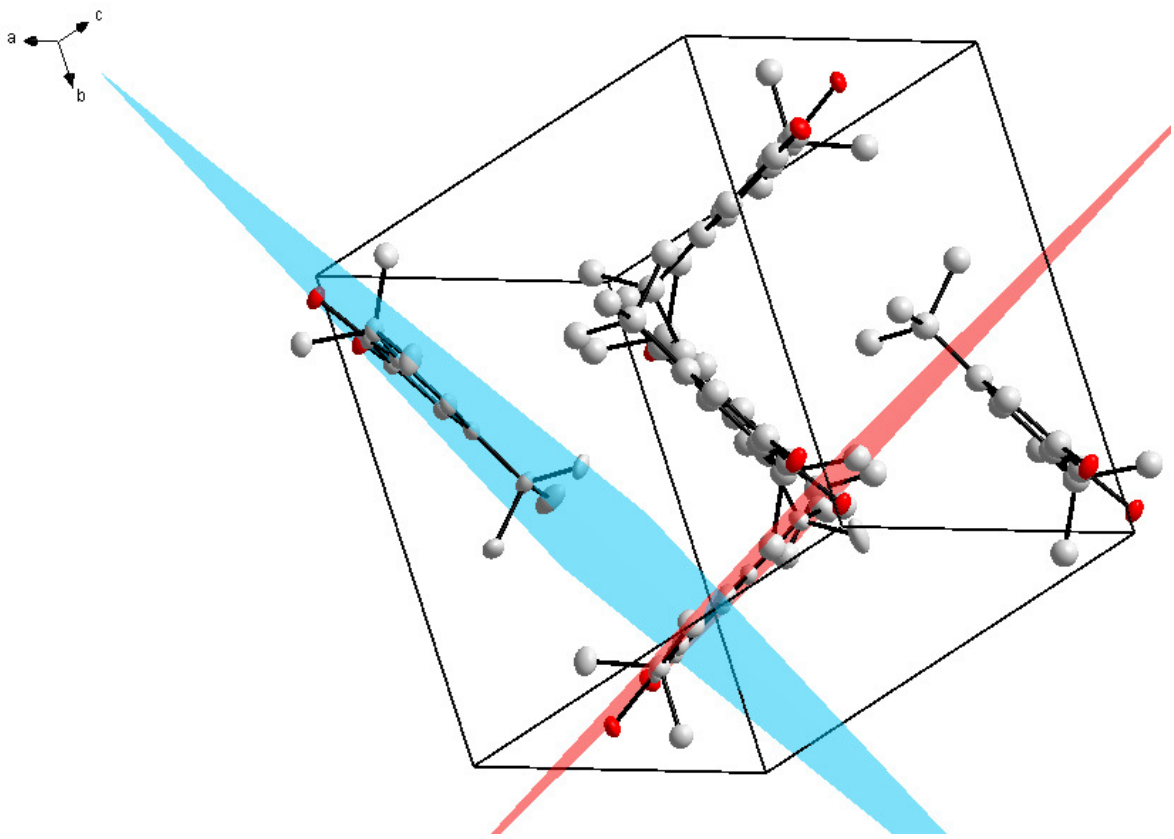

Figure 3.11Two planes in the unit cell bisecting each other. Hydrogen atoms and disorder omitted for clarity.

The packing in the unit cell of 3,5-di-*tert*-butylcatechol is in an L-like geometry and the planes that form are at an angle of 88.22° to one another (Figure 3.11). The planes are constructed through the benzene rings of the 3,5-di-*tert*-butylcatechol that are C1-6 and C9-14. The wR is high, but there is no more electron density to place atoms nor are these voids big enough to place a solvent molecule. When some of the reflections, which do not agree, are omitted the model improves, but not sufficiently.

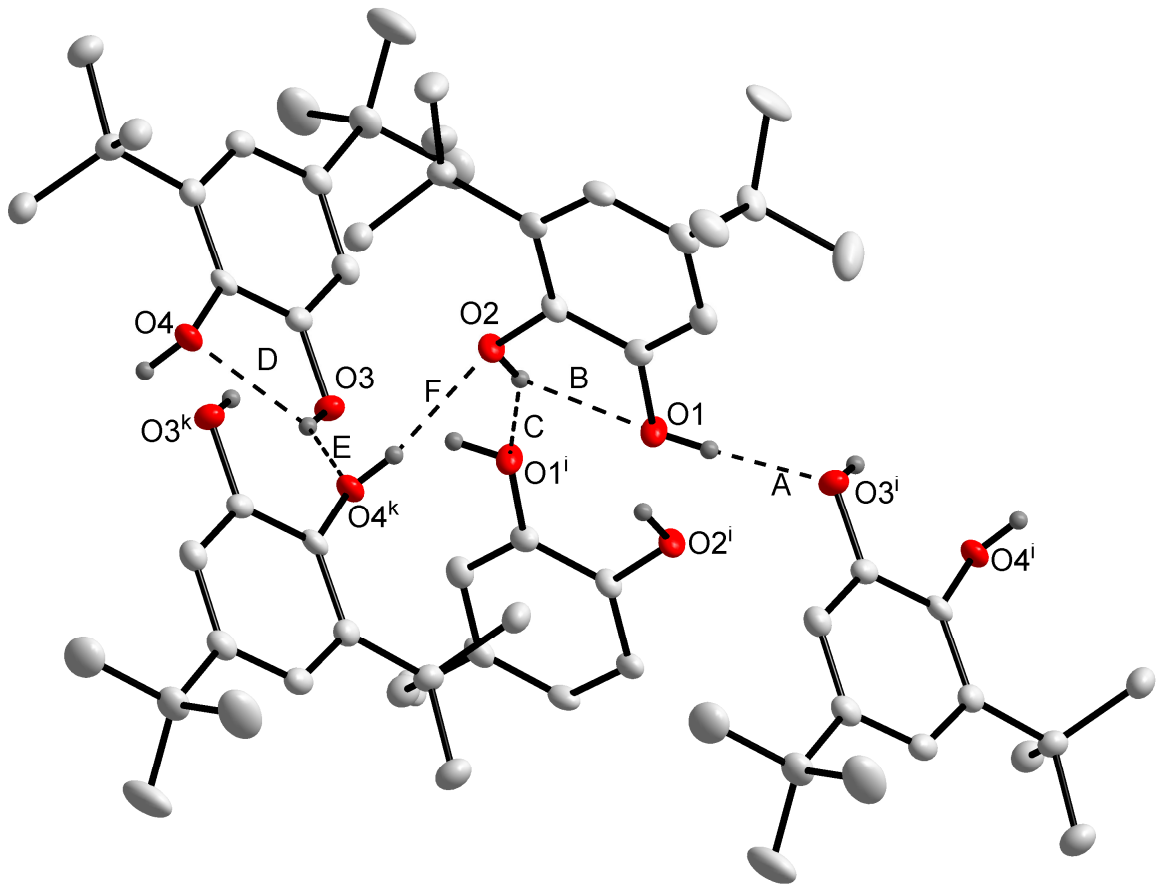

Figure 3.12 Inter- and intramolecular hydrogen-bond interactions found between 3,5-di-*tert*-butylcatechol molecules. Some *tert*-butyl groups and hydrogen atoms omitted for clarity.

The 3,5-di-*tert*-butylcatechol is stabilised by weak hydrogen interactions (Figure 3.12). The interactions are between the hydrogen on the hydroxyl groups and the oxygen of the next hydroxyl group. A complete list of all the hydrogen interactions ia given in Table 3.9, together with all the symmetry operations.

Table 3.9 Hydrogen bonds for 3,5-di-*tert*-butylcatechol [Å and °].

H-Bond	D-H...A	D-H (Å)	H...A (Å)	D----A (Å)	D-H...A (°)
A	O1 H1 O3 ^{i}	0.84	1.85	2.680(3)	169.9
B	O2 H2 O1	0.84	2.26	2.649(3)	108.1
C	O2 H2 O1^{i}	0.84	2.02	2.755(3)	145.9
D	O3 H3 O4	0.84	2.26	2.701(3)	113.0
E	O3 H3 O4 ^{k}	0.84	2.08	2.778(3)	140.7
F	O4 H4 O2^{k}	0.84	2.15	2.868(3)	143.7

i = 2-x, -y, -z
k = 3-x, -y, -z

3.6 Conclusion

In this chapter, a number of compounds, including [Cu(Memal)$_2$], [Cu(Etmal)$_2$], [Cu(Trop)$_2$] and [Cu(TropBr$_3$)$_2$] have been successfully synthesised and characterised by means of IR Spectroscopy and Elemental Analysis. The complexes were obtained in a good yield, ranging from between 84 % and 90 %. From the initial IR studies done in Chapter 3, it was postulated that the electron density on the Cu^{II} centre increases in the order [Cu(TropBr$_3$)$_2$], [Cu(Trop)$_2$], [Cu(Etmal)$_2$] and [Cu(Memal)$_2$] and that steric bulk of the complexes decreases in the same order. In the elemental analysis of [Cu(TropBr$_3$)$_2$], the calculated values differ between 0.4 % and 1.8 %. This might be because traces of water were present, if one compensates for the water in the sample, the results are much better and the calculated values become: C, 21.09 %; H, 0.76 %; O, 10.04 %; Cu, 7.79 % and Br, 60.14 %, which correlates much better with the experimental values.

The single crystal structure of [Cu(TropBr$_3$)$_2$(DMSO)$_2$] and 3,5-di-*tert*-butylcatechol was also determined. The [Cu(TropBr$_3$)$_2$(DMSO)$_2$] was solved with the DMSO molecule coordinated to the copper. This structure was compared to three similar copper structures. Consequently it was possible to determine how [Cu(TropBr$_3$)$_2$(DMSO)$_2$] differs in geometry and how the space requirements compared to other Cu complexes. It was possible to determine the manner in which the tropolone ligand coordination varies on a copper complex.

The single crystal structure of 3,5-di-*tert*-butylcatechol was solved as well as the hydrogen bonding network which results in a closed pacing mode.

An understanding of the electronic and steric properties of the Cu complexes will contribute to solving the mechanistic pathway of the oxidation of 3,5-di-*tert*-butylcatechol by molecular oxygen to the corresponding 3,5-di-*tert*-butyl-1,2-benzoquinone. These aspects will be addressed again in Chapter 4, where the actual kinetic reactivity of the four-coordinated copper complexes will be discussed.

4. Kinetic Study of the Oxidation of 3,5-di-*tert*-butylcatechol by Different Copper Complexes

4.1 Introduction

Chemical kinetics comprises the study of the rates of chemical reactions[1], which involves the precise measurement of the variation of concentrations of the reacting species with time. These measurements are conducted in such a way that a certain aspect of the chemical reaction may be studied, such as the influence of temperature, concentration and pressure variation on the reaction time, or the catalytic effect of one species involved in the reaction pathway.

While thermodynamics is primarily concerned with the initial and final state of a chemical system, it cannot yield any information about the rate of the reaction or possible detail of the intermediate states that constitute the prime concern of chemical kinetics.

The presence of time as a factor in chemical kinetics adds both interest and difficulty[2]. Furthermore, chemical kinetics reflects a statistical average state of the molecules participating in the chemical reaction[3,4]. All these factors combined yield only a general idea of the chemical reaction taking place and make interpretation a difficult science. However, it can be simplified significantly by selective manipulation of concentrations of the reacting species.

The study of the copper complexes in this investigation is considered very important and necessary in the evaluation of possible catalytic behaviour of the chemical reaction system.

---

[1] J.H. Espenson, *Chemical Kinetics and Reaction Mechanisms*, 2nd Ed, New York: McGraw-Hill, (1995).
[2] K.A. Connors, *Chemical Kinetics: Study of reaction rates in solution*, 1st Ed, New York: VCH Publishers, (1990).
[3] A.F. Frost and R.G. Pearson, *Kinetics and Mechanism*, New York: John Wiley and Sons, (1953).
[4] C. Capellos and B.H.J. Bielski, *Kinetics Systems*, New York: Wiley-Interscience, (1972).

These kinetic experiments thus assists in determining the fundamental properties of $[Cu(Memal)_2]$, $[Cu(Etmal)_2]$, $[Cu(Trop)_2]$ and $[Cu(TropBr_3)_2]$ and the rate of oxidation of 3,5-di-*tert*-butylcatechol in the presence of molecular oxygen.

In this study different mechanistic investigations were evaluated to elucidate the intrinsic mechanism of the reaction pathway:

- To determine the rate of oxidation by each of the copper(II) complexes.
- The preliminary study of the effect that the concentration of the molecular oxygen will have on the kinetics of these complexes.

It was therefore anticipated that the five-member chelating $[Cu(O,O\text{-}Bid)_2]$ complexes would show an effect on the oxidation rate due to smaller bite angles, less of a steric demand on the copper centre and the fact that the metal orbital, with regard to the ligand, is less optimal as opposed to six-member chelating $[Cu(O,O\text{-}Bid)_2]$ complexes which have more optimal metal orbital with regard to the ligand and larger bite angles, or to bimetallic copper centres. Although there was an appreciable uncertainty about the influence of electronic effect of the different ligands present in the system.

4.2 Theoretical Principles of Chemical Kinetics

4.2.1 Reaction Rates and Rate Laws

In a closed system, the rate of a chemical reaction can be defined as the rate of change with time *t* of the concentration of one of the reactants or of one of the products of the reaction. The rate is defined as a positive quantity, which is unaffected by the component whose concentration change is being measured.

For a generalised chemical reaction:

$$aA + bB \rightarrow fF + jJ \qquad \text{...Eq 4.1}$$

The rate can be expressed as a derivative because the rate almost invariably changes as time passes, as illustrated in Eq 4.2, where *t* = time and the brackets indicate concentration of the species:

$$R = -\frac{d[A]}{dt} = -\frac{d[B]}{dt} = \frac{d[F]}{dt} = \frac{d[J]}{dt} \qquad \text{...Eq 4.2}$$

In general, the rate of reaction can be a function of the concentration of all the species present in a reaction mixture. Therefore, of:

$$R = f(c_1, c_2, \dots \dots, c_j) \quad \text{...Eq 4.3}$$

Eq 4.3 is called the rate law of a given reaction and cannot be predicted from the stoichiometric equation for the overall reaction. It is defined as the experimentally determined dependence of the reaction rate on the reagent concentration.[5] The general form of the rate law is,

$$\text{Rate} = k[A]^m[B]^n \quad \text{...Eq 4.4}$$

Where k is the proportionality constant, called the rate constant. The exponents m and n are determined experimentally from the kinetic study and the sum of m + n yields the total order of the reaction. The rate constant is independent from the concentrations of A and B, but it may depend on environmental factors such as temperature and solvent. The magnitude of k will naturally depend on the particular reaction being studied.

An important objective of experimental kinetics is to propose a reasonable mechanism that will predict a rate law that is consistent with the experimentally observed rate law.

The rate law does not always depend on the concentration of the reactants/products found in the overall reaction. It can also depend on the concentration of catalysts or inhibitors that assist the reaction but which do not undergo any permanent change.

4.2.2. Reaction Order

The rate law as indicated in Eq 4.4 has experimentally determined exponents. The reaction order with respect to any one component is simply the exponent associated with the particular component in question[5]. The units of the rate constant, k, are dependent on the overall reaction order.[2] If the reaction conditions for a specific reaction are such that the concentration of one or more of the active species remain constant or nearly constant during a "run", then these concentrations may be included in the rate constant. The reaction is then said to be *pseudo* n^{th}-order, where n is the sum of the exponents of the concentrations that change during the run. This occurs in catalytic reactions, when the catalyst concentration

[5] R.B. Jordan, *Reaction Mechanisms of Inorganic and Organometallic Systems*, Oxford: Oxford University Press, Inc., (1991).

remains constant during the run, or if one reactant is in excess over another, so that during the run there is only a minute change in the concentration of the former.[6]

4.2.3. Reaction Rates in Practice

The determination of reaction rates can be simplified into a study of concentrations as a function of time. The reaction rate is rarely obtained directly from the experiment. Normally one or more concentrations, or one or more physical properties that are related to concentration, are measured as a function of time in an isothermal system. A number of kinetic runs of this type, analysed under changing conditions, provides the data needed to determine the rate expression and perhaps the variation of the rate constant along with temperature.

The concentration of a specific species can be determined by numerous methods and can generally be divided into two broad categories, namely chemical and physical. Chemical analysis implies a direct determination of one of the species by volumetric or gravimetric procedures; the former is preferred because of its speed. Any chemical method used must be more rapid with respect to the reaction being studied. The advantage of chemical analysis is that it gives an absolute value of concentration.

Physical methods are usually more convenient than chemical methods. A physical method measures some physical property of the reaction mixture that changes substantially as the reaction proceeds. Ideally, the physical property that is measured must vary in a simple manner in regard to the concentration. Common physical methods include optical methods such as polarimetry, refractometry, colourimetry and spectrophotometry; pressure measurements in gaseous reactions; nuclear magnetic resonance, conductivity, potentiometry, etc. Physical methods have the general advantage of being rapid, resulting in more experimental points being available in a given time, often without interfering with the reaction solution, as happens when, for example, chemical sampling is done for analytical purposes.[6] The data received from whatever method is used, can be used to determine the reaction by plotting the species concentration change with time.

A typical result for a kinetic run is illustrated in Figure 4.1, where the concentration c of a reactant starts at zero time at an initial value c_0 and decreases more and more slowly,

[6] J.W. Moore and R.G. Pearson, *Kinetics and Mechanism*, 3rd Ed., New York: John Wiley & Sons, Inc., (1981).

approaching zero or some equilibrium value c_∞ asymptotically. At any time, the rate would be the negative of the slope of the curve expressed in the appropriate units.

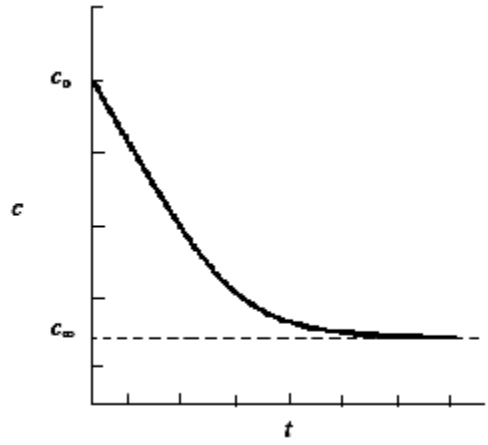

Figure 4.1 Concentration versus time for a typical reaction.[1]

A general rate equation can be determined for an nth-order reaction of a single component system. The stoichiometric equation for a single component[6] is indicated in Eq 4.5 below.

$$A \xrightarrow{k} Z \qquad \text{...Eq 4.5}$$

where Z = the concentration of the other reaction components, which have been grouped together.

The form of the rate expression becomes Eq 4.6 and this form can be integrated:

$$\frac{-d[A]}{dt} = k[A]^n \qquad \text{...Eq 4.6}$$

The limits of integration are taken as $[A_0]$ = initial concentration at t = 0 and [A] = concentration at time t, respectively.

$$-\int_{[A_0]}^{[A]} \frac{d[A]}{[A]^n} = k\int_0^t dt \qquad \text{...Eq 4.7}$$

For a single component rate expression, there are several possible reaction orders such as zero, first and second order. The integrated form of the common rate expression for zero, 1st and 2nd order reactions can be determined from Eq 4.7 and are illustrated below:

For zero order in A: $[A] = [A_0] - kt$ ...Eq 4.8

For first order in A: $\ln[A] = -kt + \ln[A_0]$ ...Eq 4.9

or can be rewritten in the exponential form, $[A] = [A_0]e^{-kt}$ ...Eq 4.10

For second order in A: $\frac{1}{[A]} = kt + \frac{1}{[A_0]}$ ...Eq 4.11

In order to determine an acceptable rate equation, the experimentally determined concentration-time data is fitted to each of the integrated expressions in turn. A linear plot is obtained only when the integrated form of the correct rate law is used. The rate constant, *k*, can then be determined from the slope of the line.[5]

A very useful technique which can be used to simplify rate equations is *pseudo-order reactions*. Suppose a reaction has a second order rate equation:

$R = k[A][D]$ ...Eq 4.12

If the concentration of D is held essentially constant, then the rate equation becomes:

$R = k_{obs}[A]$ ...Eq 4.13

The second-order reaction has been transformed into a *pseudo* first-order reaction, where k_{obs} is the *pseudo* first-order rate constant and $k_{obs} = k[D]$. As mentioned previously, there are several methods by which this reaction equation can be achieved,[2] such as:

- By having an excess concentration of D ([D] >>> [A]) so that its concentration remains essentially constant.
- Using a buffer. If the reaction medium is water and D is either a hydronium ion or hydroxide ion, the use of a buffer could hold the concentration of D reasonably constant.
- The third method is illustrated by a first-order solution reaction of a substance in the presence of its solid phase. If the dissolution rate of the solid is greater than the reaction rate of the dissolved solute, the solute concentration is maintained constant by the solubility equilibrium and the reaction becomes a *pseudo* zero-order reaction.

Spectrophotometry is very useful in kinetic measurements because each molecule has a characteristic absorption spectrum. The Beer-Lambert law[7] provides a direct linear relationship between the concentration of a species; the intensity of the incident (I_0) and transmitted (I_t) monochromatic light as well as the electromagnetic radiation which the species absorbs.

$$Abs = -\log (I_0/I_t) = \varepsilon l c \quad \text{...Eq 4.14}$$

Where l = path length, ε = extinction coefficient, c = concentration and Abs = absorbance. The total absorbance of a solution containing more than one kind of absorbent substance is simply the sum of the individual absorbencies.[8] The absorption of electromagnetic radiation can occur at any wavelength, but of particular interest to this study, is the absorption in the ultraviolet and visible region.

For the purpose of this study, the relationship between concentration and absorbance was used in order to determine the rate equation. All reactions were performed under *pseudo* first-order conditions. The change in absorbance of a solution consisting of the reaction components was plotted as a function of time after the components were mixed together. In the plot obtained, the kinetic runs can be viewed as increasing or decreasing in absorbance, which represents the changing concentration of one of the reaction components. The observed first-order rate constants for the reactions were determined from Eq 4.14:

$$A_{obs} = A_f - (A_f - A_i)e^{k_{obs}t} \quad \text{...Eq 4.15}$$

Where A_{obs} = observed absorbance at time t, A_f = final absorbance, A_i = initial absorbance, k_{obs} = *pseudo* first-order rate constant and t = time.

4.2.4. Reaction Half-Life

The reaction *half-life* ($t_{1/2}$) is defined as the time required for the reactant concentration to decay to one-half its initial value. The term is used to convey a quantitative idea of the time scale and has a quantitative relationship to the rate constant in simple cases.[5]

[7] P.W. Atkins, *Physical Chemistry*, London: Oxford University Press, (1994).
[8] D.A. Skoog, D.M. West, F.J. Holler and S.R. Crouch, *Fundamentals of Analytical Chemistry*, 8th Ed., London: Brooks/Cole, (2004).

To determine the half-life of a reaction, the following substitution is made:$[A] = \frac{[A_0]}{2}$ and t = $t_{1/2}$. in Eq 4.9, thus a first-order equation now becomes:

$$t_{1/2} = \frac{\ln 2}{k_{obs}} = \frac{0.693}{k_{obs}} \quad \text{...Eq 4.16}$$

The half-life for the other rate equations can be similarly obtained.

4.2.5. Reaction Thermodynamics[7]

The rates of most chemical reactions are very sensitive to temperature fluctuations. Arrhenius[9] gave the first temperature dependant quantitative formulation of reaction rates. The following relationship between the specific rate constant, *k*, and the absolute temperature, T was determined to be:

$$k = \mathrm{A}e^{-\mathrm{Ea/RT}} \quad \text{...Eq 4.17}$$

Where *A* and *Ea* are constants, called the pre-exponential factor and the activation energy respectively; R is the gas constant. *Ea* and *A* have different values for the forward and reverse reaction of a given chemical reaction. In practice, the reaction rate generally increases by a factor of 2 or 3 for each 10 ^{o}C rise in temperature.[6] The activation energy *Ea* and the constant *A* may be determined experimentally[10] from the values of *k* and T, by applying the logarithmic form of Eq 4.17.

$$\ln k = -\frac{\mathrm{Ea}}{\mathrm{RT}} + \ln \mathrm{A} \quad \text{...Eq 4.18}$$

4.2.6. Transition State Theory[5]

The parameters used in the transition state theory describes the temperature dependence of k_{exp}, the experimental rate constant, even for solution reactions that are much more complex than gas phases for which the original theory was formulated. Within the transition state theory, reactions are often illustrated in terms of "reaction coordinate diagrams". These are graphic plots of the energy of the system versus the "reaction coordinate", which is an ambiguous measure of the extent to which the reactant has converted to product. The transition state is the species at the highest energy point on the reaction coordinate diagram (Figure 4.2).

[9] S. Arrhenius, *Z. Phys. Chem. (Leipzig),* **4**, 226, (1889).
[10] A.E. Merbach, P. Moore, O.W. Howarth and C.H. McAteer, *Inorg. Chim. Acta*, **39**, 129, (1980).

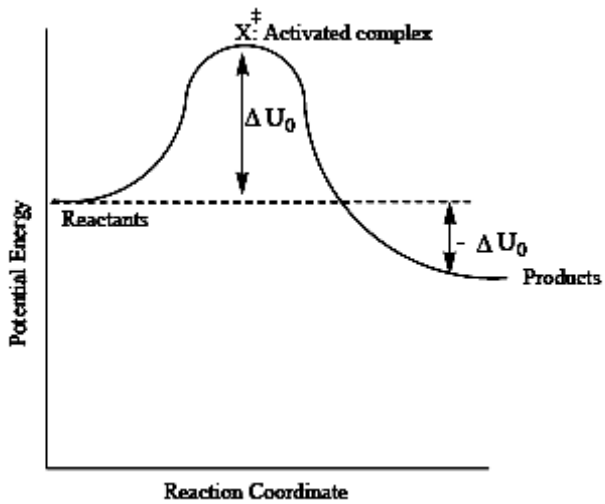

Figure 4.2 Reaction coordination diagram, where the products are more stable than the initial reactants.

The transition state theory assumes that the reaction can be described by the following sequence:

$$\mathrm{A-D} \underset{\leftrightarrows}{\overset{K^{\neq}, k_1}{}} \{\mathrm{A} \cdots \mathrm{D}\} \rightarrow \mathrm{A+D} \qquad \text{...Eq 4.19}$$

The theory proposes that the activated complex will proceed to the products A and D, when the bond has sufficient thermal energy kT, so that the vibrational frequency $v = k\mathrm{T}/h$ will be equal to the rate constant k_3 (k = Boltzman`s constant, $h$ = Planck`s constant). It also assumes that the activated complex is always in equilibrium with the reactant, so that $K^{\neq} = \frac{[\mathrm{A}\cdots\mathrm{D}]^{\neq}}{[\mathrm{A-D}]}$. If $K^{\neq}$ is a normal equilibrium constant, then

$$\frac{\mathrm{d[D]}}{\mathrm{dt}} = k_3[\mathrm{A} \cdots \mathrm{D}]^{\neq} = k_3 K^{\neq}[\mathrm{A-D}] = \frac{k\mathrm{T}}{\mathrm{h}} K^{\neq}[\mathrm{A-D}] \qquad \text{...Eq 4.20}$$

and

$$\ln K^{\neq} = -\frac{\Delta \mathrm{G}^{\neq}}{\mathrm{RT}} = -\frac{\Delta \mathrm{H}^{\neq}}{\mathrm{RT}} + \frac{\Delta \mathrm{S}^{\neq}}{\mathrm{R}} \qquad \text{...Eq 4.21}$$

where $\Delta G^{\neq}, \Delta H^{\neq}$ and $\Delta S^{\neq}$ are the molar free energy, enthalpy and entropy differences between the activated complex and the reactants. If the first-order rate expression, $\frac{d[D]}{dt} = k_{\mathrm{exp}}[A-D]$ is compared to Eq 4.20, then substitution from Eq 4.21 shows that:

$$k_{\mathrm{exp}} = \frac{k\mathrm{T}}{\mathrm{h}} \mathrm{K}^{\neq} = \frac{k\mathrm{T}}{\mathrm{h}} \exp\left(\frac{-\Delta \mathrm{G}^{\neq}}{\mathrm{RT}}\right) \qquad \text{...Eq 4.22}$$

An experimentally viable equation can be derived from substituting Eq 4.21. The logarithmic form of the equation now becomes:

$$\ln\left(\frac{k_{\text{exp}}}{\text{T}}\right) = \ln\left(\frac{k}{\text{h}}\right) - \frac{\Delta\text{H}^{\neq}}{\text{RT}} + \frac{\Delta\text{S}^{\neq}}{\text{R}} \qquad \text{...Eq 4.23}$$

The value of $-\Delta H^{\neq}/R$ can be determined from the slope of the graph of $\ln(k_{exp}/T)$ versus 1/T. The value of $\Delta S^{\neq}$ can be calculated from the intercept. The relationship in Eq 4.23 is known as the Eyring equation.[11] An established Eyring plot can be used to calculate the rate constant at varying temperatures. Non-linear Arrhenius and Eyring plots are unusual because the deviation from a linear plot indicates reactions involving equilibrium, parallel or consecutive reactions.[12]

4.3 Oxidation of 3,5-di-*tert*-butylcatechol by $[Cu(Memal)_2]$, $[Cu(Etmal)_2]$, $[Cu(Trop)_2]$ and $[Cu(TropBr_3)_2]$

4.3.1. Introduction

The catalytic oxidation of 3,5-di-*tert*-butylcatechol by a number of Cu(II) complexes, of the form $[Cu(Memal)_2]$, $[Cu(Etmal)_2]$, $[Cu(Trop)_2]$ and $[Cu(TropBr_3)_2]$, is discussed in detail in this section. The kinetic data for these reactions was determined in order to obtain a reasonable reaction mechanism. Initial rates indicate that the reaction proceeds via a first-order reaction to form 3,5-di-*tert*-1,2-benzoquinone as product.

4.3.2. Experimental

All reagents were of analytical grade. All organic solvents were pre-dried over calcium hydride and then distilled before use. The copper complexes were prepared as described in Section 3.4.

Kinetic measurements were conducted on a UV-Vis Varian Carey 50 Conc Spectrometer equipped with a Julabo F12-mV temperature cell regulator (accurate within 0.1°C) in a 1.00 cm quartz cuvette cell. GC measurements were done on a Shimadzu 2010 Chromatograph equipped with an FID detector and a J&W HP-1 capillary column (30 m x 0.25 mm x 0.25 μm). Hydrogen gas was used as the carrier gas. The temperature program used was as follows: start at 50.0 °C, ramp at 10.0 °C/ min up to 150.0 °C ramp further at 5.0 °C/ min up

[11] C.H. McAteer and P. Moore, *J. Chem. Soc., Dalton Trans.*, 353, (1983).
[12] R.G. Wilkins, *Kinetics and Mechanism of reactions of transition metal complexes*, 2nd Ed., New York: VCH Publishers, Inc., (1991).

to 320.0 °C and kept constant at 320.0 °C for 10 min. All kinetic measurements were conducted in methanol unless otherwise indicated. Data analysis was conducted by means of Microsoft Office Excel 2007[13] and MicroMath Scientist for Windows[14] Version 2.01.

The oxygen concentration was measured with a Hanna HI 9143 dissolved oxygen meter. The methanol was put under a vacuum in a sonic bath to completely degas the methanol and then molecular oxygen was bubbled through. An attempt was made to do the reaction without any oxygen, but there is a minimum of 3 ppm of oxygen in all gasses commercially available. The oxygen concentration varied between 8.13 x 10^{-6} M and 1 x 10^{-3} M. The reaction was monitored by following the rate at which the 3,5-di-*tert*-butyl-1,2-benzoquinone, as oxidation product of 3,5-di-*tert*-butylcatechol (Scheme 2.47, Section 2.6.1), forms at 395 nm. A concentration of 1.4 x10^{-4} M 3,5-di-*tert*-butylcatechol and 1.4 x 10^{-5} M of the copper complex was used for the kinetic run.

The 3,5-di-*tert*-butylcatechol concentration varied between 1.4 x10^{-4} and 1.4 x 10^{-3} M. The concentration was kept this low, in order to prevent the absorbancy level to go above 2. A stock solution of 7.12 x 10^{-3} M of 3,5-di-*tert*-butylcatechol was made up and this was diluted to obtain the right concentration for the kinetic run. All the solutions were made up with O_2 saturated methanol. Extreme care was taken to ensure that all the glassware was clean to prevent any further oxidation of the 3,5-di-*tert*-butyl-1,2-benzoquinone.

4.3.3. Mechanistic Investigation

4.3.3.1. Arguments and Results from Literature and Preliminary Experiments used

In this section the concentration of 3,5-di-*tert*-butylcatechol will be referred to as [cat] and 3,5-di-*tert*-butyl-1,2-benzoquinone as [quin]. In order to construct the complete reaction mechanism, the following arguments where utilised based on preliminary measurements, characterisation studies and literature:

1. The starting materials, $[Cu(Memal)_2]$, $[Cu(Etmal)_2]$, $[Cu(Trop)_2]$ and $[Cu(TropBr_3)_2]$ have been well characterised by IR, elemental analysis and X-ray crystallography (Section 3.4 and 3.5). The data for $[Cu(Trop)_2]$ correlates well with the data published

[13] Microsoft Office Professional Edition 2007 Copyright© 1985-2007 Microsoft Corporation.
[14] MicroMath Scientist for Windows, Version 2.01, Copyright© 1986-1995, MicoMath, Inc.

by Hasegawa *et al.*[15] and the elemental analysis is also correlates well with the theoretical data.

2. The oxygen concentration in the reaction mixture was varied by saturating the methanol with different amounts of molecular oxygen. The reaction followed limiting kinetics with respect to O_2 concentrations as can be seen in Figure 4.3.

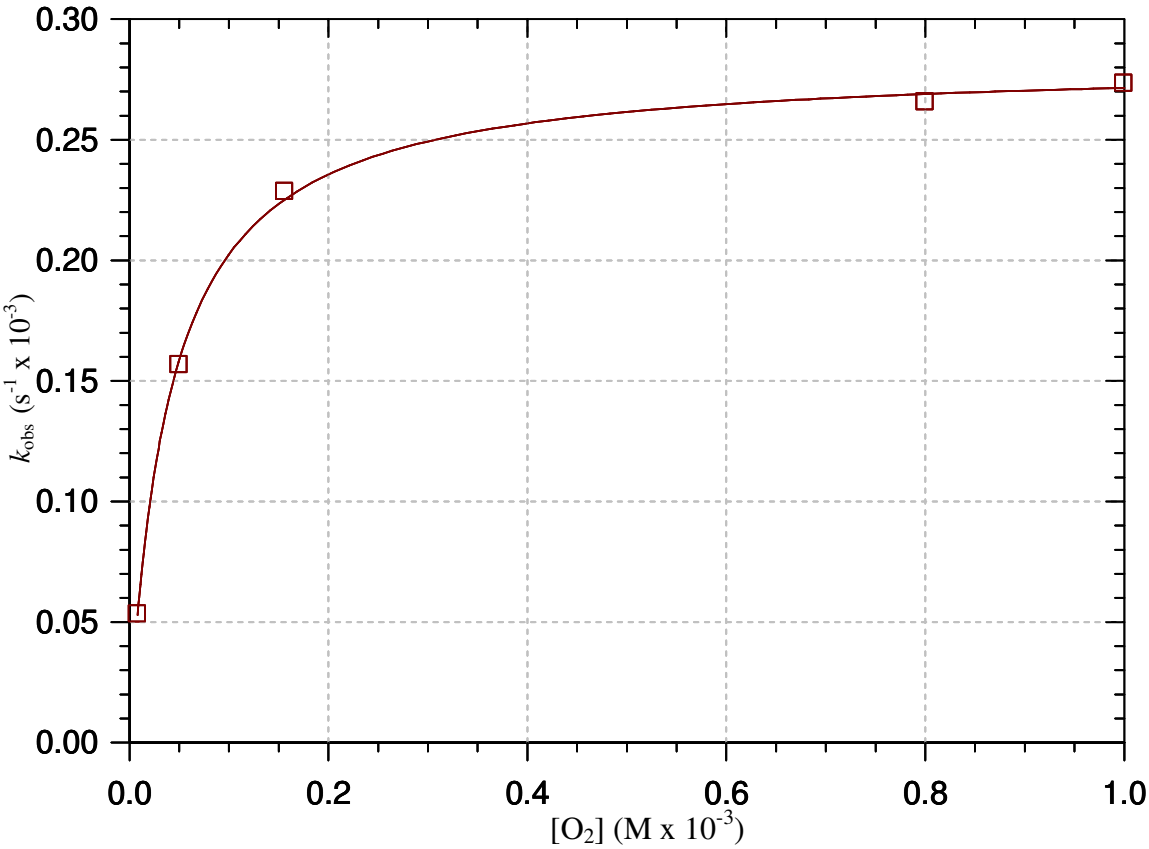

Figure 4.3 Graph of k_{obs} vs. [O_2] with [Cu(Memal)$_2$] = 1.4 x 10^{-5} M as oxidizing catalyst for 3,5-di-*tert*-butylcatechol = 1.4 x10^{-4} M in methanol at 25.0 °C, experimental points observed as well as fitted line are shown.

3. Different concentrations of the 3,5-di-*tert*-butylcatechol were used in the kinetic experiment and the formation of 3,5-di-*tert*-butyl-1,2-benzoquinone was followed at 395 nm on the UV-Vis (Figure 4.4).

[15] M. Hasegawa, Y. Inomaki, T. Inayoshi, T. Hoshi and M. Kobayashi, *Inorg. Chim. Acta*, **257**, 259, (1997).

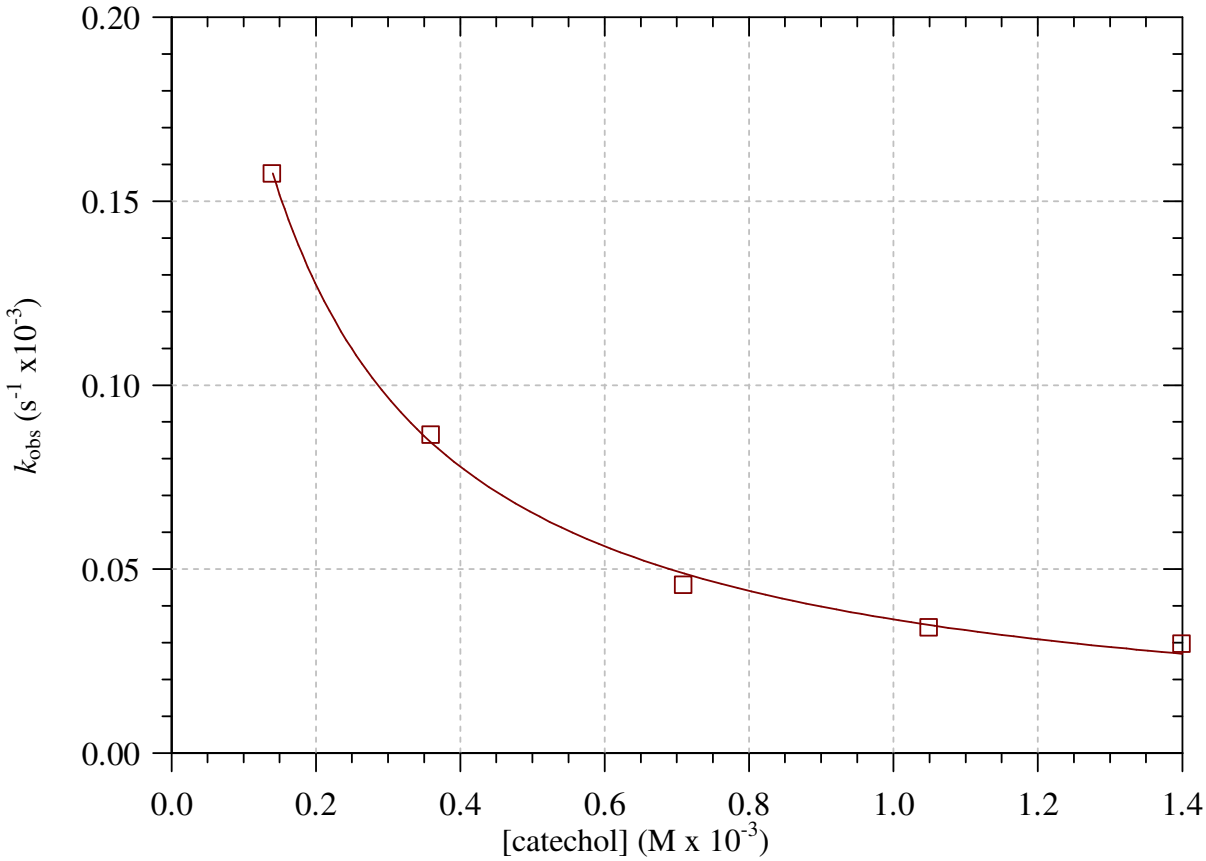

Figure 4.4 Graph of k_{obs} vs. 3,5-di-*tert*-butylcatechol concentration with [Cu(Memal)$_2$] = 1.4 x 10^{-5} M as oxidizing catalyst and [O_2] = 1 x 10^{-3} M at 25.0 °C in methanol, experimental points observed as well as fitted line are shown.

4. The kinetics were followed at 395 nm as this was the wavelength where 3,5-di-*tert*-butyl-1,2-benzoquinone absorbed the light, as shown in Figure 4.5. A tandem cuvette, with a path length of 1 cm was used to follow the kinetics. At the highest concentration the absorbance was below 2. Beer's law can be used to obtain the extinction coefficient of 3,5-di-*tert*-butyl-1,2-benzoquinone from Eq 4.14. The extinction coefficient of 3,5-di-*tert*-butyl-1,2-benzoquinone at 25.0 °C and 1 atm is 1556 M^{-1} cm^{-1} mol in methanol. This correlates well with published literature[16].

[16] K. Selmeczi, M. Reglier, M. Giorgi and G. Speier, *Coord. Chem. Rev.*, **245**, 191, (2003).

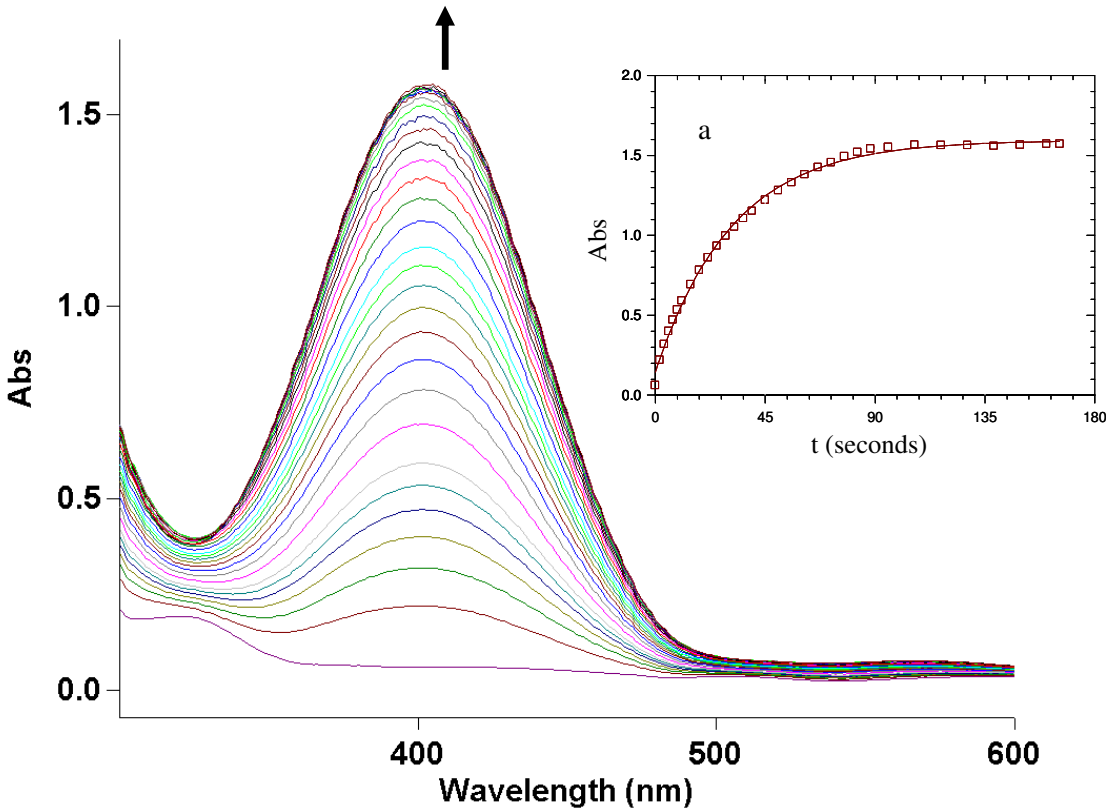

Figure 4.5 UV-Vis spectra for the formation of the 3,5-di-*tert*-butyl-1,2-benzoquinone in methanol at 25 °C. [Cu(Memal)$_2$] = 1.4 x 10^{-5} M, [O$_2$] = 1 x 10^{-3} M, Δt = 30 min, k_{obs} = 3.38 x10^{-5} s^{-1}, ε = 1556 M^{-1} cm^{-1} mol. Insert (a) consists of a graph of absorbance vs. time (seconds) for the formation of 3,5-di-*tert*-butyl-1,2-benzoquinone, experimental points observed as well as fitted line are shown.

5. 3,5-Di-*tert*-butylcatechol or 3,5-di-*tert*-butyl-1,2-benzoquinone can act as a bidentate ligand. While studying the auto-oxidation of 3,5-di-*tert*-butylcatechol by the copper complexes, it was noted that the intermediates have various possible structures and that oxidised products exist[17] as a moiety of 3,5-di-*tert*-butyl-1,2-benzoquinone in copper complexes. As can be seen in Section 3.5.3 the metal ions are the electron acceptors for reactions with 3,5-di-*tert*-butylcatechol or electron donors for reactions with 3,5-di-*tert*-1,2-benzoquinone, yielding in both cases metal ion-semiquinone complexes.[18]

6. During the kinetic investigation the sensor of the oxygen probe had a defect and some of the filling solution leaked into the methanol, causing a rapid decrease in absorbance at 322 nm just after mixing the reaction mixture, as shown in Figure 4.6. This also had the effect of further oxidation of 3,5-di-*tert*-butyl-1,2-benzoquinone. The peak at 395

[17] D.N. Horng, J.P. Chyn, K.J. Shieh, J.L. Chou and Y.S. Wen, *Acta Cryst.*, C**55,** (1999).
[18] J.S. Thompson and J.C Calabrese, *Inorg. Chem.*, **24**, (1985).

nm shifts to a shorter wavelength, indicating the complete oxidation of 3,5-di-*tert*-butyl-1,2-benzoquinone. The same complete oxidation effect was seen when some H_2O_2 was added to the solution.

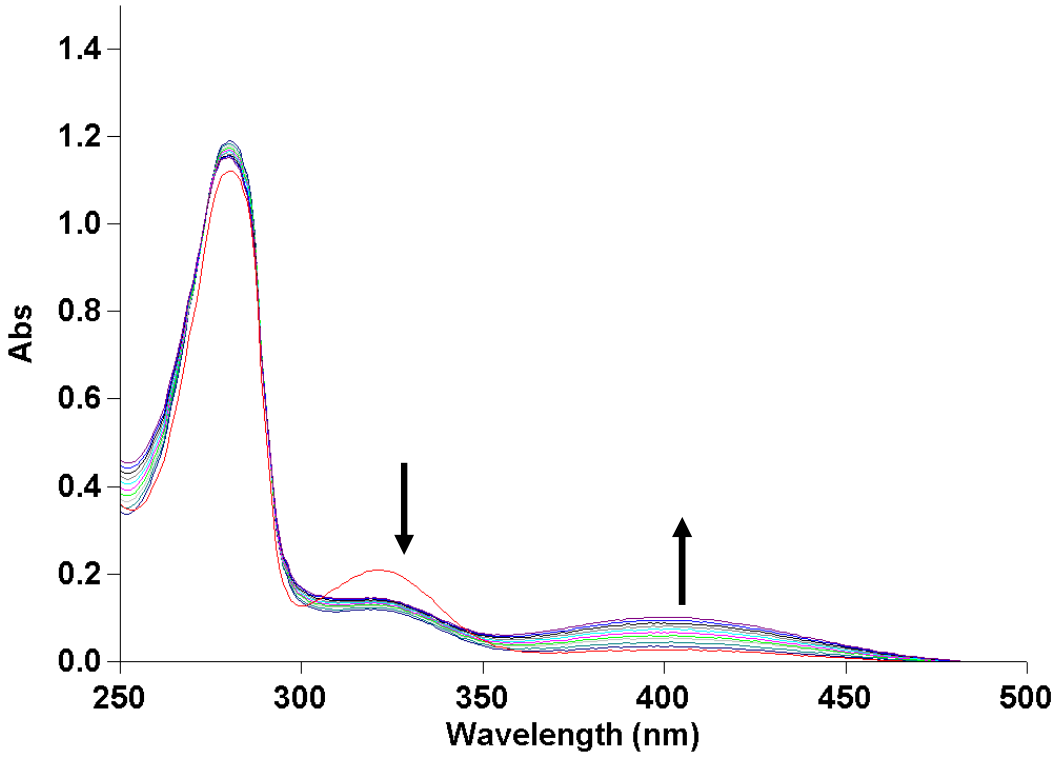

Figure 4.6 UV-Vis scan of the fast decrease in absorbance due to the filling solution of aqueous KCl in the reaction mixture.

7. The turn-over number (TON) for each of the different complexes was calculated after a period of 24 hours. From the ε calculated in no 3 above, the concentration of product formed after 24 hours could be calculated exactly and the amount of catalyst added is known and therefore the TON can be calculated. From the results obtained, it was obvious that this reaction was catalytically driven. These results correlate well to literature (Section 2.6.3).

8. The same reaction was also followed by GC, but an excess of oxygen was bubbled through the reaction mixture. Every 30 min a sample was taken and run on the GC. The formation of 3,5-di-*tert*-butyl-1,2-benzoquinone, as well as the disappearance of 3,5-di-*tert*-butylcatechol was followed on the GC.

9. In the literature, different authors proposed different mechanism, ranging from bimetallic centres[16] to mono metallic centres.[19] In Section 2.6 a thorough discussion about different mechanisms and results obtained, was presented.

4.3.3.2. Possible Reaction Mechanisms for the Catalytic Cycle

Based on the above arguments and literature, the following two possible reaction schemes for the oxidation of 3,5-di-*tert*-butylcatechol were identified:

Mechanism 1:

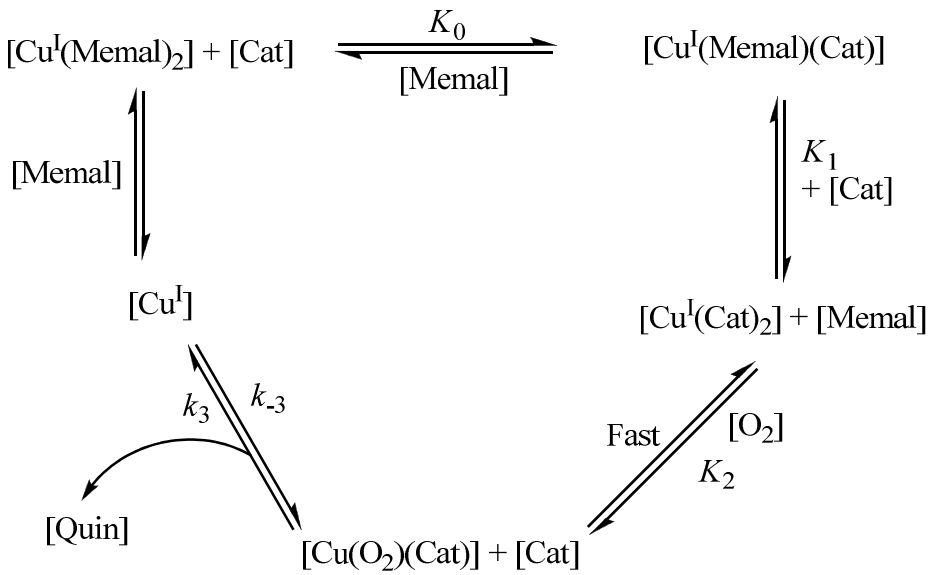

Scheme 4.1 Possible reaction scheme for the oxidation of 3,5-di-*tert*-butylcatechol by [Cu(Memal)$_2$] and molecular oxygen to form the corresponding 3,5-di-*tert*-butyl-1,2-benzoquinone.

Based on Scheme 4.1, a potential mechanism for the catalytic oxidation of 3,5-di-*tert*-butylcatechol by [Cu(Memal)$_2$] could be derived as given in the following paragraph.

The rate expression for the formation of the 3,5-di-*tert*-1,2-benzoquinone, as well as the equilibrium governing reaction in Scheme 4.1, are given by Eq 4.24 and Eq 4.25, respectively:

$$\text{Rate} = \frac{\text{d[quinone]}}{\text{dt}} = k_3[\text{Cu(O}_2\text{)(cat)}] - k_{-3}[\text{cat}] \qquad \text{...Eq 4.24}$$

$$K_2 = \frac{[\text{Cu(O}_2\text{)(cat)}][\text{cat}]}{[\text{Cu}^{\text{I}}\text{(cat)}_2][\text{O}_2]} \qquad \text{...Eq 4.25}$$

[19] A.C.D. Midoes, P.E. Aranha, M.P. dos Santos, E. Tozzo, S. Romera, R.H. de A. Santos and E.R. Dockal, *Polyhedron.*, **27**, 59, (2008).

The total metal concentration is known and is given by Eq 4.26 and this can be rearranged into Eq 4.27 and converted to Eq 4.28.

$$[\mathrm{Cu}]_{\mathrm{tot}} = [\mathrm{Cu(O_2)(cat)}] + [\mathrm{Cu^I(cat)_2}] = [\mathrm{Cu(O_2)(cat)}] + \frac{[\mathrm{Cu(O_2)(cat)}][\mathrm{cat}]}{K_2[\mathrm{O_2}]} \quad \text{...Eq 4.26}$$

$$[\mathrm{Cu(O_2)(cat)}] = \frac{[\mathrm{Cu}]_{\mathrm{tot}}}{1+\frac{[\mathrm{cat}]}{K_2[\mathrm{O_2}]}} \quad \text{...Eq 4.27}$$

$$[\mathrm{Cu(O_2)(cat)}] = \frac{[\mathrm{Cu}]_{\mathrm{tot}}K_2[\mathrm{O_2}]}{[\mathrm{cat}]+K_2[\mathrm{O_2}]} \quad \text{...Eq 4.28}$$

By substituting Eq 4.28 into Eq 4.24, the rate equation becomes Eq 4.29 and this provides us the expression of k_{obs} in Eq 4.30:

$$\mathrm{Rate} = \frac{k_3K_2[\mathrm{O_2}][\mathrm{Cu}]_{\mathrm{tot}}}{[\mathrm{cat}]+K_2[\mathrm{O_2}]} \quad \text{...Eq 4.29}$$

$$k_{obs} = \frac{k_3K_2[\mathrm{O_2}]}{[\mathrm{cat}]+K_2[\mathrm{O_2}]} + k_{-3} \quad \text{...Eq 4.30}$$

Mechanism 2:

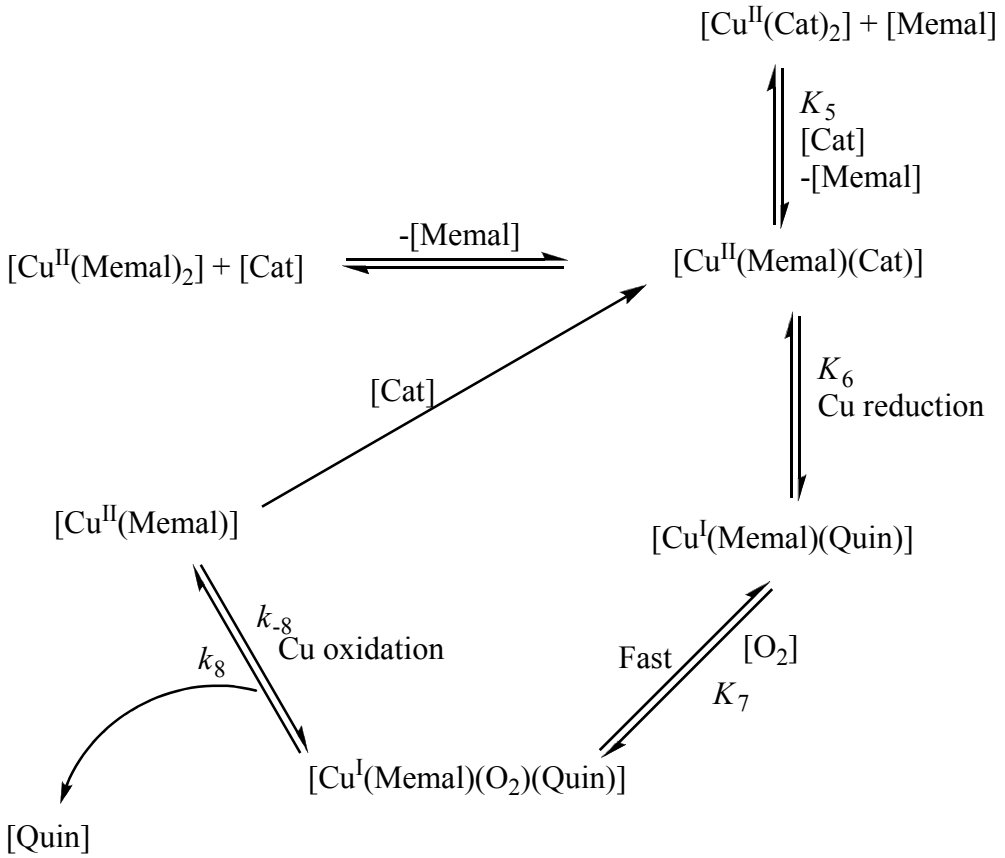

Scheme 4.2 A possible reaction scheme for the oxidation of 3,5-di-*tert*-butylcatechol by [Cu(Memal)$_2$] and molecular oxygen to form the corresponding 3,5-di-*tert*-butyl-1,2-benzoquinone.

Based on Scheme 4.2, a potential mechanism for the catalytic oxidation of 3,5-di-*tert*-butylcatechol by [Cu(Memal)$_2$] could be derived as given in the following paragraph.

The rate expression for the formation of the 3,5-di-*tert*-1,2-benzoquinone, as well as the equilibrium governing reaction in Scheme 4.2, are given by Eq 4.31 and Eq 4.32, respectively:

$$\text{Rate} = \frac{\text{d[quinone]}}{\text{dt}} = k_8[\text{Cu}^{\text{I}}(\text{mal})(\text{O}_2)(\text{quin})] \qquad \text{...Eq 4.31}$$

$$K_7 = \frac{[\text{Cu}^{\text{I}}(\text{mal})(\text{O}_2)(\text{quin})]}{[\text{O}_2][\text{Cu}^{\text{I}}(\text{mal})(\text{quin})]} \qquad \text{...Eq 4.32}$$

The total metal concentration is known and is given by Eq 4.33, which can be rearranged into Eq 4.34:

$$[\mathrm{Cu}]_{\mathrm{tot}} = [\mathrm{Cu^{I}(mal)(O_2)(quin)}] + [\mathrm{Cu^{I}(quin)(mal)}] \quad \text{...Eq 4.33}$$

$$[\mathrm{Cu^{I}(mal)(O_2)(quin)}] = \frac{K_7[\mathrm{O_2}][\mathrm{Cu}]_{\mathrm{tot}}}{1+K_7[\mathrm{O_2}]} \quad \text{...Eq 4.34}$$

Substituting Eq 4.34 in Eq 4.31 at conditions where $[O_2] >> [Cu]_{tot}$ yields Eq 4.35:

$$k_{\mathrm{obs}} = \frac{K_7[\mathrm{O_2}]}{1 + K_7[\mathrm{O_2}]^2} \quad \text{...Eq 4.35}$$

Rearranging Eq 4.36, Eq4.37 and Eq 4.38, yields Eq 4.40, Eq 4.41 and Eq 4.39, respectively, and substituting them into Eq 4.33 yields Eq 4.42.

$$K_{6\mathrm{R}} = \frac{[\mathrm{Cu^{I}(mal)(quin)}]}{[\mathrm{Cu^{II}(mal)(cat)}]} \quad \text{...Eq 4.36}$$

$$K_5 = \frac{[\mathrm{Cu^{II}(cat)_2}][\mathrm{mal}]}{[\mathrm{Cu^{II}(mal)(cat)}][\mathrm{cat}]} \quad \text{...Eq 4.37}$$

$$K_7 = \frac{[\mathrm{Cu^{I}(mal)(quin)(O_2)}]}{[\mathrm{Cu^{I}(mal)(quin)}][\mathrm{O_2}]} \quad \text{...Eq 4.38}$$

$$[\mathrm{Cu^{I}(mal)(quin)}] = \frac{[\mathrm{Cu^{I}(mal)(O_2)(quin)}]}{K_7[\mathrm{O_2}]} \quad \text{...Eq 4.39}$$

$$[\mathrm{Cu^{II}(mal)(cat)}] = \frac{[\mathrm{Cu^{I}(mal)(quin)}]}{K_{6\mathrm{R}}} \quad \text{...Eq 4.40}$$

$$[\mathrm{Cu^{II}(cat)_2}] = \frac{K_5[\mathrm{Cu^{II}(mal)(cat)}][\mathrm{cat}]}{[\mathrm{mal}]} \quad \text{...Eq 4.41}$$

$$[\mathrm{Cu}]_{\mathrm{tot}} = \underbrace{[\mathrm{Cu^{II}(cat)_2}]}_{1} + \underbrace{[\mathrm{Cu^{II}(mal)(cat)}]}_{2} + \underbrace{[\mathrm{Cu^{I}(mal)(quin)}]}_{3} + [\mathrm{Cu^{I}(mal)(quin)(O_2)}] \quad \text{Eq4.42}$$

Combining 1, 2 and 3 from Eq 4.42 with Eq 4.39, Eq 4.40 and Eq 4.41 yields Eq 4.43, Eq 4.44 and Eq 4.45.

$$[\mathrm{Cu^{I}(mal)(quin)}] = \frac{[\mathrm{Cu^{I}(mal)(O_2)(quin)}]}{K_7[\mathrm{O_2}]} \quad \text{...Eq 4.43}$$

$$[\mathrm{Cu^{II}(mal)(cat)}] = \frac{[\mathrm{Cu^{I}(mal)(quin)(O_2)}]}{K_{6\mathrm{R}}K_7[\mathrm{O_2}]} \quad \text{...Eq 4.44}$$

$$[\mathrm{Cu^{II}(cat)_2}] = \frac{K_5[\mathrm{cat}][\mathrm{Cu^{I}(mal)(O_2)(quin)}]}{[\mathrm{mal}]K_{6\mathrm{R}}K_7[\mathrm{O_2}]} \quad \text{...Eq 4.45}$$

$$[\mathrm{Cu^{I}(mal)(O_2)(quin)}] = \frac{[\mathrm{Cu}]_{\mathrm{tot}}}{1+\frac{1}{K_7[\mathrm{O_2}]}+\frac{1}{K_{6\mathrm{R}}K_7[\mathrm{O_2}]}+\frac{K_5[\mathrm{cat}]}{[\mathrm{mal}]K_{6\mathrm{R}}K_7[\mathrm{O_2}]}} \times \frac{[\mathrm{mal}]K_{6\mathrm{R}}K_7[\mathrm{O_2}]}{[\mathrm{mal}]K_{6\mathrm{R}}K_7[\mathrm{O_2}]} \quad \text{... Eq 4.46}$$

$$[\mathrm{Cu^{I}(mal)(O_2)(quin)}] = \frac{[\mathrm{mal}]K_{6\mathrm{R}}K_7[\mathrm{O_2}][\mathrm{Cu}]_{\mathrm{tot}}}{K_5[\mathrm{cat}]+[\mathrm{mal}]+[\mathrm{mal}]K_{6\mathrm{R}}+[\mathrm{mal}]K_{6\mathrm{R}}K_7[\mathrm{O_2}]} \quad \text{... Eq 4.47}$$

From Eq 4.31 and Eq 4.47 the k_{obs} for the variation in the 3,5-di-*tert*-butylcatechol concentration can be determined under the following conditions: [cat] and $[O_2]$ >> $[Cu]_{tot}$

$$k_{\mathrm{obs}} = \frac{[\mathrm{mal}]K_{6\mathrm{R}}K_7[\mathrm{O_2}]}{K_5[\mathrm{cat}]+[\mathrm{mal}]+[\mathrm{mal}]K_{6\mathrm{R}}+[\mathrm{mal}]K_{6\mathrm{R}}K_7[\mathrm{O_2}]} + k_{-8} \quad \text{...Eq 4.48}$$

$$= \frac{[\mathrm{mal}]K_{6\mathrm{R}}K_7[\mathrm{O_2}]}{K_5[\mathrm{cat}]+[\mathrm{mal}](1+K_{6\mathrm{R}}+K_{6\mathrm{R}}K_7[\mathrm{O_2}])} + k_{-8} \quad \text{...Eq 4.49}$$

For the variation in the O_2 concentration under the conditions: K_5 [cat] is small and [cat] is small:

K_7 $[O_2]$ >> K_{6R}; K_{6R} >> 1

$$k_{obs} = \frac{k_8[\mathrm{mal}]K_{6\mathrm{R}}K_7[\mathrm{O_2}]}{[\mathrm{mal}](K_{6\mathrm{R}}+K_{6\mathrm{R}}K_7[\mathrm{O_2}])} + k_{-8}$$

$$= \frac{k_8K_7[\mathrm{O_2}]}{1+K_7[\mathrm{O_2}]} \quad \text{...Eq 4.50}$$

4.3.4. Results and Discussion

The oxidation of 3,5-di-*tert*-butylcatechol by the different Cu-O,O' ligend systems was studied in methanol saturated with molecular oxygen. The formation of the 3,5-di-*tert*-1,2-benzoquinone is slow and the reaction with all four complexes was followed by UV-Vis. A variable temperature study was also done with the $[Cu(Memal)_2]$ complex. Typical kinetic data, as illustrated in Figure 4.7 below, was fitted to Eq 4.15 in order to determine the observed rate constant, $k_{\mathrm{obs.}}$

4.3.4.1. Kinetic Studies

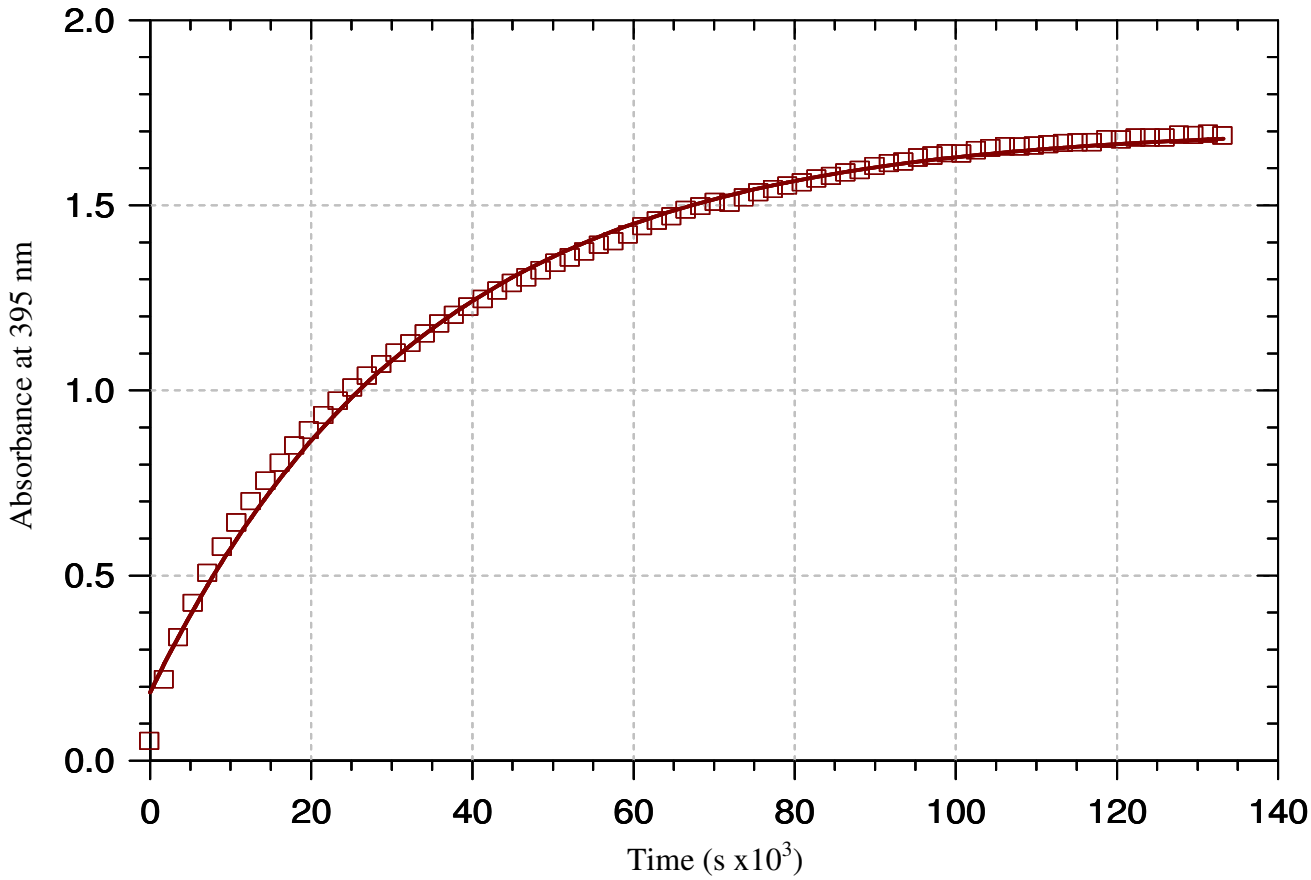

Figure 4.7 Typical UV-Vis absorbance vs. time data for the formation of 3,5-di-*tert*-butyl-1,2-benzoquinone with the oxidation of 3,5-di-*tert*-butylcatechol by [Cu(Memal)$_2$] at 395 nm in methanol saturated with O_2 at 25.0 °C. [Cu(Memal)$_2$] = 1.4x10^{-5}, [catechol] = 1.4x10^{-3} and [O_2] = 1x10^{-3}, experimental points observed as well as fitted line are shown.

a) O_2 concentration studies.

Graphs of the observed first-order rate constants, k_{obs} vs. [O_2] were plotted from the UV-Vis data and yielded a limiting relationship as the [O_2] increased (Figure 4.3) for [Cu(Memal)$_2$] as catalyst. The fits are consistent with the third step in the first proposed mechanism (Scheme 4.1), as well as the third step in the second proposed mechanism (Scheme 4.2). In both cases it is a fast equilibrium reaction. The observed *pseudo* first-order rate constant was fitted to Eq 4.37, in order to determine the rate constant for the oxidation of 3,5-di-*tert*-butylcatechol step, K_2.

The results correlated well with literature[16] in respect that there is a limiting relationship between the rate of the reaction and the concentration of O_2 in the reaction mixture. The rate of the reaction will increase as the concentration of the O_2 increases up to a certain point, and then the rate becomes independent of the O_2

concentration. The concentration where the rate becomes independent of O_2 concentration is 0.4 mM. Table 4.1 lists the rate constant determined for the oxidation of 3,5-di-*tert*-butylcatechol by [Cu(Memal)$_2$] complex as determined by UV-Vis spectroscopy at 25.0 °C.

Table 4.1 UV-Vis kinetic data obtained from Figure 4.3 from the oxidation of 3,5-di-*tert*-butylcatechol by [Cu(Memal)$_2$] at different O_2 concentration at 25.0 °C in methanol.

[O_2] x10^{-4}	k_{obs} (x 10^{-4} s^{-1})	K_2 (s^{-1})
0.08	0.53(1)	3.42(32)
0.50	1.57(4)	
1.56	2.28(15)	
8.01	2.66(8)	
10.11	2.73(8)	

b) 3,5-Di-*tert*-butylcatechol concentration studies.

Graphs of the observed first-order rate constants, k_{obs} *vs*. [cat] were plotted from the UV-Vis data and a limiting relationship was once again obtained as the [cat] increased (Figure 4.4) for all four catalysts. The fits are consistent with the fourth step in the first proposed mechanism (Scheme 4.1), as well as the fourth step in the second proposed mechanism (Scheme 4.2). In both cases it is a fast equilibrium reaction, and also the rate determining steps in both mechanisms. Table 4.2 lists the rate constants determined for the oxidation of 3,5-di-*tert*-butylcatechol by [Cu(Memal)$_2$], [Cu(Etmal)$_2$], [Cu(Trop)$_2$] and [Cu(Trop-Br$_3$)$_2$] complexes as determined by UV-Vis spectroscopy at 25.0 °C and 1 mM [O_2]. The observed *pseudo* first-order rate constant was fitted, in order to determine the rate constant for the oxidation of 3,5-di-*tert*-butylcatechol, steps k_3 and k_{-3} in Scheme 4.1.

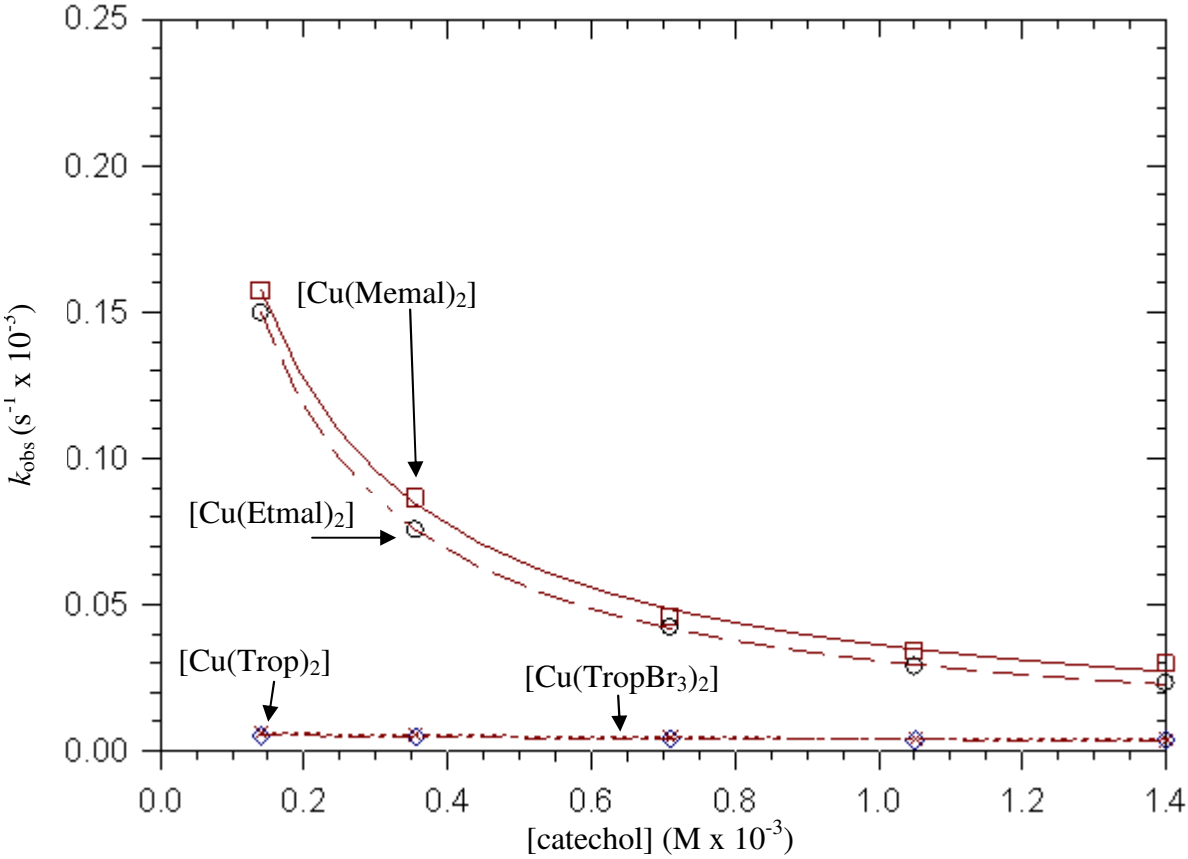

Figure 4.8 The effect of various Cu complexes on the oxidation of 3,5-di-*tert*-butylcatechol under *pseudo* first-order conditions in methanol at 25.0 °C. [Cu(R)$_2$] = 1.4 x 10^{-5} M [O_2] = 1 x10^{-3} M.

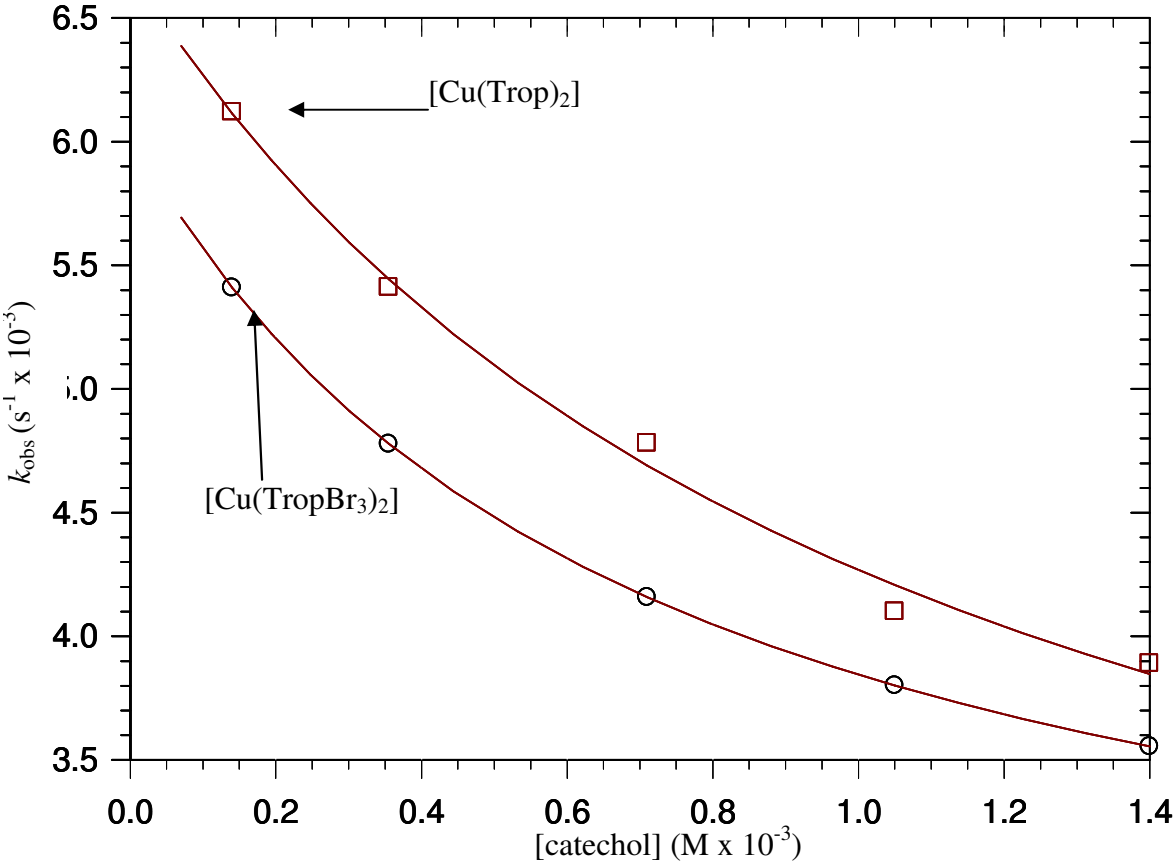

Figure 4.9 The effect of various [Cu(Trop)$_2$] and [Cu(TropBr$_3$)$_2$] on the oxidation of 3,5-di-*tert*-butylcatechol under *pseudo* first-order conditions in methanol at 25.0 °C. [Cu(R)$_2$] = 1.4 x 10^{-5} M [O$_2$] = 1 x10^{-3} M.

Table 4.2 UV-Vis kinetic data obtained from Figure 4.8 for the oxidation of 3,5-di-*tert*-butylcatechol by different [Cu(O,O-Bid)$_2$] = 1.4 x 10^{-5} M complexes at [O$_2$] = 1 x 10^{-3} M in methanol at 25.0 °C.

	k_{obs} (s^{-1} x 10^{-5})			
[cat]	[Cu(Memal)$_2$]	[Cu(Etmal)$_2$]	[Cu(Trop)$_2$]	[Cu(TropBr$_3$)$_2$]
0.00014	15.7(5)	15.0(5)	0.612(5)	0.538(6)
0.00036	8.6(3)	7.6(3)	0.541(6)	0.486(2)
0.00071	4.5(1)	4.2(8)	0.478(2)	0.411(5)
0.00101	3.4(7)	2.9(6)	0.410(2)	0.373(3)
0.00140	3.0(6)	2.3(6)	0.389(3)	0.362(9)
k_3 (x10^{-6} M^{-1} s^{-1})	370(60)	423(20)	5.0(8)	3.7(4)
k_{-3}(x 10^{-6} s^{-1})	2.2 (5.4)	0.9(10)	1.7(10)	2.3(5)

The highest TON was achieved by [Cu(Memal)$_2$] with a value of 70.4 catalytic turnovers in 24 hours, and the lowest TON was achieved by [Cu(TropBr$_3$)$_2$] 12.6 TON in 24 hours. It was confirmed that upon the introduction of additional amounts of [O$_2$], that the oxidation reaction proceeds to completion based on the amount of 3,5-di-*tert*-butyl-1,2-benzoquinone formed.

Table 4.3 TON for the different copper complexes after 24 hours. $[Cu(R)_2]$ = 1.4 x10^{-5} M, [Catechol] = 1.4 x 10^{-3} M, $[O_2]$ = 0.1x10^{-3} M and ε =1556 M^{-1} cm^{-1} mol.

Copper complex	TON in 24 hours
$[Cu(Memal)_2]$	70.4
$[Cu(Etmal)_2]$	63.8
$[Cu(Trop)_2]$	12.9
$[Cu(TropBr_3)_2]$	12.6

As can be seen from the GC results, the 3,5-di-*tert*-butyl-1,2-benzoquinone had a retention time of 17.3 min and 3,5-di-*tert*-butylcatechol had a retention time of 18.4 min. Methanol as well as acetonitrile were used as solvents, but in the case of acetonitrile the reaction stopped after only 14 % of the 3,5-di-*tert*-butyl-1,2-benzoquinone was formed and a ratio of 100:1 catalyst to 3,5-di-*tert*-butylcatechol was used. When methanol was used during the reaction, it reached completion after about 48 hours, but after that the 3,5-di-*tert*-butyl-1,2-benzoquinone was oxidised further.

Table 4.4 Results obtained by continually bubbling molecular oxygen through the reaction mixture at 25.0 °C. Different solvents, catalyst to 3,5-di-*tert*-butylcatechol ratios were used and different ways of quantification was also used.

Solvent	Catalyst : cat	UV-Vis (%)	GC(%)
Acetonitrile	100:1	16	14
Methanol	100:1	54	52
Methanol	10:1	98	96
Acetonitrile	10:1	20	21

c) Temperature studies

Temperature studies were also done on the $[Cu(Memal)_2]$ catalyst at 4 different temperatures. The studies were conducted in order to see what the effect of temperature would be on the rate of the reaction. The different temperatures that were used were 15.0 °C, 25.0 °C, 35.0 °C and 45.0 °C. The results are shown in Figure 4.10 and Table 4.5.

Table 4.5 UV-Vis kinetic data obtained from Figure 4.10 for the catalytic oxidation of 3,5-di-*tert*-butylcatechol by [Cu(Memal)$_2$] = 1.4 x 10^{-5} M in methanol at different temperatures.

	k_{obs} (s^{-1} x 10^{-4})			
[cat]	15.0 °C	25.0 °C	35.0 °C	45.0 °C
0.00014	0.60(2)	1.57(5)	4.45(3)	7.73(37)
0.00036	0.44(3)	0.86(3)	2.49(9)	2.86(10)
0.00071	0.39(1)	0.45(1)	1.83(2)	2.09(3)
0.00105	0.36(1)	0.34(1)	1.72(1)	1.58(4)
0.00140	0.34(1)	0.30(1)	1.57(2)	1.53(3)

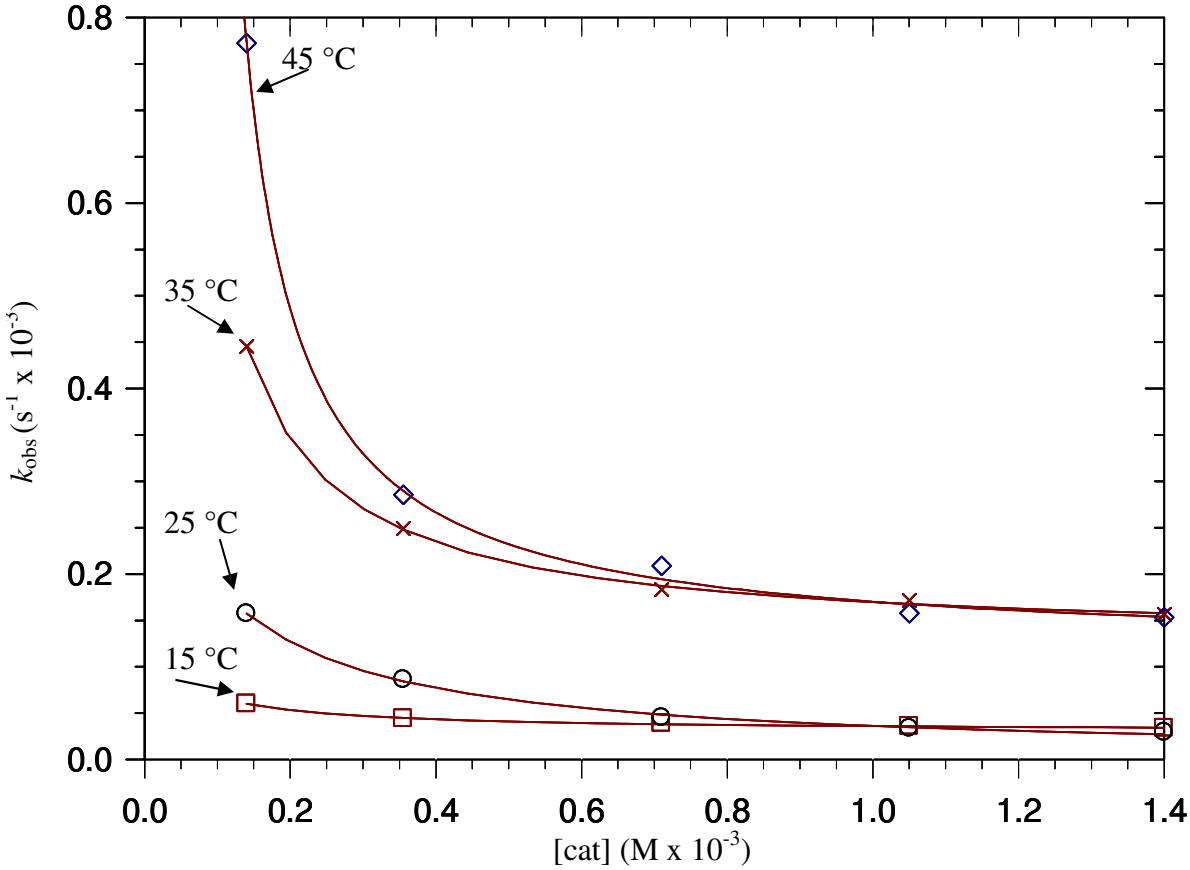

Figure 4.10 Temperature and [cat] dependants of the *pseudo* first-order rate constant for the formation of 3,5-di-*tert*-1,2-benzoquinone in methanol (λ 395 nm) [Cu(Memal)$_2$] = 1.4 x10^{-5} M and [O$_2$] = 1 x10^{-3} M, experimental points observed as well as fitted line are shown.

The product of the catalytic oxidation was isolated and both the starting material and product were characterised by ^{1}H NMR. For 3,5-di-*tert*-butylcatechol a change for two of the hydrogen peaks on the aromatic ring was observed. For the substrate, 3,5-di-*tert*-butylcatechol, peaks appear at 6.75 and 6.88 ppm with a coupling constant J = 2.1 and for the reaction product, 3,5-di-*tert*-1,2-benzoquinone, these two peaks are shifted to 6.23 and 6.95 ppm respectively with J = 2.2. This is in accordance with an ^{1}H NMR spectra of commercial 3,5-di-*tert*-1,2-benzoquinone.

4.4 Conclusion

The oxidation of 3,5-di-*tert*-butylcatechol by copper complexes has been studied as a model reaction to test the catalytic ability of the complexes as oxidation catalyst. In this the ligands were thus chosen in order to see what the effect of electronic and steric parameters would have on the rate of the reaction.

From the initial IR studies done in Chapter 3, it was postulated that the electron density on the copper(II) centre increases in the order $[Cu(TropBr_3)_2]$, $[Cu(Trop)_2]$, $[Cu(Etmal)_2]$ and $[Cu(Memal)_2]$ and that the steric bulk of the complexes decreases in the same order. The kinetic data indicates that the rates of oxidation increase in the following order:

$[Cu(TropBr_3)_2] < [Cu(Trop)_2] < [Cu(Etmal)_2] < [Cu(Memal)_2]$.

The value of k_{obs} for $[Cu(Memal)_2]$ is approximately 10 times larger than that of $[Cu(TropBr_3)_2]$.

The rate of the reaction is as expected, with the rate of oxidation increasing as the electron density around the copper centre increases, and as the steric demand around the centre decreases.

The rate of the reactions is quite slow, which might be due to the effect of inter- and intramolecular hydrogen bonding as indicated by the crystal structure determination (Section3.5). 3,5-di-*tert*-butylcatechol forms hydrogen bonds that results in a closed packing mode which might make it more difficult for the more steric demanding copper centre to reach the coordination site. The interaction of solvent molecules with the axial positions of the copper complex could most likely block the catechol from effectively coordinating with the copper complex.

An increase in temperature has a definite effect on the rate of the reaction. As expected, the rate of the reaction increases by a factor of two, for each 10.0 °C increase of temperature at the lower concentrations. At higher concentrations, there is a fivefold increase for every 20.0 °C increase.

The kinetics done using the GC compares well with that done by UV-Vis under the same conditions. When acetonitrile was used as a solvent, the reaction stopped after only 14 %

conversion took place. This is due to the fact that acetonitrile has an stronger coordination ability than methanol.

The TON of all four catalysts has been calculated and it represents what has been observed with all the other kinetic studies. The order of increase in TON is:

$[Cu(TropBr_3)_2]$, $[Cu(Trop)_2]$, $[Cu(Etmal)_2]$ and $[Cu(Memal)_2]$. With the TON of $[Cu(Memal)_2]$ almost six times larger than that of $[Cu(TropBr_3)_2]$. These results correlate well to those of other authors (Section 2.6.3).

The product of the catalytic oxidation of 3,5-di-*tert*-butylcatechol was characterised by both ^{1}H NMR, GC and UV-Vis.

The proposed mechanisms both adhere to the kinetic data. Scheme 4.1 is the preferred mechanism, because it is less complex and explains the data well. Scheme 4.2 explains the less complex mechanism of only a mono copper centre rather than a bi metallic copper centre as proposed by Selmeczi *et al.*[16] Scheme 4.2 is preferred if a Cu^I to Cu^{III} redox process were to take place in the system. It is exceptionally good because it explains a mono copper system and the term K_5 will only become active when Cu^{III} is in the system.

5. Study Evaluation

5.1. Introduction

This chapter includes a summary of the successes, the results obtained and scientific relevance of this M.Sc. study, as well as a discussion of some future research possibilities.

5.2. Scientific Relevance of the Study

One of the original motives of this study was to gain more insight in the intrinsic properties of copper. Copper complexes have received a significant amount of attention due to their ability to act as catalysts, especially in the process of oxidizing organic substrates.

The focus of the study was to understand the effect that the steric and electronic parameters would have on the ability of copper to oxidize phenolic type of compounds as well as to propose a suitable catalytic mechanism. This was done by selecting ligands that have different electronic properties and different steric bulk.

Four model complexes where successfully synthesised and characterised by IR and elemental analysis. The IR indicated an increase in electron density around the Cu^{II} centre in the following order $[Cu(TropBr_3)_2]$, $[Cu(Trop)_2]$, $[Cu(Etmal)_2]$ and $[Cu(Memal)_2]$. The elemental analysis results correlate well with that of the assumed theoretical values. The solid state structure of $[Cu(TropBr_3)_2]$ and 3,5-di-*tert*-butylcatechol was also investigated by single crystal X-ray crystallography to determine the coordination mode of the ligands and to verify the four coordinated complex.

In spite of the fact that the synthesis of the complexes were easily done, the different crystallisation techniques used in an attempt to crystallise all four copper complexes yielded only one successful crystalline solid to be investigated in detail in the X-ray study.

A kinetic investigation into the oxidation of 3,5-di-*tert*-butylcatechol by the copper complexes yielded interesting results. The systematic increase of the rate constant for the

reaction increased as the electron donating ability of the ligands increased. It indicated the order of reactivity to be as follows: order $[Cu(Memal)_2]$ > $[Cu(Etmal)_2]$ > $[Cu(Trop)_2]$ > $[Cu(TropBr_3)_2]$ which agrees with the electron density trend as indicated by the IR data. Two possible mechanisms where proposed for the four copper complexes, and both agree with the kinetic data obtained during this study.

The mechanisms are still not fully understood and other experimental procedure will have to be conducted in the future to elucidate different aspects associated therewith.

Catalytic behaviour was confirmed, and although small TON and TOF`s were achieved, the proof of concept of these copper systems, acting as oxidation catalysts, has been established.

5.3. Future Research

An interesting tendency in the reactivity of the four ligands was observed during the oxidation of 3,5-di-*tert*-butylcatechol in this study. To further understand this, additional future experiments, as listed below, should be conducted.

- An extended kinetic investigation to study the first step of the reaction. A solvent study would give further insight into a possible solvent effect in these reaction steps.
- Theoretical computational calculations would insist in understanding which parameter, steric or electronic, is the dominant factor.
- Crystallographic studies of the copper complexes and possible intermediates that forms during the reaction and possible isomers that forms to study the complex conformations.
- Modification of the bidentate ligands through either of the donor atoms onto the copper metal centre or substituent on the rings to enhance electron donating or withdrawing effects.
- Optimising the catalytic process for the oxidation of other phenolic types of systems.

Appendix

A.Data for $[Cu(TropBr_3)_2(DMSO)_2]$

Table 1.A Atomic coordinates (x 10^4) and equivalent isotropic displacement parameters ($Å^2$ x 10^3) for $[Cu(TropBr_3)_2(DMSO)_2]$. U(eq) is defined as one third of the trace of the orthogonalized U^{ij} tensor.

	x	y	z	U (eq)
Br(05)	6817(1)	-1196(1)	5341(1)	14(1)
Br(03)	5323(1)	1141(1)	5223(1)	17(1)
Br(07)	9040(1)	544(1)	4996(1)	23(1)
Cu	7500	2500	5000	11(1)
O(01)	8058(2)	1676(1)	4984(4)	11(1)
O(02)	6666(2)	1898(1)	5063(4)	13(1)
C(07)	7993(3)	532(2)	5051(7)	13(1)
C(04)	6344(3)	125(2)	5183(7)	13(1)
C(06)	7697(3)	-92(2)	5103(7)	13(1)
C(02)	6851(3)	1292(2)	5089(6)	10(1)
C(01)	7655(3)	1167(2)	5043(6)	11(1)
C(05)	6969(3)	-272(2)	5173(6)	12(1)
C(03)	6298(3)	803(2)	5152(7)	12(1)
O(1)	7999(2)	2482(2)	8321(4)	15(1)
S(1)	8507(1)	1922(1)	9295(2)	13(1)
C(1)	9412(3)	2028(3)	8828(7)	23(1)
C(2)	8821(3)	2128(3)	11705(7)	20(1)

Table 2.A Bond lengths (Å) and angles (°) for $[Cu(TropBr_3)_2(DMSO)_2]$.

Bond	Distance (Å)	Bond angle	Angle (°)
Br(05)-C(05)	1.909(4)	O(02)#1-Cu-O(02)	180.00(18)
Br(03)-C(03)	1.901(5)	O(02)#1-Cu-O(01)#1	82.08(13)
Br(07)-C(07)	1.900(5)	O(02)-Cu-O(01)#1	97.92(13)
Cu-O(02)#1	1.951(3)	O(02)#1-Cu-O(01)	97.92(13)
Cu-O(02)	1.951(3)	O(02)-Cu-O(01)	82.08(13)
Cu-O(01)#1	1.957(3)	O(01)#1-Cu-O(01)	180.000(1)
Cu-O(01)	1.957(3)	O(02)#1-Cu-O(1)	89.88(12)
Cu-O(1)	2.392(3)	O(02)-Cu-O(1)	90.12(12)
Cu-O(1)#1	2.392(3)	O(01)#1-Cu-O(1)	91.72(12)
O(01)-C(01)	1.274(5)	O(01)-Cu-O(1)	88.28(12)
O(02)-C(02)	1.277(5)	O(02)#1-Cu-O(1)#1	90.12(12)
C(07)-C(06)	1.382(6)	O(02)-Cu-O(1)#1	89.88(12)
C(07)-C(01)	1.426(6)	O(01)#1-Cu-O(1)#1	88.28(12)
C(04)-C(03)	1.382(6)	O(01)-Cu-O(1)#1	91.72(12)
C(04)-C(05)	1.388(6)	O(1)-Cu-O(1)#1	180.000(1)
C(04)-H(04)	0.95	C(01)-O(01)-Cu	113.4(3)
C(06)-C(05)	1.379(6)	C(02)-O(02)-Cu	114.1(3)
C(06)-H(06)	0.95	C(06)-C(07)-C(01)	131.7(4)
C(02)-C(03)	1.419(6)	C(06)-C(07)-Br(07)	113.9(3)
C(02)-C(01)	1.480(6)	C(01)-C(07)-Br(07)	114.5(3)
O(1)-S(1)	1.503(3)	C(03)-C(04)-C(05)	128.8(4)
S(1)-C(2)	1.784(5)	C(03)-C(04)-H(04)	115.6
S(1)-C(1)	1.785(5)	C(05)-C(04)-H(04)	115.6
C(1)-H(1A)	0.98	C(05)-C(06)-C(07)	128.7(4)
C(1)-H(1B)	0.98	C(05)-C(06)-H(06)	115.7
C(1)-H(1C)	0.98	C(07)-C(06)-H(06)	115.7
C(2)-H(2A)	0.98	O(02)-C(02)-C(03)	119.7(4)
C(2)-H(2B)	0.98	O(02)-C(02)-C(01)	114.7(4)
C(2)-H(2C)	0.98	C(03)-C(02)-C(01)	125.6(4)
		O(01)-C(01)-C(07)	119.3(4)
		O(01)-C(01)-C(02)	115.7(4)
		C(07)-C(01)-C(02)	125.0(4)
		C(06)-C(05)-C(04)	128.9(4)
		C(06)-C(05)-Br(05)	115.1(3)
		C(04)-C(05)-Br(05)	116.1(3)
		C(04)-C(03)-C(02)	131.4(4)
		C(04)-C(03)-Br(03)	114.3(3)
		C(02)-C(03)-Br(03)	114.3(3)
		S(1)-O(1)-Cu	119.79(17)
		O(1)-S(1)-C(2)	105.7(2)
		O(1)-S(1)-C(1)	105.3(2)
		C(2)-S(1)-C(1)	99.2(2)
		S(1)-C(1)-H(1A)	109.5

S(1)-C(1)-H(1B)	109.5
H(1A)-C(1)-H(1B)	109.5
S(1)-C(1)-H(1C)	109.5
H(1A)-C(1)-H(1C)	109.5
H(1B)-C(1)-H(1C)	109.5
S(1)-C(2)-H(2A)	109.5
S(1)-C(2)-H(2B)	109.5
H(2A)-C(2)-H(2B)	109.5
S(1)-C(2)-H(2C)	109.5
H(2A)-C(2)-H(2C)	109.5
H(2B)-C(2)-H(2C)	109.5

Symmetry transformations used to generate equivalent atoms: #1 -x+3/2,-y+1/2,-z+1

Table 3.A Anisotropic displacement parameters ($Å^2$ x 10^3) for $[Cu(TropBr_3)_2(DMSO)_2]$.

	u11	u22	u33	u23	u13	u12
Br(05)	15(1)	9(1)	17(1)	0(1)	5(1)	-1(1)
Br(03)	13(1)	13(1)	29(1)	-1(1)	10(1)	-1(1)
Br(07)	14(1)	14(1)	44(1)	2(1)	13(1)	0(1)
Cu	12(1)	7(1)	15(1)	-1(1)	6(1)	-1(1)
O(01)	13(2)	8(2)	13(2)	-1(1)	6(1)	-2(1)
O(02)	11(2)	9(2)	19(2)	-3(1)	6(2)	-2(1)
C(07)	8(2)	16(2)	13(3)	3(2)	1(2)	0(2)
C(04)	8(2)	18(2)	13(3)	2(2)	2(2)	-4(2)
C(06)	11(2)	13(2)	14(3)	1(2)	2(2)	2(2)
C(02)	13(2)	10(2)	6(2)	-2(2)	0(2)	-2(2)
C(01)	12(2)	11(2)	6(2)	-1(2)	0(2)	-1(2)
C(05)	18(3)	9(2)	9(3)	-1(2)	3(2)	-3(2)
C(03)	9(2)	14(2)	15(3)	1(2)	4(2)	0(2)
O(1)	17(2)	13(2)	14(2)	1(1)	3(2)	5(1)
S(1)	12(1)	13(1)	14(1)	1(1)	4(1)	1(1)
C(1)	14(3)	38(3)	17(3)	-9(2)	5(2)	3(2)
C(2)	19(3)	26(3)	14(3)	3(2)	2(2)	4(2)

Table 4.A. Hydrogen coordinates (x 10^4) and isotropic displacement parameters (Å^2 x 10^3) for $[Cu(TropBr_3)_2(DMSO)_2]$.

	x	y	z	U(eq)
H(04)	5886	-99	5215	16
H(06)	8042	-443	5087	15
H(1A)	9338	1929	7518	34
H(1B)	9805	1729	9617	34
H(1C)	9590	2483	9094	34
H(2A)	8378	2093	12189	31
H(2B)	9021	2580	11865	31
H(2C)	9236	1826	12384	31

B. Data for 3,5-di-*tert*-butylchatechol

Table 1.B Atomic coordinates (x 10^4) and equivalent isotropic displacement parameters (Å^2 x 10^3) for 3,5-di-*tert*-butylchatechol. U(eq) is defined as one third of the trace of the orthogonalized U^{ij} tensor.

	x	y	z	u (eq)
O(2)	11416(2)	846(2)	768(2)	18(1)
O(1)	8996(3)	1291(2)	-102(2)	21(1)
C(01)	9220(4)	2077(3)	568(2)	17(1)
C(02)	10467(4)	1822(3)	1035(3)	17(1)
C(03)	10778(4)	2553(3)	1746(2)	17(1)
C(04)	9801(4)	3552(3)	1916(2)	19(1)
C(05)	8553(4)	3842(3)	1433(3)	19(1)
C(06)	8263(4)	3068(3)	759(3)	20(1)
C(7)	7558(4)	4976(3)	1613(3)	22(1)
C(8)	12124(4)	2256(3)	2301(3)	20(1)
C(81)	12280(4)	3210(4)	3002(3)	30(1)
C(82)	13577(4)	2180(3)	1504(3)	23(1)
C(83)	11932(4)	1072(3)	2980(3)	27(1)
C(71A)	8449(8)	6032(6)	1004(6)	28(2)
C(72A)	6098(8)	5042(7)	1112(7)	38(2)
C(73A)	7136(10)	5172(7)	2708(5)	37(2)
C(72B)	5988(10)	4586(8)	2146(8)	35(3)
C(71B)	7563(12)	5729(8)	679(7)	36(3)
C(73B)	8093(11)	5683(8)	2435(8)	30(2)
O(3)	13786(3)	-1575(2)	534(2)	20(1)
O(4)	16113(3)	-436(2)	867(2)	19(1)
C(09)	14115(4)	-1651(3)	1518(2)	18(1)
C(10)	15342(4)	-1122(3)	1703(2)	16(1)
C(11)	15684(4)	-1219(3)	2703(3)	19(1)
C(12)	14725(4)	-1861(3)	3474(3)	20(1)

C(13)	13468(4)	-2389(3)	3298(3)	20(1)
C(14)	13178(4)	-2274(3)	2297(3)	20(1)
C(15)	17020(4)	-631(3)	2960(3)	20(1)
C(151)	16788(4)	704(3)	2782(3)	25(1)
C(152)	18486(4)	-1049(4)	2285(3)	27(1)
C(153)	17207(4)	-949(4)	4093(3)	29(1)
C(16)	12479(4)	-3075(3)	4191(3)	24(1)
C(161)	11065(5)	-3465(4)	3876(3)	36(1)
C(162)	12003(5)	-2319(4)	5094(3)	44(1)
C(163)	13371(5)	-4208(4)	4528(4)	43(1)

Table 2.B Bond lengths (Å) and angles (°) for 3,5-di-*tert*-butylchatechol.

Bond	Distance (Å)	Bond Angle	Angle (°)
O(2)-C(02)	1.386(4)	C(02)-O(2)-H(2)	109.5
O(2)-H(2)	0.84	C(01)-O(1)-H(1)	109.5
O(1)-C(01)	1.378(4)	O(1)-C(01)-C(02)	116.0(3)
O(1)-H(1)	0.84	O(1)-C(01)-C(06)	122.2(3)
C(01)-C(02)	1.381(5)	C(02)-C(01)-C(06)	121.8(3)
C(01)-C(06)	1.383(5)	C(01)-C(02)-O(2)	118.6(3)
C(02)-C(03)	1.401(4)	C(01)-C(02)-C(03)	120.5(3)
C(03)-C(04)	1.396(5)	O(2)-C(02)-C(03)	120.9(3)
C(03)-C(8)	1.534(5)	C(04)-C(03)-C(02)	116.4(3)
C(04)-C(05)	1.399(5)	C(04)-C(03)-C(8)	122.4(3)
C(04)-H(04)	0.95	C(02)-C(03)-C(8)	121.1(3)
C(05)-C(06)	1.392(4)	C(03)-C(04)-C(05)	124.0(3)
C(05)-C(7)	1.529(5)	C(03)-C(04)-H(04)	118
C(06)-H(06)	0.95	C(05)-C(04)-H(04)	118
C(7)-C(71B)	1.422(10)	C(06)-C(05)-C(04)	117.4(3)
C(7)-C(73A)	1.464(8)	C(06)-C(05)-C(7)	120.8(3)
C(7)-C(72B)	1.553(9)	C(04)-C(05)-C(7)	121.8(3)
C(7)-C(71A)	1.571(8)	C(01)-C(06)-C(05)	119.9(3)
C(7)-C(72A)	1.581(8)	C(01)-C(06)-H(06)	120.1
C(7)-C(73B)	1.585(9)	C(05)-C(06)-H(06)	120.1
C(8)-C(81)	1.535(4)	C(71B)-C(7)-C(73A)	133.3(6)
C(8)-C(82)	1.537(5)	C(71B)-C(7)-C(05)	111.4(4)
C(8)-C(83)	1.539(5)	C(73A)-C(7)-C(05)	113.1(4)
C(81)-H(81A)	0.98	C(71B)-C(7)-C(72B)	114.5(6)
C(81)-H(81B)	0.98	C(73A)-C(7)-C(72B)	64.5(6)
C(81)-H(81C)	0.98	C(05)-C(7)-C(72B)	106.5(4)
C(82)-H(82A)	0.98	C(71B)-C(7)-C(71A)	41.8(5)
C(82)-H(82B)	0.98	C(73A)-C(7)-C(71A)	110.1(5)
C(82)-H(82C)	0.98	C(05)-C(7)-C(71A)	107.2(4)
C(83)-H(83A)	0.98	C(72B)-C(7)-C(71A)	144.8(5)
C(83)-H(83B)	0.98	C(71B)-C(7)-C(72A)	63.6(6)
C(83)-H(83C)	0.98	C(73A)-C(7)-C(72A)	109.2(5)

C(71A)-H(71A)	0.98	C(05)-C(7)-C(72A)	113.1(4)
C(71A)-H(71B)	0.98	C(72B)-C(7)-C(72A)	52.9(5)
C(71A)-H(71C)	0.98	C(71A)-C(7)-C(72A)	103.7(5)
C(72A)-H(72A)	0.98	C(71B)-C(7)-C(73B)	108.8(6)
C(72A)-H(72B)	0.98	C(73A)-C(7)-C(73B)	41.0(5)
C(72A)-H(72C)	0.98	C(05)-C(7)-C(73B)	111.0(4)
C(73A)-H(73A)	0.98	C(72B)-C(7)-C(73B)	104.5(6)
C(73A)-H(73B)	0.98	C(71A)-C(7)-C(73B)	72.3(5)
C(73A)-H(73C)	0.98	C(72A)-C(7)-C(73B)	134.7(5)
C(72B)-H(72D)	0.98	C(03)-C(8)-C(81)	111.7(3)
C(72B)-H(72E)	0.98	C(03)-C(8)-C(82)	109.9(3)
C(72B)-H(72F)	0.98	C(81)-C(8)-C(82)	107.3(3)
C(71B)-H(71D)	0.98	C(03)-C(8)-C(83)	109.7(3)
C(71B)-H(71E)	0.98	C(81)-C(8)-C(83)	108.1(3)
C(71B)-H(71F)	0.98	C(82)-C(8)-C(83)	110.1(3)
C(73B)-H(73D)	0.98	C(8)-C(81)-H(81A)	109.5
C(73B)-H(73E)	0.98	C(8)-C(81)-H(81B)	109.5
C(73B)-H(73F)	0.98	H(81A)-C(81)-H(81B)	109.5
O(3)-C(09)	1.377(4)	C(8)-C(81)-H(81C)	109.5
O(3)-H(3)	0.84	H(81A)-C(81)-H(81C)	109.5
O(4)-C(10)	1.395(4)	H(81B)-C(81)-H(81C)	109.5
O(4)-H(4)	0.84	C(8)-C(82)-H(82A)	109.5
C(09)-C(14)	1.383(5)	C(8)-C(82)-H(82B)	109.5
C(09)-C(10)	1.384(5)	H(82A)-C(82)-H(82B)	109.5
C(10)-C(11)	1.402(4)	C(8)-C(82)-H(82C)	109.5
C(11)-C(12)	1.399(5)	H(82A)-C(82)-H(82C)	109.5
C(11)-C(15)	1.542(5)	H(82B)-C(82)-H(82C)	109.5
C(12)-C(13)	1.403(5)	C(8)-C(83)-H(83A)	109.5
C(12)-H(12)	0.95	C(8)-C(83)-H(83B)	109.5
C(13)-C(14)	1.384(5)	H(83A)-C(83)-H(83B)	109.5
C(13)-C(16)	1.531(5)	C(8)-C(83)-H(83C)	109.5
C(14)-H(14)	0.95	H(83A)-C(83)-H(83C)	109.5
C(15)-C(151)	1.516(5)	H(83B)-C(83)-H(83C)	109.5
C(15)-C(152)	1.535(5)	C(7)-C(71A)-H(71A)	109.5
C(15)-C(153)	1.537(5)	C(7)-C(71A)-H(71B)	109.5
C(151)-H(15A)	0.98	H(71A)-C(71A)-H(71B)	109.5
C(151)-H(15B)	0.98	C(7)-C(71A)-H(71C)	109.5
C(151)-H(15C)	0.98	H(71A)-C(71A)-H(71C)	109.5
C(152)-H(15D)	0.98	H(71B)-C(71A)-H(71C)	109.5
C(152)-H(15E)	0.98	C(7)-C(72A)-H(72A)	109.5
C(152)-H(15F)	0.98	C(7)-C(72A)-H(72B)	109.5
C(153)-H(15G)	0.98	H(72A)-C(72A)-H(72B)	109.5
C(153)-H(15H)	0.98	C(7)-C(72A)-H(72C)	109.5
C(153)-H(15I)	0.98	H(72A)-C(72A)-H(72C)	109.5
C(16)-C(162)	1.525(5)	H(72B)-C(72A)-H(72C)	109.5
C(16)-C(163)	1.533(6)	C(7)-C(73A)-H(73A)	109.5

C(16)-C(161)	1.536(5)	C(7)-C(73A)-H(73B)	109.5
C(161)-H(16A)	0.98	H(73A)-C(73A)-H(73B)	109.5
C(161)-H(16B)	0.98	C(7)-C(73A)-H(73C)	109.5
C(161)-H(16C)	0.98	H(73A)-C(73A)-H(73C)	109.5
C(162)-H(16D)	0.98	H(73B)-C(73A)-H(73C)	109.5
C(162)-H(16E)	0.98	C(7)-C(72B)-H(72D)	109.5
C(162)-H(16F)	0.98	C(7)-C(72B)-H(72E)	109.5
C(163)-H(16G)	0.98	H(72D)-C(72B)-H(72E)	109.5
C(163)-H(16H)	0.98	C(7)-C(72B)-H(72F)	109.5
C(163)-H(16I)	0.98	H(72D)-C(72B)-H(72F)	109.5
		H(72E)-C(72B)-H(72F)	109.5
		C(7)-C(71B)-H(71D)	109.5
		C(7)-C(71B)-H(71E)	109.5
		H(71D)-C(71B)-H(71E)	109.5
		C(7)-C(71B)-H(71F)	109.5
		H(71D)-C(71B)-H(71F)	109.5
		H(71E)-C(71B)-H(71F)	109.5
		C(7)-C(73B)-H(73D)	109.5
		C(7)-C(73B)-H(73E)	109.5
		H(73D)-C(73B)-H(73E)	109.5
		C(7)-C(73B)-H(73F)	109.5
		H(73D)-C(73B)-H(73F)	109.5
		H(73E)-C(73B)-H(73F)	109.5
		C(09)-O(3)-H(3)	109.5
		C(10)-O(4)-H(4)	109.5
		O(3)-C(09)-C(14)	117.3(3)
		O(3)-C(09)-C(10)	120.5(3)
		C(14)-C(09)-C(10)	122.2(3)
		C(09)-C(10)-O(4)	116.2(3)
		C(09)-C(10)-C(11)	120.2(3)
		O(4)-C(10)-C(11)	123.5(3)
		C(12)-C(11)-C(10)	116.4(3)
		C(12)-C(11)-C(15)	121.1(3)
		C(10)-C(11)-C(15)	122.5(3)
		C(11)-C(12)-C(13)	123.9(3)
		C(11)-C(12)-H(12)	118
		C(13)-C(12)-H(12)	118
		C(14)-C(13)-C(12)	117.6(3)
		C(14)-C(13)-C(16)	122.1(3)
		C(12)-C(13)-C(16)	120.3(3)
		C(09)-C(14)-C(13)	119.7(3)
		C(09)-C(14)-H(14)	120.1
		C(13)-C(14)-H(14)	120.1
		C(151)-C(15)-C(152)	109.5(3)
		C(151)-C(15)-C(153)	107.8(3)
		C(152)-C(15)-C(153)	107.1(3)

C(151)-C(15)-C(11)	110.1(3)
C(152)-C(15)-C(11)	110.6(3)
C(153)-C(15)-C(11)	111.8(3)
C(15)-C(151)-H(15A)	109.5
C(15)-C(151)-H(15B)	109.5
H(15A)-C(151)-H(15B)	109.5
C(15)-C(151)-H(15C)	109.5
H(15A)-C(151)-H(15C)	109.5
H(15B)-C(151)-H(15C)	109.5
C(15)-C(152)-H(15D)	109.5
C(15)-C(152)-H(15E)	109.5
H(15D)-C(152)-H(15E)	109.5
C(15)-C(152)-H(15F)	109.5
H(15D)-C(152)-H(15F)	109.5
H(15E)-C(152)-H(15F)	109.5
C(15)-C(153)-H(15G)	109.5
C(15)-C(153)-H(15H)	109.5
H(15G)-C(153)-H(15H)	109.5
C(15)-C(153)-H(15I)	109.5
H(15G)-C(153)-H(15I)	109.5
H(15H)-C(153)-H(15I)	109.5
C(162)-C(16)-C(13)	110.3(3)
C(162)-C(16)-C(163)	110.4(4)
C(13)-C(16)-C(163)	108.4(3)
C(162)-C(16)-C(161)	108.5(3)
C(13)-C(16)-C(161)	112.7(3)
C(163)-C(16)-C(161)	106.6(3)
C(16)-C(161)-H(16A)	109.5
C(16)-C(161)-H(16B)	109.5
H(16A)-C(161)-H(16B)	109.5
C(16)-C(161)-H(16C)	109.5
H(16A)-C(161)-H(16C)	109.5
H(16B)-C(161)-H(16C)	109.5
C(16)-C(162)-H(16D)	109.5
C(16)-C(162)-H(16E)	109.5
H(16D)-C(162)-H(16E)	109.5
C(16)-C(162)-H(16F)	109.5
H(16D)-C(162)-H(16F)	109.5
H(16E)-C(162)-H(16F)	109.5
C(16)-C(163)-H(16G)	109.5
C(16)-C(163)-H(16H)	109.5
H(16G)-C(163)-H(16H)	109.5
C(16)-C(163)-H(16I)	109.5
H(16G)-C(163)-H(16I)	109.5
H(16H)-C(163)-H(16I)	109.5

Table 3.B Anisotropic displacement parameters ($Å^2$ x 10^3) for 3,5-di-*tert*-butylchatechol.

	u11	u22	u33	u23	u13	u12
O(2)	16(1)	16(1)	24(1)	-10(1)	-3(1)	1(1)
O(1)	17(1)	21(1)	28(1)	-12(1)	-6(1)	1(1)
C(01)	18(2)	16(2)	17(2)	-4(1)	-1(1)	-4(1)
C(02)	16(2)	13(2)	21(2)	-5(1)	0(1)	0(1)
C(03)	16(2)	20(2)	16(2)	-4(1)	1(1)	-5(1)
C(04)	22(2)	18(2)	17(2)	-7(1)	2(1)	-5(1)
C(05)	19(2)	15(2)	21(2)	-2(1)	4(1)	-3(1)
C(06)	17(2)	19(2)	22(2)	-2(1)	-1(1)	-2(1)
C(7)	19(2)	16(2)	32(2)	-8(1)	0(2)	2(1)
C(8)	20(2)	25(2)	18(2)	-7(1)	-2(1)	-2(1)
C(81)	28(2)	38(2)	30(2)	-18(2)	-9(2)	2(2)
C(82)	19(2)	29(2)	22(2)	-6(1)	-5(1)	-2(2)
C(83)	30(2)	33(2)	20(2)	-2(2)	-7(2)	0(2)
C(71A)	34(4)	15(3)	31(4)	-3(3)	4(3)	1(3)
C(72A)	25(4)	27(4)	66(6)	-16(4)	-15(4)	5(3)
C(73A)	46(5)	31(4)	25(4)	-4(3)	11(3)	19(4)
C(72B)	21(4)	20(5)	60(7)	-14(4)	9(4)	4(3)
C(71B)	49(7)	19(5)	34(5)	-2(4)	-2(5)	13(4)
C(73B)	31(5)	17(5)	42(5)	-14(4)	-4(4)	9(4)
O(3)	21(1)	25(1)	15(1)	-2(1)	-4(1)	-4(1)
O(4)	16(1)	23(1)	15(1)	-2(1)	2(1)	-1(1)
C(09)	18(2)	20(2)	15(2)	-5(1)	-2(1)	2(1)
C(10)	15(2)	16(2)	15(2)	-3(1)	4(1)	0(1)
C(11)	16(2)	21(2)	19(2)	-5(1)	-2(1)	3(1)
C(12)	20(2)	23(2)	17(2)	-4(1)	-3(1)	4(1)
C(13)	20(2)	18(2)	20(2)	-2(1)	2(1)	1(1)
C(14)	17(2)	19(2)	21(2)	-3(1)	0(1)	-1(1)
C(15)	22(2)	23(2)	17(2)	-2(1)	-5(1)	0(1)
C(151)	25(2)	26(2)	26(2)	-5(2)	-7(2)	-2(2)
C(152)	20(2)	39(2)	26(2)	-9(2)	-8(2)	2(2)
C(153)	30(2)	37(2)	24(2)	-3(2)	-11(2)	-4(2)
C(16)	23(2)	24(2)	21(2)	3(1)	1(1)	-3(2)
C(161)	34(2)	37(2)	33(2)	4(2)	0(2)	-13(2)
C(162)	45(3)	52(3)	31(2)	-15(2)	18(2)	-18(2)
C(163)	42(3)	41(3)	38(2)	17(2)	4(2)	1(2)

Table 4.B Hydrogen coordinates (x 10^4) and isotropic displacement parameters ($Å^2$ x 10^3) for 3,5-di-*tert*-butylchatechol**.**

	x	y	z	u (eq)
H(2)	10928	336	587	27
H(1)	8156	1456	-280	31
H(04)	9996	4066	2388	23
H(06)	7409	3219	432	24
H(81A)	13151	2994	3341	46
H(81B)	11375	3274	3529	46
H(81C)	12412	3972	2585	46
H(82A)	14432	1994	1864	35
H(82B)	13694	2940	1081	35
H(82C)	13530	1557	1057	35
H(83A)	12793	885	3334	41
H(83B)	11867	443	2543	41
H(83C)	11013	1135	3493	41
H(71A)	8720	5896	272	42
H(71B)	9360	6087	1290	42
H(71C)	7822	6772	1072	42
H(72A)	6375	4904	380	57
H(72B)	5574	5826	1171	57
H(72C)	5438	4435	1474	57
H(73A)	6503	5910	2775	56
H(73B)	8040	5228	3001	56
H(73C)	6582	4510	3081	56
H(72D)	6077	4082	2786	53
H(72E)	5574	4144	1680	53
H(72F)	5322	5288	2309	53
H(71D)	6921	6448	819	54
H(71E)	7185	5315	177	54
H(71F)	8587	5942	397	54
H(73D)	8087	5174	3084	46
H(73E)	7413	6386	2560	46
H(73F)	9109	5925	2168	46
H(3)	14248	-1031	163	30
H(4)	16818	-854	553	28
H(12)	14937	-1945	4158	24
H(14)	12340	-2620	2145	23
H(15A)	17641	1069	2948	38
H(15B)	15867	973	3228	38
H(15C)	16704	933	2056	38
H(15D)	18637	-1912	2399	41
H(15E)	19325	-684	2470	41
H(15F)	18433	-818	1554	41
H(15G)	17358	-1810	4229	44

H(15H)	16306	-665	4550	44
H(15I)	18076	-575	4224	44
H(16A)	10472	-3897	4473	53
H(16B)	11352	-3980	3316	53
H(16C)	10467	-2766	3638	53
H(16D)	11375	-2768	5661	66
H(16E)	11435	-1598	4867	66
H(16F)	12894	-2105	5333	66
H(16G)	12755	-4656	5103	65
H(16H)	14278	-4001	4751	65
H(16I)	13651	-4692	3945	65

Table 5.B Torsion angles (°) for 3,5-di-*tert*-butylchatechol.

O(1)-C(01)-C(02)-O(2)	2.8(5)
C(06)-C(01)-C(02)-O(2)	-176.9(3)
O(1)-C(01)-C(02)-C(03)	-178.7(3)
C(06)-C(01)-C(02)-C(03)	1.6(5)
C(01)-C(02)-C(03)-C(04)	-2.2(5)
O(2)-C(02)-C(03)-C(04)	176.3(3)
C(01)-C(02)-C(03)-C(8)	177.7(3)
O(2)-C(02)-C(03)-C(8)	-3.8(5)
C(02)-C(03)-C(04)-C(05)	0.7(5)
C(8)-C(03)-C(04)-C(05)	-179.2(3)
C(03)-C(04)-C(05)-C(06)	1.3(5)
C(03)-C(04)-C(05)-C(7)	-177.3(3)
O(1)-C(01)-C(06)-C(05)	-179.2(3)
C(02)-C(01)-C(06)-C(05)	0.5(5)
C(04)-C(05)-C(06)-C(01)	-1.9(5)
C(7)-C(05)-C(06)-C(01)	176.7(3)
C(06)-C(05)-C(7)-C(71B)	-60.3(6)
C(04)-C(05)-C(7)-C(71B)	118.3(6)
C(06)-C(05)-C(7)-C(73A)	134.0(5)
C(04)-C(05)-C(7)-C(73A)	-47.4(6)
C(06)-C(05)-C(7)-C(72B)	65.2(6)
C(04)-C(05)-C(7)-C(72B)	-116.2(5)
C(06)-C(05)-C(7)-C(71A)	-104.5(4)
C(04)-C(05)-C(7)-C(71A)	74.1(5)
C(06)-C(05)-C(7)-C(72A)	9.1(6)
C(04)-C(05)-C(7)-C(72A)	-172.3(4)
C(06)-C(05)-C(7)-C(73B)	178.3(5)
C(04)-C(05)-C(7)-C(73B)	-3.0(6)
C(04)-C(03)-C(8)-C(81)	-2.7(5)
C(02)-C(03)-C(8)-C(81)	177.4(3)
C(04)-C(03)-C(8)-C(82)	-121.7(3)
C(02)-C(03)-C(8)-C(82)	58.4(4)

C(04)-C(03)-C(8)-C(83)	117.1(4)
C(02)-C(03)-C(8)-C(83)	-62.8(4)
O(3)-C(09)-C(10)-O(4)	5.7(5)
C(14)-C(09)-C(10)-O(4)	-174.6(3)
O(3)-C(09)-C(10)-C(11)	-179.0(3)
C(14)-C(09)-C(10)-C(11)	0.8(5)
C(09)-C(10)-C(11)-C(12)	-0.2(5)
O(4)-C(10)-C(11)-C(12)	174.7(3)
C(09)-C(10)-C(11)-C(15)	-178.9(3)
O(4)-C(10)-C(11)-C(15)	-4.0(5)
C(10)-C(11)-C(12)-C(13)	-0.5(5)
C(15)-C(11)-C(12)-C(13)	178.2(3)
C(11)-C(12)-C(13)-C(14)	0.7(5)
C(11)-C(12)-C(13)-C(16)	-179.9(3)
O(3)-C(09)-C(14)-C(13)	179.2(3)
C(10)-C(09)-C(14)-C(13)	-0.5(5)
C(12)-C(13)-C(14)-C(09)	-0.2(5)
C(16)-C(13)-C(14)-C(09)	-179.6(3)
C(12)-C(11)-C(15)-C(151)	-114.4(4)
C(10)-C(11)-C(15)-C(151)	64.3(4)
C(12)-C(11)-C(15)-C(152)	124.6(3)
C(10)-C(11)-C(15)-C(152)	-56.8(4)
C(12)-C(11)-C(15)-C(153)	5.4(5)
C(10)-C(11)-C(15)-C(153)	-175.9(3)
C(14)-C(13)-C(16)-C(162)	-128.5(4)
C(12)-C(13)-C(16)-C(162)	52.1(5)
C(14)-C(13)-C(16)-C(163)	110.5(4)
C(12)-C(13)-C(16)-C(163)	-68.9(4)
C(14)-C(13)-C(16)-C(161)	-7.2(5)
C(12)-C(13)-C(16)-C(161)	173.4(3)

Table 6.B Hydrogen bonds for 3,5-di-*tert*-butylchatechol (Å) and (°).

D-H...A	d(D-H)	d(H...A)	d(D...A)	<(DHA)
O(1)-H(1)...O(3)#1	0.84	1.85	2.680(3)	169.9
O(2)-H(2)...O(1)	0.84	2.26	2.649(3)	108.1
O(2)-H(2)...O(1)#1	0.84	2.02	2.755(3)	145.9
O(3)-H(3)...O(4)	0.84	2.26	2.701(3)	113
O(3)-H(3)...O(4)#2	0.84	2.08	2.778(3)	140.7
O(4)-H(4)...O(2)#2	0.84	2.15	2.868(3)	143.7

Symmetry transformations used to generate equivalent atoms:
#1 -x+2,-y,-z #2 -x+3,-y,-z